The Relative Roles of Dynamics and Control in Bipedal Locomotion

by

Shawn Michael O'Connor

A dissertation submitted in partial fulfillment
of the requirements for the degree of
Doctor of Philosophy
(Biomedical Engineering)
in The University of Michigan
2009

Doctoral Committee:

Professor Art D. Kuo, Chair
Professor Beverly D. Ulrich
Associate Professor Daniel P. Ferris
Assistant Professor Kathleen H. Sienko

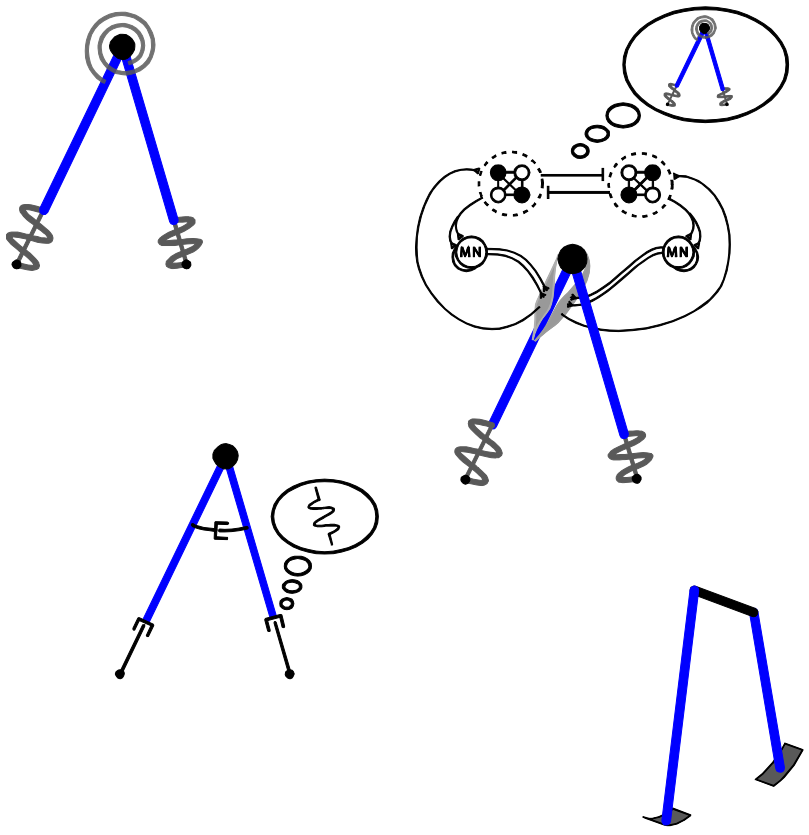
MN
MN

I would like to thank…

Prof. Art Kuo for his mentorship and for helping me grow as an independent researcher.

The HBCL Lab: Peter, Steve, Karl, John, Andrew, Wisit, Megan, and Yiqi for their good advice, good conversations, help collaboration, and many laughs.

Dan Ferris and the HNL lab for generously allowing me to use their lab space and for their helpful feedback along the way.

Steve DeWeerth, Shane and the Neurolab for helping me get my start in research.

My Mom and Dad for their constant love, generous support, and for inspiring me to follow my dreams. Thank you for all of your sacrifices. I could not have asked for better parents.

My brothers, Kevin and Bret, for a great childhood and for lessons they teach me about living a happy and meaningful life

Danny for being a great roommate and the many hours of fun we had not doing research.

My fiancée, Antoinette, for undying support during rough times, fun and laughter during good times, and love throughout. I am so thankful that I can share my life with you.

Table of Contents

List of Figures

List of Tables

Abstract

The Relative Roles of Dynamics and Control in Bipedal Locomotion

by

Shawn Michael O'Connor

Chair: Art D. Kuo

The traditional view of motor control predicates that the central nervous system dictates the motions of the body through muscle activation. An alternative view suggests that movement may be governed by body dynamics alone without need for neural control. Both philosophies have merits, but neither represents a complete solution for robust and efficient behavior. We proposed an integrated view of control and dynamics and investigated how the natural dynamics of the limbs influence control strategies used to pattern and stabilize walking. We explored how features of human walking, traditionally absent in passive walking models, are gained by adding compliance. This compliant behavior essentially models work performed by muscle and tendon and predicts energetic costs measured in human walking. We also countered the notion that walking and running can best be described by stiff and compliant leg behavior, respectively. We showed that the amount and proportion of mechanical energy in the legs distinguishes between gaits much more so than leg compliance or other properties. However, some control is needed to provide spring-like actuation and could be afforded by reflex loops and neural oscillators located in the spinal cord. We used a compliant walking model to study how the feedforward and feedback nature of central pattern generators (CPGs) can be optimally combined to produce steady walking motions. Our findings suggest that CPGs serve a primary role to filter sensory

information rather than to simply generate motor commands. Finally, three-dimensional passive walkers indicate that the fore-aft component of walking may be self stable, whereas lateral motion remains unstable and requires control, as through active foot placement. We tested whether healthy humans exhibit such direction-dependent control by applying low-frequency perturbations to the visual field and measuring foot placement during treadmill walking. We found step variability to be nearly ten times more sensitive to lateral perturbations than fore-aft, suggesting that the central nervous system gains fore-aft stability through uncontrolled behavior. Our results may have implications for the development of novel prosthetics, more energy efficient robots, and the rehabilitation of a broad set of neuromuscular and physical disorders that cause locomotor impairment.

Chapter 1. Introduction

The goal of this thesis is investigate how the natural dynamics of the limbs influence control strategies used by the human nervous system during locomotion. We will employ simple passive dynamic models with actuation (Figure 1.1a) to generate testable predictions regarding feedback control and sensory processing strategies related to gait. We first explore how a simple model with spring-like behavior can reproduce much of the two-dimensional dynamics of human walking (Figure 1.1b). This compliant behavior essentially models the need for work done by muscle and tendon to redirect the vertical motion of the body and speed up swing leg motion and can be used to study energetic costs of locomotion. Some control is needed to supply this spring-like actuation and could be potentially provided by reflex loops and neural oscillators located in the spinal cord (Figure 1.1c). We seek to understand how this rhythmic control of limb behavior can be understood in terms of feedforward and feedback control and how disturbances affect this tradeoff. Finally, three-dimensional passive walkers (Figure 1.1d) must be actively stabilized in the lateral direction. We explore how the dynamic needs for walking stability dictate how visual sensory information is integrated for balance control. While topics of this work cover a broad range of motor control issues, they are tied to the common theme of passive dynamics. Our results have implications for the development of novel prosthetics, more energy efficient robots, and the rehabilitation of a broad set of disorders that cause locomotor impairment.

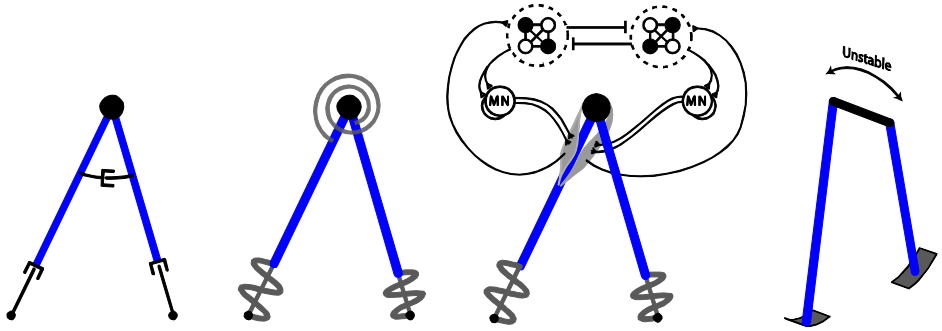

Figure 1.1. Simple models of locomotion. **a**. A generic model of two-dimensional locomotion with linear actuators placed along the legs and a rotational actuator between them. **b**. Actuation can be replaced with axial springs along the legs and a torsional spring between them to model compliant limb behavior. **c**. Control is needed to provide spring-like actuation and could be potentially afforded by reflex loops and neural oscillators located in the spinal cord. **d.** Three-dimensional passive walking models are unstable in the lateral direction and require active stabilization, as through foot placement.

Motivations

Movement is the primary means by which humans are able to express themselves and interact with the outside world. The complex functions of the human neuromuscular system allow people to execute a near infinite number of movements, but are also vulnerable to a diverse array of diseases, birth defects, and injury. Impairments may occur at any of three levels: sensory input (vision, vestibular, proprioceptive), neural processing, and motor output (muscle activation). These impairments can lead to the partial or complete loss of the ability to walk. These disorders can greatly affect quality of life and may even be life threatening to some, especially the elderly, by increasing the risk of falls.

Prosthetics

Over one million Americans have experienced limb loss, a majority of whom are lower limb amputees that rely on a prosthetic foot for mobility (Dillingham et al. 2002). Transtibial amputees minimally expend 15% more metabolic energy than intact persons to walk at the same speed or over the same distance (Barth et al. 1992; Gailey et al. 1994; Herbert et al. 1994) and this cost is much higher for bilateral or transfemoral amputees. All groups would greatly benefit from a prosthetic limb that could improve their walking economy. Walking prostheses must also be designed to accommodate the practical needs of every-day life, which includes not only walking but also sitting, standing, climbing stairs, etc. Traditional prosthetics appear to accommodate these needs, as well as aesthetic appeal, with a relatively rigid prosthetic surrounded by a rubber skin-like material. Designs may then be modified to make them more comfortable for walking, using compliance to absorb shocks at heel-strike. The most commonly prescribed foot prosthesis in the U.S. is the Solid Ankle Cushioned Heel (SACH) foot, which is comprised of a wooden keel with a rubber wedge included at the heel. More recent prosthetic designs (Dynamic Elastic Response feet) have incorporated elasticity through the use of carbon fiber composites, to not only improve comfort but also store and return elastic energy which in theory may reduce necessary muscle work to walk. However, it is unclear how elasticity can be best incorporated into a prosthetic to improve energy economy. This limitation is clear, since amputees still expend significantly more energy than intact individuals even when walking on compliant feet. In fact, no compliant prosthetic has significantly reduced the energy requirements of gait as compared to the SACH foot (Torburn 1996, Schmalz 2002, Casillas 1995, Barth 1992). In contrast, the modeling of running as a spring-mass system has provided significant insight into the design of running prosthetics, with the result that Paralympic athletes are approaching competitive finishes with their able-bodied counterparts. We sought to develop a greater understanding of how elasticity

can be beneficially used in walking gaits and also explore energetic trade-offs that exist with this feature (Chapter 2). We also explore how the compliant modes of walking compare to those of running gaits and suggest a common framework to understand both gaits (Chapter 2). We believe the successful implantation of compliance in a running prosthesis may be similarly applied to walking.

Robotics

With proper design, adding elasticity to walking robots could greatly improve their energy economy and controllability. Many current approaches to walking robots use actuators placed at the joints to drive the limbs through prescribed trajectories, creating a walking motion but at the price of high energy and control costs (Hirai et al. 1998). On a separate path, the field of passive dynamics has produced a series of walking machines that are powered by gravity and are remarkably efficient. Building on these concepts, small amounts of actuation have been added to passive machines so that they can walk on level ground, resulting in gaits with comparable mechanical efficiency to humans (Collins et al. 2005). However, even these robots are at a disadvantage given current limits on energy storage capacity. Adding elasticity to the legs could potentially yield robots that have far superior energy efficiency over humans. While a robot could use a passive spring to perform positive and negative work with appropriate timing, a person must always use a combination of muscle and tendon to perform this work, at a significant metabolic cost. Theoretically, an elastic legged robot would require very little additional mechanical work from an actuator such as a motor if friction is kept small and the springs are properly tuned for the desired gait. We explore limits on the efficiency of an elastic walking machine and suggest methods to improve energy economy (Chapter 2).

Elasticity in walking machines could also potentially allow for more robust robotic control schemes. Rigid walkers inevitably suffer from abrupt velocity changes at the semi-impulsive heel-strike events of the step-to-step transition. These sudden changes in velocity and corresponding changes in sensor signals (as from an accelerometer or gyroscope) tend to wreak havoc on estimation control schemes that use sensory feedback to update an internal model of the system states. These errors can be reduced when only using position sensors, but then valuable velocity information may be lost. Gains on sensory feedback can be increased to allow better tracking of sudden changes in state, but this approach is limited by sensor noise and inaccuracies. By softening the impacts at heel-strike, an elastic walking robot could potentially be more robust to the tradeoffs between sudden changes in state and sensor noise. Furthermore, a machine with

compliant legs may provide terrain independence since the dynamic effects of changing terrain stiffness may be filtered out when passed through the leg spring.

Motor control

We also seek a basic understanding of the motor control principles that underlie gait. We are primarily concerned with identifying the feedback strategies used during gait and understanding how sensory information is processed for use in feedback control. Feedback strategies determine how motor commands are generated based on the perceived states of the body. Sensory processing refers to how information from sensory receptors is processed to gain knowledge of body movement.

We believe our work also has relevance for the development of detection protocols and treatments for a broad set of neuromuscular disorders that cause locomotor impairment. Identification of gait related feedback strategies could be useful for designing assistive orthotics, and locomotor and balance training regimens. The framework of state estimation to be used in this paper may explain on a systematic level how sensory information is processed for walking control and may lead to improvements in our understanding of how to treat and assist patients with sensory loss or deficits. For example, recent evidence suggests that augmentation strategies directed at providing alternate forms of sensory information may offset losses of other sensory inputs (Sienko et al. 2009). A better understanding of how sensory information is integrated during walking is needed to further develop these assist strategies. Also, the walking models to be developed in this proposal may be useful for predicting the outcomes, or expected performance of individuals with varying levels of sensory or motor impairment. These models could be used to detect early onset of a neuromuscular disease or even evaluate the effectiveness of an ongoing treatment.

Balance and Falls

Humans use visual and other sensory information to perform active feedback corrections necessary to maintain balance. Understanding of the neural and muscular mechanisms responsible for this feedback has largely been gained through the study of upright standing. In particular, the sensory contributions of vision, proprioception, and vestibular sensation to standing balance have been extensively investigated and applied in clinical practice. In comparison, the sensory roles for walking balance are not well understood, even though more than half of all falls in elderly groups occur during some form of locomotion (Blake et al. 1988; Gabell et al. 1985; Niino et al. 2000). For walking, there have been very few analogues to standing balance tests, where senses are

perturbed and the resultant balance corrections are measured (Oddsson et al. 2004; Wall et al. 2002). Furthermore, the dynamics of walking and standing are different and therefore sensory information may be used differently. Mechanical models of walking indicate that lateral balance is more difficult than fore-aft, likely the reverse of normal standing. In Chapter 4 we examine the visual contribution to dynamic balance during walking, contrasted to standing posture.

Background

From the inverted pendulum to passive dynamic walking

Bipedal walking has traditionally been studied within the inverted pendulum paradigm, where the center of mass (COM) exchanges potential and kinetic energy as the body rises and falls over a rigid stance leg. Inverted pendulum walking models are advantageous for their simplicity and provide us with a conceptual understanding of how the walking motion can be very efficient (Cavagna and Margaria 1966). While these models were useful for conceptualizing efficient stance limb behavior, they could not take a complete step. Tad McGeer was the first to bridge the gap between the energy efficient inverted pendulum concept and powered robots that could functionally walk. Inverted pendulum models did not have a swing leg and even so it was not known what control or actuation had to be added to produce a functional gait. In contrast, the current approaches to walking robots used actuators placed at the joints to drive the limbs through prescribed trajectories, creating a walking motion but at the price of high energy and control costs (Hirai et al. 1998). Taking his inspiration from gliders which maintain lift and fly under gravity power alone, McGeer examined whether the simple dynamic modes of coupled pendulums and gravity power were enough to produce a passive cyclic walking motion. He demonstrated that the natural pendulum motion of a stance and swing leg connected by a pin joint at the hip could produce a motion remarkably similar to human leg motions during gait. With the appropriate dynamic parameters he found that impact of the swing foot at heel-strike was sufficient to reset the walking cycle and produce a stable gait (McGeer 1990b) without the need for control and little energy input. Garcia et al. simplified this model further to an irreducible limit, such that the inertia of the legs converged to zero relative to that of a point mass pelvis, and demonstrated that this model retains passive stability even though the only parameter is slope (Garcia et al. 1998). Rigid legged passive walkers have not only served as important tools for studying the stability and control of walking (Alexander 1995; McGeer 1991) but have also made powerful predictions about the mechanical and metabolic cost of walking. Such models have produced substantial predictions validated by human walking experiments, such as the preferred speed-step length relationship (Kuo 2001), which is largely comprised of the cost of producing longer steps (Kuo

2002a) and cost of swinging the leg faster (Doke et al. 2005). These models have also predicted the cost of taking wider steps (Donelan et al. 2001) and suggested why humans save energy by creating a roll-over shape with their foot (Adamczyk et al. 2006).

However, even passive dynamic walking models lack the ability to reproduce basic features often measured in human walking, including a significant double support period and non-pendular ground reaction forces. Passive walkers have traditionally relied on sequential impulsive collisions, labeled push-off and heel-strike, to transfer momentum from the stance leg to the swing leg. Double-support is then modeled as an infinitesimally small event. The stance leg of these models are also rigid such that the COM moves over the stance foot as an inverted pendulum, and the leg produces force normal to the direction of movement. Consequently, the COM trajectory follows an arc of constant radii, and the stance leg performs no work on the COM during single support. Both of these features, lack of double-support and pendulum kinetics during single support, fail to resemble those of human walking.

Passive dynamics and compliance in human gait

Compared to passive dynamic walking models, human legs appear remarkably compliant. During normal walking, double-support comprises between 10% and 30% of the gait cycle (Murray et al. 1984) and the extension of the trailing leg performing push-off and compression of leading leg experiencing heel-strike experience significant overlap. Though pendular motion is significant, the limbs also perform work on the COM during single support such that the ground reaction forces and COM trajectory look different from those produced by an inverted pendulum. Since the work performed on the COM during single support cannot be explained entirely by pendulum motion, it is reasonable to assume that this work on the COM may derive from the extension and compression of legs. In fact, the effective leg length changes significantly during walking (Lee and Farley 1998) by bending of the knee and ankle joints, and compressing tissue such as the pads of the feet or cartilage in the knee. Such movement may have an associated stiffness or elasticity from active and passive muscle properties and compliance of the tendons and ligaments. The movement would also likely have a degree of damping from joint friction, padding of the foot, and motion of visceral and fatty tissue. Limb compression is advantageous because it extends the double-support period, which reduces peak impact forces during heel-strike, and allows events such as push-off to occur on a time scale over which muscle can generate force. Some of these components, especially tendons, serve as energy storage and release devices, reducing the need for muscles to produce positive work and thereby metabolic

cost (Alexander 1990). Research has shown that a significant portion of push-off work is performed by tendon (Fukunaga et al. 2001; Ishikawa et al. 2005) and it is the ankle extension in push-off that appears to be responsible for the second hump of the ground reaction force seen in normal walking (Pandy and Berme 1988).

Human walking is controlled with feedback from an array of sensory organs

Three groups of sensors are thought to have primary responsibility in locomotion as well as posture control: proprioceptors, vestibular organs and vision (Horak and Macpherson 1995). Proprioception provides the perception of movement and spatial orientation of the body segments. This sensory pathway is largely dominated by muscle spindles, which are located within muscle and are sensitive to stretch, providing direct information about muscle length and the rate of length change. Two types of vestibular organs provide information regarding movement of the head. Semicircular canals are located in the inner ear and detect angular velocity of the head by sensing the viscous motion of fluid within the canals. The otolith organs contain sets of hair cells coupled to crystal-like masses and act as linear accelerometers. Vision provides information about rotational and translational motion of the visual field relative to the head. Other visual cues such as optic flow and motion parallax also provide information about heading and orientation (Bardy et al. 1996, Warren et al. 2001).These three sensory pathways are thought to contribute to the control of walking because a wealth of studies have shown that stimulation or inhibition of the proprioceptive (Mazzaro et al. 2004), vestibular (Fitzpatrick et al. 1999, Harris et al. 2000), or visual system (Bardy et al. 1996, Warren et al. 1996, Harris et al. 2000, Warren et al. 2002) affect the stability of the walking motion and/or ability to follow a desired trajectory.

Sensory feedback is processed by a series of hierarchical motor control loops in the spinal cord, brainstem, and forebrain

More complex sensory information is used at each successive level to generate motor commands that specify more complicated aspects of the locomotion task. The lowest level of control arises in the spinal cord which is also the final pathway for all motor control signals. The spinal cord contains neuronal circuits that mediate a variety of local reflexes and rhythmic patterns which make use of proprioceptive sensory feedback. This combination of reflexive and rhythmic circuits is thought to pattern the basic walking motion, as evidenced by the fact that spinalized cats can produce stepping patterns that resemble normal walking (Lovely et al. 1986). The next level of the motor control hierarchy is in the brain stem. The brain stem partially acts as a relay center, modulating the behavior of reflexive and other spinal circuits through projections to the spinal cord, and integrating inputs from the cerebral cortex. The brainstem also contributes to the control

of more complex but automatic movements such as the control of posture and balance by integrating visual, vestibular, and proprioceptive information. The cortex is the highest level of motor control and produces highly complex movements, mostly of a voluntary nature, by projecting directly to the spinal cord and regulating circuits in the brainstem. This level is primarily responsible for initiating locomotion and anticipatory control, such as obstacle avoidance.

Sensory feedback is also weighted differently depending on task and context

Evidence suggests that humans weight proprioceptive sensory information differently during walking and standing. During normal standing, vibration applied to the various muscles of the lower leg, which activates stretch receptors, causes a significant tilt in whole body posture, whereas this stimulation causes no significant changes in the walking motion (Courtine et al. 2006). Evidence also suggests that sensory information may experience phase dependent modulation during locomotion. When galvanic vestibular stimulation was applied to subjects at either heel strike, mid-stance, or toe-off, resulting foot placement was dependent on the time when stimulation was delivered. Changes in foot placement were significantly larger at heel contact than when stimulation was delivered at mid-stance (Bent et al. 2004). Reflexes driven by proprioceptive signals also appear to be phasically modulated during the gait cycle of walking and during repetitive arm cycling (Zehr 2005).

Imperfect sensing and physical disturbances make control more difficult

Individual sensors provide incomplete information about the motion of local body segments and are subject to noise. *Sensor noise* is present due to limits on sensory precision and loss of accuracy by transmission of sensory information through multiple synapses and along axons (Kuo 2005). Sensory information is also incomplete in several regards. The sensors act as filters because they have dynamics: for example, the semicircular canals act like high-pass filters and information is lost when low frequency content is removed. The sensors may also only be sensitive to certain types of motion: for example, the otilith organs only provide information about linear acceleration and not velocity or position. Information from the otoliths is also ambiguous in the sense that they cannot distinguish between gravity and linear acceleration. Individual sensor information can also be incomplete in a global sense since information about joint movement and head movement must be combined to provide a sense of body orientation. Physical disturbances are random external perturbations that cannot be predicted or corrected for ahead of time such as experience when walking over uneven terrain. Motor output variability also contributes to uncertainty and represents random fluctuations in muscle force in response to a

motor command. We collectively refer to random physical disturbances and motor output variability as *process noise*. This sensor and process uncertainty is significant even for healthy persons and often magnified due to locomotor impairments or aging (van Beers et al. 2002, Horak et al. 1989). Control theory may offer insight into possible neural strategies used during locomotion, especially given knowledge of these uncertain conditions under which locomotion is achieved. For example, direct feedback can compensate for process noise but is not robust to sensor error. Such a control strategy would make direct use of sensory information and be highly sensitive to sensor noise or sensor conflict and even unstable when these sensor errors are large.

Feedback control can be distinguished from sensory processing

We define sensory processing as the act of combining, shaping, or filtering raw sensory signals received directly from sensory afferents with the aim of improving their quality or translating them into a more useful representation. Examples include removing noise or unwanted frequency content from sensory signals or combining sensory information from many local joints to produce some representation of whole body motion. We define feedback control as the act of using sensory information to generate motor commands in order to control the dynamic behavior of the body and create an intended motion. The distinction between sensory processing and feedback control is shown in Figure 1.2, which depicts a block diagram of our most basic understanding of how purposeful movement is accomplished with sensory feedback. In this paradigm, sensory signals from the body sensors, which are corrupted by noise, are processed or filtered by some neural components, which may have access to efference copies of motor commands. The processed sensory signals are then used for feedback control, which translates processed sensory information into motor commands. The particular feedback control strategy and type of sensory processing are selected by the nervous system based on the task at hand, external variables, and

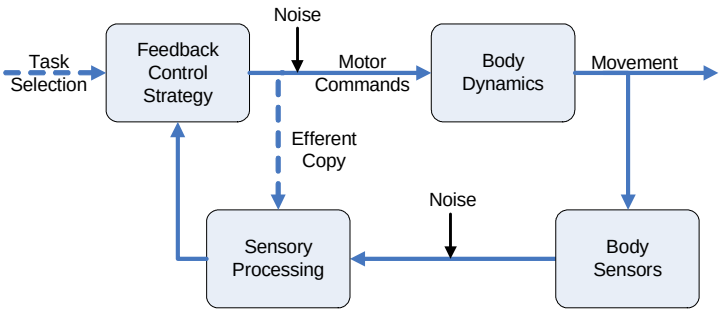

Figure 1.2. A generalized motor control diagram incorporating sensory feedback. Motor commands from the nervous system cause muscles to contract which produces movement through the body dynamics. Motion is detected by body sensors. Sensory signals from body sensors are corrupted by noise and then filtered through by some sensory processing strategy which may have access to efference copies of the motor commands. The processed sensory information is then translated into motor commands by a feedback control strategy.

prior experience. In this diagram, it is possible that no sensory processing takes place, whereby sensory signals are used directly to produce motor commands (direct feedback).

Rhythmic control of the limbs during locomotion

The presence of rhythmic pattern generating circuits located in the spinal cord has been well established in vertebrates over the past century. These circuits are thought to contribute to the basic walking motion, as evidenced by the fact that spinalized cats can produce stepping patterns that resemble normal walking (Grillner and Wallen 1985). However, over time, the role of feedback in generating these rhythms has been a point of debate. Charles Sherrington was one of the first to demonstrate that decerebrate cats could produce basic stepping motions and largely attributed these motions to reflexes (Sherrington 1911). Sherrington proposed that simple reflexes are the fundamental units of movement and that complex tasks are produced by combining these reflexes. Around the same time, Thomas Graham Brown also isolated the spinal contributions of the stepping pattern (Brown 1914). However, he found that spinalized cats could produce stepping motions even when the afferents fibers were cut, suggesting that sensory feedback was not necessary to produce rhythmic motor behavior. These two competing ideas, central versus peripheral generation of rhythmic behavior, co-existed through much of the 20th century.

By the mid-1980's research emerged that demonstrated voluntary movements and even more stereotyped movements such as walking could be completed following de-affererentation (sensory feedback channels blocked or severed) (Knapp et al. 1963, Rothwell et al. 1982, Marsden et al. 1984). From these findings emerged the concept of the motor program, a set of pre-constructed motor commands that contain the correct muscle activation sequence to complete a movement in the absence of sensory feedback. It was suggested that motor programs, and not reflexes, are the fundamental component of movement (MacKay-Lyons 2002). Today, the presence of spinal neural networks that produce rhythmic motor commands even when isolated from afferent feedback is well established for a large number of vertebrates (MacKay-Lyons 2002). For example, isolated spinal cords from neonate rats are still able to produce fictive locomotor signals even when afferent fibers are dissected (Grillner and Wallén 1985). These neural networks are generally referred to as "central pattern generators" though this naming is largely the product of studies in invertebrates where the specific pattern generating neurons can be isolated. In humans, the existence of central pattern generators is still under speculation and most of our understanding of how they apply to humans is drawn as extensions from other vertebrate models.

With the discovery of central pattern generators, emphasis shifted toward feedforward motor pattern generation and away from patterns created solely through reflexive sensory feedback pathways. However, sensory feedback is known to play an important role in normal behavior (Cohen 1992), and feedforward control alone is known to perform poorly in the presence of disturbances. Furthermore, when limb dynamics and the metabolic cost of a motion is significant, movements are also likely to be more efficient when driven by sensory feedback.

Despite our evolving comprehension of the neural components of movement, we still lack a framework to understand how sensory feedback should be processed and combined with more feedforward components to produce efficient and accurate movements. We are left with two ideas about CPGs that are seemingly at odds: 1) CPGs can produce feedforward rhythmic bursting activity even when sensory feedback is removed. 2) CPG oscillation can be entrained or modified with sensory feedback and this feedback is important for normal movement. However, modern control systems have long used an approach called state estimation to make use of feedforward and feedback behavior for processing sensory information and responding to disturbances.

State Estimation

State estimation is a method for processing sensory information whereby states of the system to be controlled are estimated by filtering sensory feedback and copies of motor command signals through an internal representation of the system dynamics (Figure 1.3). Optimal state estimation control is known to make ideal use of sensory information in the presence of both sensory and process noise. A state estimation controller is comprised of an internal, forward model that estimates system states, $\hat{x}$, and the associated sensory output, $\hat{y}$ (estimates are denoted by the hat symbol). The internal, forward model predicts the next state of a system given the current state and an efference copy of the motor command, u. The estimated states are then used to time and scale a control input, u, for feedback control. Errors in sensory prediction, e, are used to update the internal model through an estimator feedback gain, L. In the terms of human locomotion, the system states would be represented by a set of body states that describe joint motion and movement of the head, the sensory output would be represented by a set of firing patterns of the sensory organs (vision, vestibular, and proprioceptive) and the control input would be represented by a set of motor command signals sent to muscle. Under this interpretation, the estimator feedback gain, L, would represent the weighting of sensory information. This control scheme can be described by a linear set of differential equations, (1)-(4), which model the dynamics of the body, the sensors, and the estimator or internal model. Also modeled within these equations is the

effect of sensory noise, *v*, represented as random unexpected errors added to the sensory inputs, and process noise, *w*, represented as unexpected forces applied to the body. If *x* represents a vector of body states and *y* a vector of sensory inputs, *L* will be manifested as a matrix of sensory weightings. The major task when developing a state estimation controller is determining the estimator feedback gain, *L*, which determines how strongly estimation errors update the internal model of the body states. There are many control strategies for choosing *L*, but the optimal state estimator, or Kalman filter, design approach in particular has been shown to minimize the variance of the estimation error (Simon 2001). The Kalman filter was originally developed for spacecraft navigation but today is used in a great variety of controls applications.

(1) $\dot{x} = Ax + Bu + w$

(2) $y = Cx + Du + v$

(3) $\hat{\dot{x}} = A\hat{x} + Bu - L(\hat{y} - y)$

(4) $\hat{y} = C\hat{x} + Du$

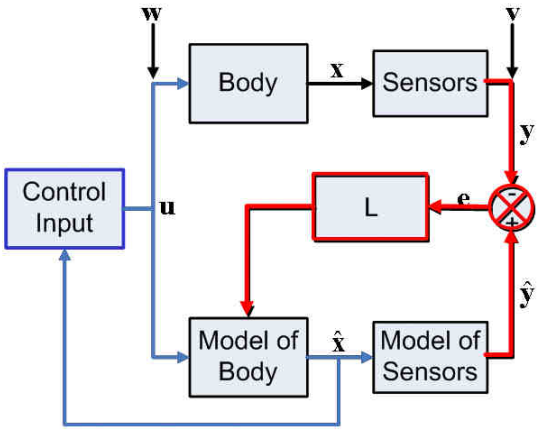

Figure 1.3. Diagram of a state estimation control scheme. A state estimation controller is comprised of an internal, forward model that estimates system states, $\hat{x}$, and the associated sensory output, $\hat{y}$ (estimates are denoted by the hat symbol). The internal, forward model predicts the next state of a system given the current state and an efference copy of the motor command, u. The estimated states are then used to time and scale a control input, u, for feedback control. Errors in sensory prediction, e, are used to update the internal model through an estimator feedback gain, L.

In this design approach, the major determinants of the sensory weightings are the stability of the system to be controlled, the level of process noise, and the level of sensor noise. Optimal state estimation control predicts that sensory weightings be larger for sensory information corresponding to unstable modes and smaller for sensory information that is noisy. Essentially the estimator feedback gain, *L*, scales the controller between feedback and feed forward control. For very large entries in the *L* matrix, the internal model will nearly exactly follow the sensed body state and the control would mimic the direct feedback controller mentioned previously. If the entries of *L* are zeros, sensory feedback would be cut off and the controller would mimic a pure feed forward controller. Intermediate choices of *L* produce a controller somewhere between these

two types of control, whereby sensory information (feedback) is filtered through an internal model of the body dynamics (feed forward).

Most importantly, state estimation control describes how sensory information from multiple sensors is processed and combined to provide information about the states of the body. State estimation does not imply how this processed sensory information is used to generate motor commands (feedback control strategy) nor what body states are used by the nervous system. It is our basic hypothesis that sensory processing is performed during locomotion in a manner akin to state estimation, where sensory information is filtered through an internal representation of the body dynamics.

Standing and Walking Balance

Scientific understanding of standing balance is extensive and guides clinical assessment of balance disorders. The unstable orientation of upright stance is known to be balanced by corrective joint torques that are generated through feedback control (Horak and Macpherson 1996; Johansson and Magnusson 1991; Peterka 2002a). Successful control must ultimately maintain the center of pressure (COP) within the base of support or else risk a fall. While a portion of this control presumably involves spinal reflexes (Allum 1983; Carpenter et al. 1999), active control must also be performed by higher centers such as the brain stem and cerebellum, where vision, vestibular sensing, and proprioception are integrated and processed for controlling the body center of mass (COM) motion relative to the support surface. These sensory channels are all known to contribute to this feedback because their stimulation elicits body sway and COP movement (see review by Peterka 2002a). The evidence also suggests that the sensory channels are weighted differently depending on the task (Cordo and Nashner 1982; Fitzpatrick et al. 1994), quality of the sensory channels (Mahboobin et al. 2005; Oie et al. 2002; Peterka and Loughlin 2004; Speers et al. 2002) and age (Peterka and Black 1990). Sensory weightings are quantified in postural experiments by perturbing the sensory inputs, such as through movement of a support platform, visual field, and galvanic stimulation, and measuring resultant balance corrections, such as changes in COP, kinematics, or muscle activity. Such research has contributed to the development of quantitative clinical measurements for assessing sensory and balance deficits. Perhaps the best known is computerized dynamic posturography, which selectively removes or renders inaccurate vision and ankle proprioception and quantifies postural responses. The test data can be used to objectively identify and distinguish a variety of sensory and motor impairments that affect balance control. This tool is useful for the diagnosis of vestibular

disorders, since these patients are generally unable re-weight visual sensory channels (Peterka 2002a; Peterka and Benolken 1995). Not only are different sensors weighted differently, but even a single modality such as vision can contain multiple attributes that may themselves be weighted differentially (Streepey et al. 2007a). Vision is sensitive to multiple directions of visual field motion (Movshon et al. 1985), and the importance of these directions may depend on the dynamics of the task or the degree of feedback stabilization that must be provided by the central nervous system.

The sensory contributions to walking balance have been less significantly explored and it is unclear as to what outcomes should be measured to assess this balance. As in standing, the inverted pendulum motion of the head, arms, and torso (HAT) must be stabilized (Winter 1995) and oscillations of the visual field are known to induce upper body sway during walking (Bardy et al. 1996; Warren et al. 1996). Posture control is likely coupled with gait frequency (Kay and Warren 2001), however, it is unclear to what degree HAT dynamics affects whole-body walking balance. Foot placement may be more important since dynamic balance is minimally achieved by redirecting the motion of the whole body COM as support is transferred from one leg to another. The location of the swing foot at heel-strike significantly affects this redirection (Donelan et al. 2001; Kuo et al. 2005; McGeer 1990b). However, sensory weightings for walking balance measured from foot placement are difficult to isolate because foot placement can be used to steer, adjust speed, and balance the body. Galvanic stimulation (Bent et al. 2004; Jahn et al. 2000), muscle vibration (Courtine et al. 2007), and shifts of the visual field (Jahn et al. 2001) cause subjects to veer away from an intended straight path. In these cases one cannot assign these outcomes to balance corrections or the adjustment of heading or speed. To isolate the effect of foot placement on walking balance, an experiment must ensure that subjects do not significantly change heading or average speed over time. Typically, therapists must rely on functional measures of walking performance, such as ability to walk with narrow step widths, with eyes closed, or while rotating the head back and forth, to qualitatively assess walking balance. Other functional tests such as a 5m timed-up-and-go test (TUG) and Dynamic Gait Index (DGI) are useful for assigning a measureable score and are significantly correlated with risk of falling in elderly groups (Morris et al. 2007; Whitney et al. 2004). However, there has been no clinical analogue to the dynamic posturography test to quantitatively assess the sensory contributions related to walking balance. If the sensory requirements for walking are very different from standing, diagnosing sensory balance impairment solely based on standing tests may be incomplete.

Mechanical walking models and human walking studies show that dynamic stability may be different from postural stability, and that implies visual and other sensory contributions may be different. Two-dimensional passive walking models can walk down an incline without active control of foot placement. In these models, the combination of pendulum limb behavior, collisions, and gravity power are sufficient to produce stable, periodic walking motions resembling human gait. These models suggest that the passive properties of the limbs may largely dictate and stabilize the basic stepping pattern in the sagittal plane (McGeer 1990b) and that the nervous system need only supply energy and support body weight. Three-dimensional passive walking models (see Figure 1a) retain passive stability in the anterio-posterior (AP) direction but are unstable in the medio-lateral (ML) direction (Kuo 1999). Some degree of high level active control would therefore necessary to balance lateral but not sagittal motion. In the frontal plane, active control of lateral balance would likely involve visual and vestibular sensation and the integration of these sensory inputs with proprioception in higher centers such as the brain stem and cerebellum. Experiments in human subjects suggests that the lateral walking motion is stabilized by lateral foot placement or adjustment of step width (Dean et al. 2007b; Donelan et al. 2004b) and that vision is used for guiding this foot placement (Bauby and Kuo 2000a). In the sagittal plane, passive stability of foot placement could be gained indirectly by reflexive and rhythmic circuits in the spinal cord which make use of proprioceptive sensory feedback to support body weight and supply energy to the gait.

Such stability contrasts with normal standing, which is unstable and requires high level neural control in both the ML and AP directions. However, empirical evidence indicates that standing is more unstable in the AP direction (Anand et al. 2003; Marigold and Eng 2006). Standing stability may be altered with changes in foot placement configuration. The tandem or Sharpened Romberg stance, where the feet are placed heel-to-toe, is likely to have reversed directional stability. In this case, the AP direction, which now has a much larger base of support is the more stable direction compared to the ML direction, which has a reduced base of support.

Aims

This thesis will use passive dynamic principles to study motor control schemes that pattern and supply energy for the basic walking motion and stabilize walking balance through corrective foot placement. We will represent these specific aspects of the walking task with reduced dynamic walking models. These walking models are complicated enough to produce specific features of the walking task but simple enough that feedback rules can be generically represented. In the case of generating the rhythmic walking motion, we use a simple model with legs that extend and compress like linear springs to reproduce and study the major features of sagittal plane walking motions (Chapter 2). We then compare walking and running gaits produced from the same model and offer insight into how these dynamic modes are differentially produced (Chapter 3). We also show that a state estimation scheme can be used to explain sensory processing within control loops responsible for generating this basic walking pattern (Chapter 4). To represent the balancing task of walking, we will use a simple 3D passive walker which maintains balance through active lateral foot placement. We demonstrate that visual sensory information is weighted based on predicted requirements of active stabilization by applying low frequency visual perturbations to human subjects during treadmill walking (Chapter 5).

Chapter 2. Passive Dynamic Walking on Axial Compliant Legs

Abstract

Rigid legged walking models cannot reproduce basic features observed in human gait, such as a smooth COM trajectories and significant duration of the step-to-step transition. These models also cannot account for the timing and amount of work performed by the legs during gait. We analyze a simple passive bipedal model that uses axially compliant legs to gain these features. The addition of springs at the end of the legs results in a smoother walking motion with a finite double-support period where positive and negative work occurs simultaneously. A variety of walking and running gaits can be produced by varying a two stiffness parameters and adjusting initial conditions. The total mechanical energy of the model is closely correlated with speed and leg and hip spring stiffness parameters can be used to tune the stance and swing periods, respectively. Analysis of model stability reveals that there are three neutrally stable modes and one critical mode that is unstable when gaits demonstrate symmetry. Dissipation and leg mass stabilize non-symmetric walking gaits but requires an energy source to replace dissipated energy. Arcs added to the feet reduce this cost and are necessary to extend the speed range of walking gaits beyond 1.4 m/s. For a model with arc feet (radius 30% leg length), moderate damping (damping ratio = 0.1), and an anthropomorphic mass distribution of the legs, the cost of transport is only 20% that of a human, suggesting that an elastic walking robot could gain stability at low energetic cost. Assuming that positive work done by the leg springs is analogous to active work performed by muscle, we show that the cost of performing work on the center of mass over a step is similar to measurements recorded in human walking. At normal walking speed, the model was able to predict the work performed during the push-off and collision phases within 8% and 2%, respectively. Push-off and heel-strike work can be minimized by 18% with choice of an optimal overlap of the push-off and heel-strike phases, suggesting that gait parameters such as duty factor can be tuned for energetic economy.

Introduction

Inverted pendulums and passive dynamics

Bipedal walking has traditionally been studied within the inverted pendulum paradigm, where the center of mass (COM) exchanges potential and kinetic energy as the body rises and falls over a rigid stance leg. Inverted pendulum walking models are advantageous for their simplicity and provide us with a conceptual understanding of how the walking motion can be very efficient (Cavagna and Margaria 1966). Passive dynamic walking models further expanded this concept by adding a dynamic swing leg to the inverted pendulum. McGeer demonstrated that passive pendular motion of a stance and swing leg and impulsive collisions at heel-strike are sufficient to reset the walking cycle and produce a stable gait (McGeer 1990b). Passive models have also proven to be useful for making testable predictions about the energetics and control of walking (Kuo 2001).

Rigid legged models, however, fail to produce a significant double support period or account for the timing and amount of work performed by the legs during a step. Passive walkers have traditionally relied on sequential impulsive collisions, labeled push-off and heel-strike, to transfer momentum from one rigid leg to another. Double-support is then modeled as an infinitesimally short event. Given a rigid stance leg the COM moves over the stance foot as an inverted pendulum, and the leg produces force normal to the direction of movement. Consequently, the COM trajectory follows an arc of constant radii, and the stance leg performs no work on the COM during single support. Both of these features, lack of double-support and pendulum kinetics during single support, fail to resemble those of human walking. Adding degrees of freedom (DOF) to these models seems to be the obvious approach in order to achieve these features but may obscure conceptual understanding if the model becomes too complex. The question remains: Can we add features to rigid legged models and gain human-like kinematics and kinetics and still retain a conceptual understanding of how the model produces these features?

Leg dynamics of human gait

Compared to passive dynamic walking models, human legs appear remarkably compliant. During normal walking, double-support comprises between 10% and 30% of the gait cycle (Murray et al. 1984) and the positive work produced during push-off and negative work during heel-strike experience significant overlap (Kuo et al. 2005). Though pendular motion is significant, the limbs also perform work on the COM during single support such that the ground reaction forces and COM trajectory look different from those produced by an inverted pendulum.

Since the work performed on the COM during single support cannot be explained entirely by pendulum motion, it is reasonable to assume that this work on the COM may derive from the extension and compression of legs. In fact, the effective leg length changes significantly during walking (Lee and Farley 1998) by bending of the knee and ankle joints, and compressing tissue such as the pads of the feet or cartilage in the knee. In terms of developing a more human-like walking model, this knowledge suggests that it makes sense to include leg compression.

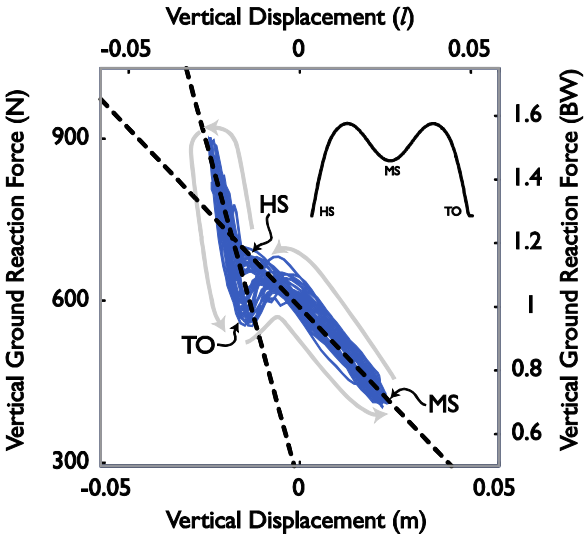

Figure 2.1. Elastic behavior of the leg can be approximated by viewing the vertical ground reaction force in comparison to leg extension/compression (representative subject data for 10 steps at 1.25 m/s). The slope of this curve at a time point represents the instantaneous vertical stiffness. The force-displacement relationship is approximately linear in the separate phases of double and single support. The double support period is roughly twice as stiff as the single support period. Time points of heel-strike (HS), mid-step (MS), and toe-off (TO) are marked on subject data and cartoon inset of vertical force w.r.t time over a period of ground contact.

Experimental data suggests that it may be reasonable to approximate leg behavior with a single leg stiffness parameter. Rather than modeling individual stiffness or muscle force at each joint, a single global leg stiffness can be used to characterize the interaction of the force produced by the legs and the movement of the center of mass (Holt et al. 2003). This global leg stiffness becomes apparent upon viewing the relationship between vertical ground reaction force and vertical displacement of the center of mass (Figure 2.1) during normal walking. A linear relationship between these variables was originally used to justify modeling running as a spring-mass system (McMahon and Cheng 1990). In walking there appear to be two regions that demonstrate a linear relationship between force and displacement, which coincide with the double and single support phases. The double support phase appears roughly twice as “stiff” as the single support phase which is reasonable for two leg springs approximately in parallel. Perhaps the best justification for using a single leg spring to model leg actuation is knowledge that a model with linear elasticity along the leg already works well for running (McMahon and Cheng 1990). Since the same mechanical system (the leg) is used by

humans for both walking and running, it seems reasonable to also model walking with compliant legs.

We propose that adding leg extension/compression features with an associated stiffness to previous rigid legged walkers will produce gait features that more closely resemble those of human walking. While real legs are made up of both active (muscle) and passive (tendon, ligament, etc.) components, we will approximate the global behavior of the legs as that of a passive linear spring. Indeed, several attempts at modeling parts of the walking cycle indicate that human-like movements and forces are produced by adding elasticity to the legs (Alexander 1992; Geyer et al. 2006; Siegler et al. 1982). However, these models all prescribed aspects of the walking motion in some way. For example, Alexander's model of compliant walking prescribed the force profile under feet. The axial legs in this model then only acted to filter the interaction of the force profile and center of mass. The model of Geyer et al., produces a robust space of walking and running gaits by modifying only three parameters. However, this model does not incorporate swing leg dynamics and sets the angle of attack of the leading leg at heel-strike. Incorporating this type of control in a walking robot would require high-gain feedback to accurately target the angle of attack at each heel-strike. Humans do not appear to use end point control to fix the angle of attack, as will be later shown in Chapter 4. We believe that incorporating swing leg dynamics are beneficial for exploring what minimal level of control is necessary to achieve a walking gait. Actuation can be simply added to the hip in the form of a passive torsional spring which speeds up the natural motion of the legs (Kuo 2002a). By modeling the motion of the swing leg and treating the torsional stiffness as a model parameter we can create a mechanical cost function for forced leg swing (Kuo 2001) and examine how speeding up the oscillation of the swing leg affects gait parameters.

We seek to determine whether the walking motion can be completely determined through the interaction of elasticity and passive dynamics. Analysis of this model will incorporate parameter studies, stability analysis, and work principles relating to energetics in order to gain a better understanding of the principles governing biped walking. Foremost, we are interested in understanding how the addition of elasticity within the passive dynamic walking framework will allow a more faithful representation and understanding of human walking.

Methods

Model

We present a compliant walking model that is capable of closely approximating a variety of gaits by varying a small number of model parameters and initial conditions. The compliant dynamic biped walking model (Figure 2.2) is comprised of a point mass at the hip, two legs with mass and rotational inertia and mass-less arc feet. Axial springs are located between the legs and feet and a torsional hip spring connects the two legs. All of the mass in the model is assumed to be above the legs' axial springs. As should be expected from other compliant walking models (Alexander 1992; Geyer et al. 2006), our model is capable of producing a wide-variety of locomotion gaits, including walking and running, simply by varying the initial conditions and model parameters of the gait. As will be demonstrated, the type of gait and gait parameters, such as speed and step length, determine the energetic and stability properties of a movement cycle. Our analysis will focus attention on the dynamics of the model with small leg mass and point feet, but we will consider parametric effects of adding inertia and dissipation to the legs. We will further focus on results from the analysis of walking-like motions and will refer to similar analysis for running gaits. The following chapter will broaden our analysis to an array of gaits including running and skipping.

The generic model has 6 degrees of freedom, and therefore 6 position states and 6 velocity states, as well as 7 physical parameters to be varied. The position states are x, the horizontal location of the pelvis, y, the vertical location of the pelvis, θ_{st}, the angle of the stance leg with respect to vertical, θ_{sw}, the angle of the swing leg with respect to vertical, δ_{st}, the extension of the stance leg, and δ_{sw}, the extension of the swing leg. At minimum, the model requires only two physical parameters; the stiffness of the leg spring, K_{leg}, and the stiffness of the hip spring, K_p. This simplification results when the inertia of the legs is assumed to be very small compared to the inertia at the hip. In a human, the leg stiffness represents the average stiffness of the stance limb during ground contact. The hip stiffness is representative of the average effort about the hip to force leg swing. Other physical parameters also considered include: M_p, the mass of the pelvis; M_t, the mass of the legs; I_t, the rotational inertia of the legs; c, the distance along the leg between the foot and leg mass center; and r, the radius of the foot. Finally, to consider the consequences of dissipation, we also added damping to the leg springs, with damping ratio ζ. To balance energy lost to dissipation, we added two sources of energy input: potential energy in the form of a slope γ, and a thrust coefficient, r_t, that pumps energy into the leg springs in the second half of the

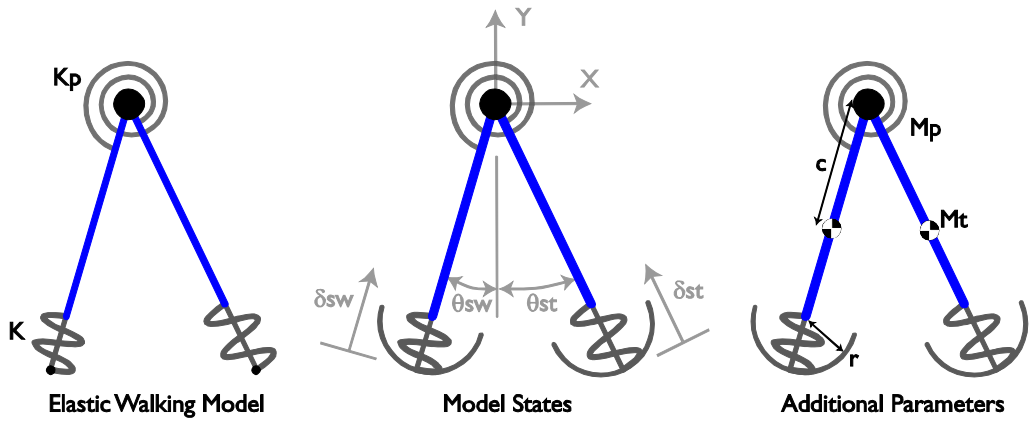

Figure 2.2. The compliant passive walking model has six degrees of freedom (middle): the angle of the stance and swing legs, θ_{st} and θ_{sw}, the displacement of the axial leg springs, δ_{st} and δ_{sw}, and the horizontal and vertical location of the pelvis, x and y. The model also has seven physical parameters (left): axial leg stiffness, K_{leg}, torsional hip stiffness, K_p, (right): mass of the pelvis, M_p, mass of the leg, M_t, rotational inertia of the legs, I_t, the distance along the leg between the hip and leg mass center, c, and the radius of the foot, r. When the leg inertia and radius of the foot are made irreducibly small (left), the model is greatly simplified and only has two physical parameters, K_{leg} and K_p

contact period. All parameters and states are non-dimensionalized by total mass, m, leg length, l_o, and the gravitational constant, g.

Our model combines the features of previous rigid anthropomorphic passive walkers (McGeer 1990b) with the added feature of elastic leg extension and compression. It should also be noted that our model is very similar to the model used by McGeer to describe passive dynamic running (McGeer 1990b), with the added capability of simulating simultaneous contact of both feet (double support) and generic transitioning between contact phases. If the mass and rotation inertia of the legs are made irreducibly small (for limit as mass approaches zero), the model converges to a compliant version of the simplest walking model (Garcia et al. 1998).

We found that gaits are not unique for a given set of stiffness parameters. If speed is fixed, there are a finite number of different walking and running gaits. Allowing speed to vary, there are an infinite number of fixed point solutions, across a range of speeds. In previous rigid legged models, the gait speed was determined by an energy balance between that lost during the heel-strike collision and energy added by a slope or impulsive push-off. With small leg mass and conservative leg spring behavior, this energy balance is implicitly achieved and thus elastic gaits exists over a range of speeds. Energy is conserved because the heel-strike collision axial to the

leg transfers energy safely to the leading leg spring and negligible energy is lost from the impact of the small leg mass in a direction normal to the leg. To narrow our analysis and find unique gait solutions, we chose to add an additional parameter, the overall mechanical energy of the model, E, which will be shown to closely correlate with speed. This parameter sets a bound on the available initial conditions for a set of stiffness values, with the result that only two walking gaits exist for a given set of parameters, a symmetric and an asymmetric walking gait. As will be explained later, these gaits have very similar initial conditions but very different stability properties. Symmetry simply implies that the motion of the gait looks the same whether viewed forwards or backwards in time. Since a stance leg transitions to swing by smoothly leaving the ground (toe-off), symmetry requires that the transition from swing back to stance mirror toe-off and also be smooth (non-impulsive). As was found for a passive bipedal runner (McGeer 1990a), symmetric gaits conserve energy, even with significant leg mass. When adding dissipation to the model, symmetric gaits disappear, but asymmetric gaits still exist.

A reduced model is used when simulating single and doubles support phases. The 12 model states (6 position, 6 velocity) reduce to 8 and then 4 independent states as ground contact constraints are applied when one and two feet are on the ground, respectively. The number of independent states is reduced further by the condition that a leg spring is locked when that leg is off the ground. Therefore, there are 6 independent states during single support and 4 independent states during double support. The initial conditions of a step, which occurs at the beginning of double-support, are therefore fully described by the four states, $[\theta_{st}\ \theta_{sw}\ \dot{x}\ \dot{y}]$. These states are similar to those used to describe the initial conditions of a spring-mass runner, with the added state, θ_{sw}, to describe the position of the swing leg (McMahon and Cheng 1990). While these initial state variables are useful for visualizing the rectilinear movement of the COM, we found that another set of initial conditions, $\left[\theta_{st}\ \theta_{sw}\ \dot{\theta}_{st}\ \dot{\delta}_{st}\right]$ are more useful for interpreting the resultant eigenvectors from stability analysis and comparing the relative amounts of spring-mass and inverted pendulum-like behavior.

Simulation

Differential equations describing the motion of the compliant legged model were created using the Dynamics Workbench, an equation of motion generator developed by Art Kuo. The state vector, *x*, is comprised of the position states, *q*, and velocity states, *u*,

$$x = \begin{bmatrix} q \\ u \end{bmatrix} \tag{1}$$

where $u = \dot{q}$. The differential equation describing the motion of the system is simply

$$\dot{x} = \begin{bmatrix} u \\ \dot{u} \end{bmatrix} \tag{2}$$

where $\dot{u}$ is given by

$$[M] \cdot [\dot{u}] = [F] \tag{3}$$

In Equation 3, *M* is a mass matrix that represents the spatial distribution of the mass of the model and *F* represents conservative force components such as gravity and spring forces. The equations of motion are listed in the Matlab code in Appendix 2.2. While these differential equations as a whole may appear complex, they simply describe the movement of a system of coupled pendulums bouncing on a spring. The portion of the EOM associated with the force produced by the spring was modified to add damping. The damping coefficient, *B*, will be determined based on the damping ratio, ζ, of the mass spring system and the leg stiffness (Equation 4).

$$\zeta = B / \sqrt{4\, K_{leg}} \tag{4}$$

The presence of leg springs also introduces a mechanism by which to perform some level of active control, whether by feedback, feedforward, or a combination of the two, and thereby maintain a steady walking pattern and speed when damping and large physical disturbances are present. By controlling the set point of the leg springs, energy can be added to or removed from the system, thereby compensating for energy fluctuations from disturbances and damping. The set point may be adjusted to add energy by increasing it in proportion to the stance leg angle in the second half of the gait cycle (Equation 5). The proportional constant, r_t, will be labeled the ratio of thrust, as in (McGeer 1990a).

$$\delta_0 = \begin{cases} -r_t \cdot \theta_{st}\,, & \theta_{st} \le 0 \\ 0\,, & \theta_{st} > 0 \end{cases} \tag{5}$$

Real-time control of the leg spring stiffness could also serve as a means of active control but will not be explored here. With combined damping and stance thrust, the new stance leg spring force will be calculated by Equation 6 with the trailing leg spring force calculated similarly during double support.

$$F_{st} = -K_{leg} \cdot (\delta_{st} - \delta_0) - B \cdot \dot{\delta}_{st} \tag{6}$$

Walking simulations were developed to integrate the equations of motion, handle discrete events such as heel-strike and toe-off, and apply a smooth or impulsive transition to the next continuous phase. For example, when the force produced by the trailing leg falls to zero during double-support, the model recognizes a toe-off event and smoothly transitions to single support, applying a ground contact constraint for the stance leg and locking the swing leg spring in place. It is important to note that we do not prescribe an order for which the gait events must occur, a method typically used t constrain possible gaits produced by a model. During single support, the stance leg force may fall to zero, initiating a smooth transition to a flight phase or the swing leg may contact the ground, in which case the simulation will solve for an impulsive collision with the ground, and then transition to double support.

Repeatable gaits or limit cycles were found using a first-order Newton shooting method, which linearizes the step-to-step function, *f(x)*, about an initial guess for the fixed point. The step-to-step function calculates the model states at the end of a step, x_{k+1}, given the initial condition states at the start of a step, x_k (Equation 7). This function is determined by simulating the model dynamics (integrating the equations of motion) through an entire step (from heel-strike to heel-strike). A limit cycle is achieved if there is an initial condition, *x**, such that Equation 8 is satisfied, in which case *x** is labeled a fixed point. The step-to-step transition function is linearized around the fixed point (Equation 9) through a first order Taylor expansion. By substituting Equation 7 into 9, we can solve for matrix A (Equation 10), which is the Jacobian of the step-to-step function. This Jacobian is then directly used in a shooting method to reduce the error between x_k and x_{k+1} to zero. To find a fixed point solution, the Jacobian is computed iteratively until convergence. Similar root finding methods were used to adjust the model parameters to find gaits with specific speed, step length, and duty factor parameters. We only report gaits for which a limit cycle could be found but did not exclude gaits based on any stability requirement. Unstable gaits were previously excluded from the gait analysis of a similar compliant walking model (Geyer et al. 2006). We believe this restriction likely limits a significant parameter space of viable gaits.

$$x_{k+1} = F(x_k) \qquad (7)$$

$$x^* = F(x^*) \qquad (8)$$

$$x_{k+1} \approx F(x^*) + \frac{\partial F(x)}{\partial x}\Big|_{x^*}(x_k - x^*) \qquad (9$$

$$\Delta x_{k+1} \approx \frac{\partial F(x)}{\partial x}\Big|_{x^*} \cdot \Delta x_k = A \cdot \Delta x_k \qquad (10)$$

Typically, these search methods are rather sensitive to the initial guess condition, and a bad guess can prevent a solution from ever being found. Experience has given us the following rule of

thumb to find an initial estimate. It is usually adequate to step ahead to the time period at the middle of double support and assume a rough symmetry. Then, $\dot{x}$ can be set to the desired forward gait speed, $\dot{y}$ to zero. The leg angles, θ_{st} and θ_{sw}, can be of equal and opposite magnitude and set by the desired step length, s, such that $\sin\theta_{st} = s/1.9$. From there, one can forward simulate the rest of the step to recover a plausible set of initial conditions after heel-strike. The initial conditions can then be used with the Newton shooting method.

The dimensionality of the system can be further reduced by choice of energy and symmetry constraints. Though 4 initial states are necessary to define the conditions at the beginning of a step, we need only search through three states to find new gaits when energy, E, is assumed to be fixed. Given the initial states, θ_{st} , θ_{sw}, and $\dot{y}$, the gravitational and elastic potential energy and vertical kinetic energy may be calculated. With total mechanical energy fixed, we need only assume the remaining energy to be horizontal kinetic energy to solve for $\dot{x}$. The search space is further limited to two states when searching for symmetric gaits, in which case $\dot{y}$ is known to be zero at the middle of double support.

The eigenvalues of the Jacobian matrix can also be used to assess the local stability of a limit cycle. In relation to walking balance, the most general definition of stability describes the ability to "not fall down" when moving through an environment of disturbances. This stability is presumably obtained by actively rejecting disturbances and imbalances through neuromuscular control. However, this definition allows no quantitative description of stability and is only assessed after failure has already occurred. We will quantitatively describe stability by calculating the local asymptotic stability of the passive dynamic walking models used in this paper. Local stability refers to the ability to reject small disturbances, or disturbances that don't move the model very far from the state about which the stability was calculated. The eigenvalues of the Jacobian matrix are used to describe this local stability of a gait about the fixed point. The eigenvalues provide information about the factor by which a perturbation grows or decays at the next step. An eigenvalue with magnitude less than unity suggests that a perturbation shrinks over successive steps and indicates stability. An eigenvalue greater than one suggests that the perturbation will grow with each step and will eventually cause the model to fall down if it is not attracted to a nearby stable gait. This stability measure is useful for suggesting where active control would be needed to stabilize unstable modes against small disturbances.

Results

Axial leg compliance makes model dynamics more human-like

We found that the addition of springs at the end of the legs results in a smoother walking motion with a finite double-support period and characteristic ground reaction. We first searched for a walking gait that had typical gait parameters found at normal walking speeds (speed = 1.25 m/s (0.4), step length = 0.69 m (0.69), duty factor = 0.60; nominal units (dimensionless units)) and found a symmetric and non-symmetric gait for these parameters. These gaits will from now on be referred to as the 'nominal' gaits. We used known initial conditions from the simplest walking model of Garcia et al. at the same speed and step length as a starting point. Details of the model parameters and initial conditions of these gaits are provided (Table 2.1) along with a depiction of the motion of the model while walking over a complete stride (Figure 2.3). Without directly comparing these motions with actual human data, at first glance we note that several features appear that are qualitatively similar to observed human walking gaits: 1) The COM motion is smooth and continuous, 2) The stance not leg does not remain rigid while supporting body weight during single support, 3) Support is transferred from one leg to another over a significant portion of the gait cycle, i.e. double support does not occur instantaneously, 4) The vertical ground reaction forces are characteristically double peaked.

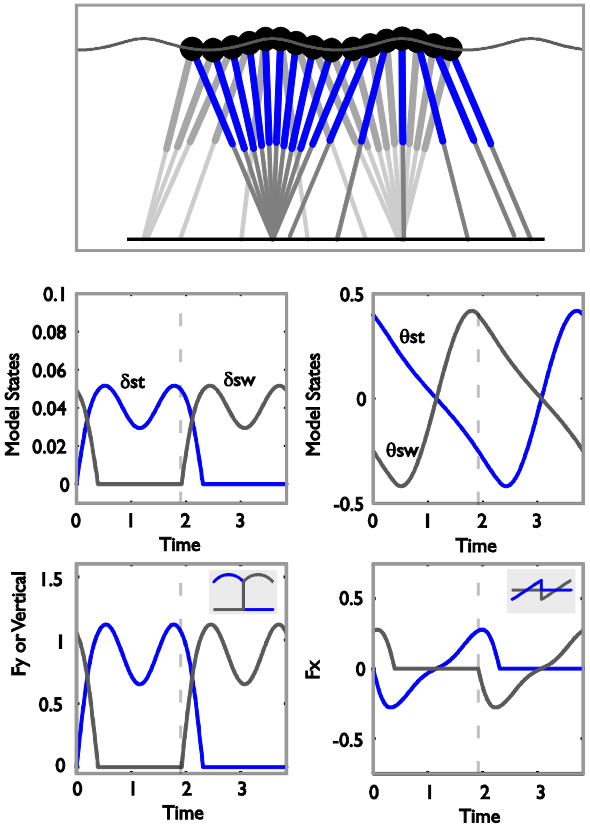

Figure 2.3. Model kinematics and ground reaction forces for a nominal walking gait at 1.25 m/s. As seen from the cartoon (top), the COM motion smoothly oscillates up and down as the limbs continuously swing back and forth. The model states (middle) reveal a similar story, where the legs switch between inverted pendulum and pendulum behavior in the stance and swing phases, respectively. The COM also exhibits spring-mass behavior along the direction of the leg. Ground reaction forces (bottom) exhibit a characteristic M-shape in the vertical direction and Z-shape in the horizontal direction. Inset are similar force traces produced from a rigid legged walking model for comparison.

Table 2.1. Model Parameters of Nominal Gaits

	E	K_{leg}	K_p	r
Symmetric Model Parameters	1.05	22	3.96	0
Non-symmetric Model Parameters	1.05	22	4.54	0

	Speed	Step Length	Duty Factor (Double Support)
Model Gait Parameters	0.40	0.69	0.60 (0.20)
Dimensional Gait Parameters	1.25 m/s	0.69 m	0.60 (0.20)

We define the start of the walking cycle as the time point immediately after the leading foot touches the ground and becomes the new stance leg, marking the beginning of double-support. During double-support, the velocity of the COM is directed upward as the trailing leg spring extends, performing positive work, while the leading leg spring contracts and performs negative work. Double-support ends and single support begins as the trailing leg leaves the ground, determined by the conditions that take-off occurs when the trailing leg force vanishes. During single support, the trailing leg swings from the hip as a pendulum. During this time, the hip moves over the stance foot as an inverted pendulum while also bouncing on top of the stance spring. Since the legs are relatively close to vertical during normal walking, the bouncing motion or displacement of the leg spring largely resembles the characteristic double-humped shape of the vertical ground reaction forces seen in normal human walking. Both single support and the step end when the swing leg makes contact with the ground ahead of the stance foot. A stride is complete after one more step where the model returns to the original configuration at the first heel strike. It should be noted that we neglect the fact that the swing leg moves through the ground at the middle of single support. This is an acceptable allowance considering that adding knees would eliminate this problem without the need for additional control (McGeer 1990c).

Compliant walking gaits are defined by speed, step length, and duty factor

While gaits of previous rigid legged models have been fully defined by speed and step length, the compliant model also requires some description of the amount double support to sufficiently describe a unique gait. We define the double support period as the fraction of a step for which both legs are in contact with the ground. In this paper, we use duty factor to describe the amount of leg contact because it will be later useful for also describing running gaits. Duty factor is

defined as the fraction of a stride over which the stance leg contacts the ground and is related to the fraction of double support (Equation 11).

$$T_{ds} = 2 \cdot T_{df} - 1 \tag{11}$$

A duty factor greater than 0.5 implies a period of time exists when both legs are in contact with the ground. A duty factor less than 0.5 implies that a period of flight occurs between successive leg contacts. Increasing duty factor past 0.5 generally results in a greater percentage of positive work from push-off and negative work from heel-strike that are performed simultaneously.

Compliant walking model reproduces timing and shape of human kinetic traces over a step but over-exaggerates amplitudes

While modeling the legs with elastic compliance generally produces features resembling a walking gait, it remains to be seen how well the model approximates the actual kinetics measured during human walking. More specifically, we ask whether adding a spring in series with a rigid leg will produce accurate ground reaction forces (matching well with human data) and if not, what additional model features are necessary to improve the approximation. Correlation between kinematics measured from human data and those measured from the model is a simple way to evaluate the power of our simplification that global leg behavior during walking can be well approximated by a simple linear spring.

We compared the ground reaction force and individual limb COM work rate curves (Figure 2.4) produced by the compliant walking model with published averaged human walking data (Donelan et al. 2002a). Both curves reflect the effort produced from an individual leg over a stride. We measured the rate of work performed on the model COM by each leg using the individual limbs method (Donelan et al. 2002b), defined as the vector dot product of each leg's ground reaction force against the COM velocity. We used the nominal gait with a speed of 1.25 m/s, step length of 0.69 m, and duty factor of 0.6, to compare with human walking data at 1.25 m/s, step length of 0.70±0.03 m, and approximate duty factor of 0.6. The ground reaction forces produced in simulation appear to match the qualitative features of the human forces, most notable producing a double-humped pattern on the vertical ground forces. The vertical forces of the springy walker show a much larger difference between the maximum vertical force and the vertical force at mid-stance than the human data, resulting in larger excursions of the center of mass, as also observed in Geyer et al. Comparing the horizontal forces, the model again qualitatively matches the human shape profile with negative force in the first half of stance and positive force in the second half but again over-exaggerates amplitude.

We also discovered that compliant legs individually perform work on the COM similarly to humans during normal walking. The model, like humans, produces the four distinct phases of COM work: collision, preload, rebound, and push-off. The collision phase begins after heel-strike, when the leading leg accepts the weight of the body while compressing, thus performing negative work on the COM. In the first half of single support the leg extends under load, producing positive work in rebound. In the second half of single support, the leg again compresses under load, performing negative work in preload. Finally, just before heel-strike and throughout double support, the trailing leg lengthens as it releases the load of the body, producing positive work in push-off. The COM work performed in each of these phases can be found by calculating the area under the instantaneous COM work rate curves over the time period of each phase. In previous rigid legged models, the total negative work performed on the COM was equal to the negative work performed during the collision. For the compliant model, and human walking, the total negative work is the sum of the negative work performed during collision and preload. Likewise, the total positive work is the sum of the work performed in rebound and push-off. Accounting for the additional work performed during rebound and preload may be important when using the model to predict how metabolic cost might change across different gaits. However, like the ground reaction forces, the COM work curve of the model shows much greater excursions about zero than does the human data. These excursions, basically the bouncing up and down of the COM on the stance spring, would likely match the human data better if the springs had damping and other features such as significant leg inertia added to the model. However, we first explore the simple solution of increasing the arc radius of the foot from zero (point foot).

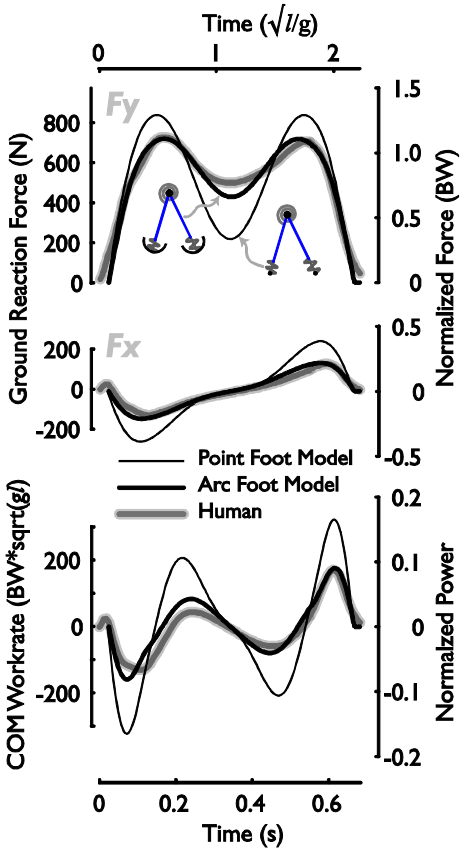

Figure 2.4. Comparison of ground reaction force and individual limb COM work rate curves from averaged human subject data at 1.25 m/s (Donelan et al. 2002a) with those produced from two elastic models at the same gait parameters. Compared are reduced elastic models with point feet and arc feet of radius 0.3. Model curves show strong correlation with human data but adding an arc foot greatly improves the correlation of the model and human data.

Arc feet increases the comparison with human kinetics

Simple passive dynamic walking models predict that redirection of the COM velocity during double support requires step-to-step transition work which decreases quadratically with increasing arc radius of the foot. Work requirements decrease with increasing radius because the distance between the points of contact of the leading and trailing leg during double support decreases with radius, reducing the angle through which the COM velocity must be redirected. An extreme example occurs when the radius of the foot equals leg length. In this theoretical case, no work is required to redirect the body at heel-strike because the body transitions between continuous modes of rolling. Experimental work in our lab tested this hypothesis by attaching rigid arc shapes of various radii to the bottoms of rigid boots worn by human subjects (Adamczyk et al. 2006). They found that mechanical work performed on the COM did decrease by a quadratic power law for increasing arc radius. The net metabolic work rate also decreased with increased arc radius to a minimum of 0.30 (expressed as a fraction of leg length) and then increased for larger radii. This metabolically advantageous radius of 0.3 was also previously found to be produced as an effective 'roll-over shape' of the knee-ankle-foot in human gait (Hansen et al. 2004).

With sufficient experimental justification, we added an arc radius of 0.3 to the model and searched for gaits that again matched the speed, step length, and duty factor of the average human data. Remarkably, adding a significant radius to the feet was sufficient to drastically reduce the excursions of the force and power traces (Figure 2.4). For example, the point-foot version produced 75% more work during collision than the average human subject. By adding arcs to the feet the collision worked dropped to within 2% of the human data, suggesting that an arc foot compliant walking model can somewhat accurately predict this mechanical cost of human gait. The push-off work for the arc foot model is also within 9% of the human data. However, the arc foot model exceeds the rebound work of the human data by 120%. The other measured amounts of work performed by the models in each of the four gait phases are compared with the human data in Table 2.2. The overshoot of rebound work can be explained by the undamped elasticity of the leg springs. In the compliant model the work produced in the four phases are closely coupled. For example, the amount of positive work performed by the spring in rebound is dependent upon the amount of energy that was stored in the spring during the collision phase. A similar correlation is found in human gait, whereby the rebound work increases with the collision work (Kuo et al. 2005). Adding damping to the leading leg spring could potentially leave the total work

performed during collision relatively unmodified but reduce the amount of available spring energy to be returned in rebound.

We also calculated correlation coefficients between the model and human data traces (Table 2.3). While the correlations with the point mass foot model were quite high, adding arc foot to the model improved all of the correlation coefficients to at least 0.93. Despite the large forces and work rate produced by the point mass foot compliant model, the force and work rate profiles generally matched the shape of those produced by the human subjects, evidenced by the relatively high correlation coefficients. This result suggests that the point mass model does at least account for the timing of force and work production, though not the amplitude. It is worth it at this point to note again that we did not 'tweak' or optimize the model parameters to find gaits that closely matched the human data or reduce the error between them. We simply searched for model gaits that matched the average speed, step length, and duty factor of the human subjects and used whatever model parameters were required to achieve those gait parameters. The closeness of the model and human data found by matching gait parameters highlights the usefulness of this model for comparing experimental human data and model results.

Table 2.2. Comparison of individual limb COM work in four phases of gait for two compliant walking models and averaged human subject data at 1.25 m/s. Values are in non-dimensional units of work. Values in parentheses indicate the percent difference between the model and corresponding human measurement.

Phase	Collision	Rebound	Preload	Pushoff
Human	0.0232	0.0067	0.0124	0.0250
Point Foot Model	0.0405 (75%)	0.0379 (465%)	0.0379 (205%)	0.0405 (62%)
Arc Foot Model	0.0228 (2%)	0.0148 (120%)	0.0148 (20%)	0.0228 (9%)

Table 2.3. Correlation coefficients, *R*, between ground reaction force and individual limb COM work rate curves produced from two compliant walking models and average human subject data at 1.25 m/s.

	Vertical Ground Reaction Force	Horizontal Ground Reaction Force	COM Work Rate
Point Foot Model	0.93	0.99	0.85
Arc Foot Model	0.99	0.99	0.93

Effect of Parameters

Three system parameters, K_p, K_{leg}, and E were varied individually about those of the nominal walking gait (Figure 2.3), while the other parameters were held constant. For each new parameter combination, we found a fixed point or set of initial conditions using a first-order Newton shooting method. Results of varying these parameters on gait properties are shown and discussed below. Walking gaits were found for a small range of energy values E = [0.99, 1.10] and a large range for the spring constants K_p = [1.1, 25.0], and K_{leg} = [2.2, 49.3].

The effects of the changes in model parameters on initial conditions are reported in Appendix 2.1 and summarized here. The amount of energy in the system significantly influences the horizontal velocity of the COM, $\dot{x}$, which grows with increasing energy and is closely related to forward speed. The magnitude of the leg angles and therefore step length also increases with E. The leg spring stiffness, K_{leg}, predominately affects the vertical velocity of the COM and the angle of the stance leg at heel-strike. As the leg spring becomes stiffer, the vertical velocity of the COM increases (decreases in magnitude) and the angle of the stance leg decreases. A shallow stance leg angle is needed to balance the effect of increasing leg stiffness on overall vertical stiffness, such that the vertical COM velocity is re-directed with proper timing (McMahon and Cheng 1990).The stiffness of the hip spring has the largest comparative effect on the angle of the swing leg and to a lesser degree the horizontal velocity of the COM. We find that the angle of the swing leg increases as the hip spring becomes stiffer.

Speed is determined by varying the energy parameter

Overall, our parameter study suggests that adding energy to the gait is the simplest way to increase the speed of the model (Figure 2.5). Energy appears to have a significant effect on the walking speed, step length, and magnitude of the ground reaction forces. Since the stride period remains relatively constant as speed increases, we suggest that increasing the energy increases the walking speed largely through an increase in step length. Besides increasing walking speed, increasing the energy of the system also increases the portion of energy associated with spring compression. The increase in spring compression is demonstrated by the fact that the maximum vertical ground reaction force (Appendix 2.1) also increases with energy. Since the leg stiffness is held constant, we associate the increased ground reaction forces with increased excursion of the COM along the length of the spring. We can attribute the larger peak ground reaction forces to longer steps which require larger push-off and collision work, and thus more energy stored in the springs and larger spring deflections. The difference between the maximum and minimum ground

reaction force increases with peak force simply because the average force over a stride must equal body weight. The period of leg swing appears to be decoupled from the energy parameter while the stance period shows some decrease over the energy range. We can likely attribute the decreased stance period to the increase in step length, and thus the difference in leg angles during double support. In running gaits, the vertical stiffness increases with leg angle for constant leg stiffness (Farley et al. 1993; McMahon and Cheng 1990) and leads to decreases in period of stance contact. Walking then appears to show a similar trend, whereby the stance period and thus step period decreases naturally for faster speeds.

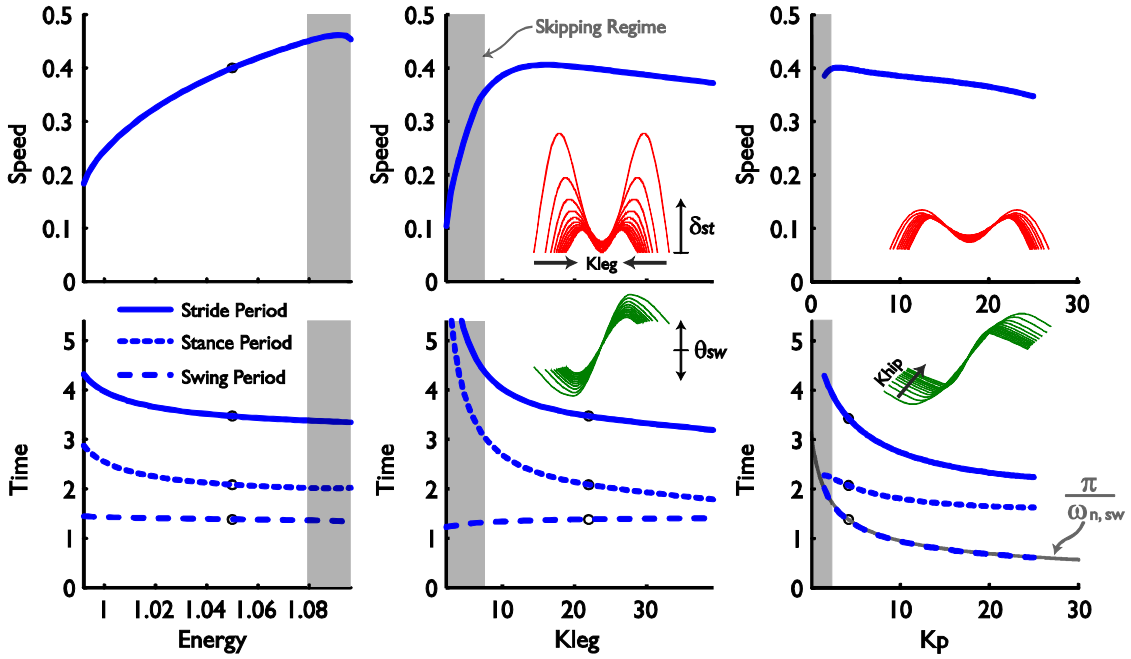

Figure 2.5. Gait parameters as a function of varied stiffness and energy parameters. Adding energy to the gait is the simplest way to increase the speed of the model. The stance period and thus step period decreases naturally for these faster speeds. Skipping gaits naturally appear for large energy or small stiffness values and can occur over a range of speeds. The stiffness parameters show a lesser affect on speed for normal walking gaits. Leg stiffness primarily determines the frequency of the spring-mass oscillation (middle inset) and thus adjusts the stance period. Leg stiffness provides little control over the swing period. Consequently the stride period also decreases with increased stiffness. The hip stiffness parameter predominantly determines the period of swing by adjusting the natural frequency of the swing leg (right inset), with this period closely correlated to one-half period of the oscillation. Hip stiffness shows much less of an effect on stance period, and therefore stride period also decreases for increased hip stiffness. Nominal gait (E = 1.05, Kleg = 22, Kp = 3.96) marked by ‘o’.

Faster walking speeds lead to skipping

We also see that for increasing energy, the walking gaits end around a speed of 0.45 (≈ 1.4 m/s), because at this point the stance leg begins to leave the ground at mid-stance (force at mid-stance goes to zero) (Appendix 2.1). Inverted pendulum models can approach a theoretical maximum speed of 1 (≈ 3 m/s) before the required centripetal force approaches gravity, lightening the contact force at the foot, and causing the pendulum to leave the ground at mid-step. The pendular motion of the compliant model is also similarly speed limited; however, in this case the centripetal terms act on the undamped spring-mass mode. These combined effects allow a large portion of the stored energy from the collision phase to be released during rebound for fast speeds (centripetal), for large heel-strike collisions (spring-mass), or a combination of the two. The amount of rebound can be sufficient for the model to leave the ground at mid-stance, even at speeds below 0.2, for gaits that store sufficient energy in the stance spring during collision. In our parameter study these slow speed gaits were found for low leg stiffness values (Figure 2.5). The end of the walking gaits, where the stance leg leaves the ground around mid-stance, is marked by the beginning of the skipping regime. We found that by continuing the simulations into the flight phase after the stance leg leaves the ground and allowing the stance phase to resume once the stance foot returned to the ground, we could simulate an entire step of skipping. Limit cycles were found for a range of skipping gaits. Generally, skipping gaits are found by following some increase in stance compression, usually accomplished by increasing step length, during the collision phase and continuing that change after the model leaves the ground during stance.

Arc feet and leg mass are necessary to extend the speed range of walking gaits

It would be useful for the model to walk at faster speeds to study a larger range of bipedal gait. The speed limit of 0.45 is well below the walk-to-run transition speed of 0.71 (≈ 2.2 m/s) for a typical human. Extending the speed range of the walking gaits would be especially important for robotics applications that exploit compliant legs. These machines could adopt a skipping gait at faster speeds, but we generally find this gait to be energetically costly and rather unstable. If skipping were energetically advantageous at some speed between modest walking and running speeds, we would also expect this gait to be more prevalent in nature (lively toddlers not withstanding). It would likely be more energetically favorable to exploit the model parameters in some way to extend the speed range for increasing energy. Entering the skipping regime is really a matter of storing too much energy in the stance spring during collision. Increasing the stiffness of the hip spring can reduce step length for relatively constant speed and therefore cause collision work to increase more slowly than if energy were increased alone. However, we found that

increasing the hip stiffness with energy provided minimal improvement in the walk-to-skip transition speed (0.47). Adding an arc foot to the model may be a better choice since it was already shown to drastically reduce the energy stored in collision. For an arc foot radius of 0.3 increasing energy still leads to an increase in speed, but skipping does not occur until an E of 1.13 and speed of 0.55 (≈ 1.7 m/s). By adding leg mass to the arc foot model with approximate anthropomorphic inertial parameters (c = 0.635, M_t = 0.16), this speed range can be expanded past 0.60. Centripetal effects of arm and leg mass appear to similarly impact the speed range of human walking (Kram et al. 1997). However, this speed is still below the walk-to-run transition speed of 0.71, suggesting that damping may be required for even faster speeds.

Two stiffness parameters determine step frequency and duty factor

The stiffness parameters are most useful for adjusting the timing of the stance and swing periods. Leg stiffness shows little effect on the speed of the gait within the walking regime. At very low stiffness values, the model takes on a slow speed skipping gait with large double support periods that borders on forward hopping on both legs. Adjusting leg stiffness appears to be more useful for patterning the gait parameters at a particular speed. We can best understand the effect of leg stiffness by considering the spring mass motion of the COM along the stance leg during a stride. The spring mass motion is largely determined by the natural frequency of the mass with respect to the leg spring, especially for slow speeds, and small step lengths (small angle approximation). As speed increases, the oscillation of the leg spring is also affected by the pendulum to which it is coupled (ex: centripetal effects grow with speed). The relationship between the natural frequency of the spring-mass system and the actual frequency of compression/extension is further complicated by the double support period, when two leg springs engage the COM motion, and approximately double the apparent stiffness. However, we can largely approximate the oscillation of leg compression as being correlated with the stiffness of the leg spring and we might estimate the overall frequency of oscillation to be between the natural frequency of a single leg spring and the natural frequency of two springs in parallel. For increasing leg stiffness, the frequency of the axial leg motion increases (inset Figure 2.5) and the period over which the leg completes two compression extension cycles, the stance period, decreases. In contrast, leg stiffness has little effect on frequency of leg swing and thus the single support period remains unchanged. For decreasing stance period and relatively constant swing period, both the duty factor and stride period decrease with leg stiffness. Thus step length is also reduced for increasing leg stiffness with the relatively constant speed over the leg stiffness range.

As with leg stiffness, the hip stiffness parameter, K_p, provides little control over the walking speed. The stiffness of the hip spring largely affects the other gait parameters through the natural frequency of swing leg oscillation. In contrast, the other parameters showed very little control of the swing leg motion. The swing period decreases and frequency of leg swing increases as hip stiffness is increased (inset Figure 2.5). However, the frequency of leg spring oscillation remains largely unchanged. Duty factor and the double support fraction then increase with hip stiffness largely by decreasing the step period for relatively constant stance period. Intuitively, larger hip spring stiffness will speed up the motion of the swing leg, causing heel-strike to occur sooner and earlier in the push-off phase. For a stiffer hip spring, the step frequency increases while the walking speed remains relatively constant.

We can compare the swing period of the model with those of a freely swing inverted pendulum. For an inverted pendulum with the same inertial properties as the swing leg, the period of one half cycle is inversely proportional to the natural frequency of the pendulum (Equation 12). When comparing this theoretical period with that produced by the model, we found that the

$$t_{sw} = \frac{\pi}{\omega_{n,sw}} \qquad \omega_{n,sw=\sqrt{1+K_p}} \tag{12}$$

swing period is almost entirely defined by the half-cycle period of the free motion of an inverted pendulum. This finding was similarly found for a passive running model (McGeer 1990a), and implies that the spring-mass motion has very little effect on the swing leg dynamics.

In summary, we found that the overall speed of the gait is simply determined by the mechanical energy in the system set by the initial conditions. To increase speed, one need only temporarily inject energy into the gait to achieve a new steady state for the same stiffness parameters. The stiffness parameters largely adjust the gait parameters at a given speed and this effect can be understood by a relatively decoupled spring-mass motion along the leg and pendulum motion about the hip. We can think of the leg stiffness as adjusting the frequency of the spring-mass mode or period of stance duration and the hip stiffness as adjusting the frequency of the inverted pendulum mode or swing period. The actual initial conditions are also just as important as energy, which only sets a bound on the initial conditions. We have only considered walking gaits so far, but as we will show later, choice of initial conditions for constant energy adjusts the relative amplitudes and phasing of the spring-mass and pendulum modes and largely explains the differences between walking and running gaits.

Humans may increase leg and hip stiffness for increasing walking speed to adjust metabolic cost

How might humans adjust these parameters for faster walking speeds? We have shown that simply increasing the energy of the gait is enough to increase speed and step length. However, increasing energy by itself leads to a set of gaits with excessive step length that fall far off the known preferred speed-step length relationship (data not shown). Humans tend to walk faster by increasing both their step length and step frequency. Therefore, the stiffness parameters must also likely be adjusted for increased speed. The relationship between model parameters is very complex and we found no simple rule that falls out a priori that would tell us specifically how to adjust the stiffness parameters with energy to exactly follow the preferred speed-step length relationship. However, we do have a general idea how these parameters individually affect the gait parameters. To follow the preferred relationship, step frequency must increase with speed and therefore leg or hip stiffness must also increase. Either parameter could be used to increase the step frequency, but increasing them together allows the duty factor to remain within an allowable window. Recall, K_{leg} and K_p have opposite effects on duty factor. We did find that increasing K_{leg} and K_p by a rule of thumb 4:1 ratio generally maintained duty factor within a narrow window. However, further adjusting the stiffness parameters relative to one another could be used to advantageously adjust duty factor with speed. Duty factor does decrease for faster walking speeds in humans (Murray et al. 1984) and does so more drastically than can be explained by the model for increasing energy alone. This result emphasizes that leg stiffness may increase with walking speed since using leg stiffness alone to increase step frequency would result in increased duty factor. Increasing leg stiffness with speed may then distinguish walking from running, which is thought to maintain relatively constant leg stiffness over a range of running speeds. This hypothesis has yet to be tested experimentally in human subjects. However, it is also important to emphasize that adjustment of leg stiffness or hip stiffness is not required for walking at faster speeds but may be adjusted based on some other criteria such as choosing a preferred step length and duty factor to minimize metabolic cost at a particular speed.

Stability analysis reveals three neutrally stable modes and one critical for stability

Stability analysis shows that the model is generally neutrally stable given conservative behavior, but there is a critical mode that can lead to instability. Rigid passive walkers are locally stable for a subset of parameter values and initial conditions but are generally sensitive to large disturbances. It would be beneficial for a compliant walker to also demonstrate some level of passive stability to minimize the requirements for active stabilization against disturbances. Stability information is gained through a linearization of the step-to-step function about a fixed

point and calculating the eigenvalues and eigenvectors of the resultant Jacobian matrix. Analysis of a gait associated with normal walking shows that the model has three neutrally stable eigenvalues and one eigenvalue that is either stable or unstable based on the symmetry of the gait (Table 2.4). We find that two gaits exist for the same model parameters: an unstable symmetric gait and a neutrally stable non-symmetric gait. This difference in stability is derived from the manner in which the swing foot hits the ground at heel-strike.

The non-symmetric gait has one stable mode that we associate with the pendulum motion of a leg over a stride (indicated by the small $\dot{\delta}_{st}$ component in the eigenvector). Each leg moves smoothly from stance phase to swing phase as the force under that leg falls to zero. However, the transition back from swing to stance may be very discontinuous based on the symmetry of the gait (Figure 2.6). In the non-symmetric gait the swing foot hits the ground with both axially and normal velocity, meaning that the swing foot experiences an impulsive force in a direction normal to the leg axis, abruptly stopping this component of velocity and enforcing foot contact. The collision in the axial direction occurs over significant time because the leg spring cannot transmit an impulse along its axis. The impulsive normal force scales to the normal velocity of the stance foot, and

Table 2.4. Step-to-step stability of the walking cycle for a symmetric and non-symmetric gaits with parameters E = 1.05, Kleg = 22 Kp = 3.96

	Mode	Speed	Spring		Pendulum
			Symmetric Gait		
			Magnitude	± Phase	
	Eigenvalue	1.00	0.99	± 2.69	1.48
Eigenvector	θ_{st}	0.45	0.33	± 1.58	0.47
	θ_{sw}	0.39	0.22	± 2.23	0.71
	$\dot{\theta}_{st}$	0.36	0.54	± 0.61	0.53
	$\dot{\delta}_{st}$	0.72	0.75	± 0.00	0.05
			Non-Symmetric Gait		
			Magnitude	± Phase	
	Eigenvalue	1.00	0.99	± 2.69	0.68
Eigenvector	θ_{st}	0.48	0.33	± 1.59	0.52
	θ_{sw}	0.44	0.22	± 2.26	0.67
	$\dot{\theta}_{st}$	0.39	0.54	± 0.61	0.53
	$\dot{\delta}_{st}$	0.65	0.75	± 0.00	0.11

therefore provides a method for the dynamics to regulate the swing leg velocity, even though this collision causes no noticeable loss in energy for very small leg mass. Whether a perturbed swing leg approaches heel-strike with too little or two much velocity compared to the nominal limit cycle, the results is the same, the collision arrests the motion of the swing leg. The new angular velocity of the leg is then dictated by the COM velocity normal to the leg. It is interesting that this stability is gained without energy dissipation, owing to the fact that the leg mass infinitesimally small. Adding mass to the legs would not be expected to change this stability, though it would be carried out for significant energy dissipation. A non-symmetric gait with significant leg mass would then require the model to walk on a shallow slope or use some form of energy input.

In comparison, the symmetric gait has an unstable pendulum mode along a very similar eigenvector direction. For symmetric gaits, the transition from swing phase to is smooth because the velocity of the swing foot is parallel to the leg axis (Figure 2.6). However, if this gait is perturbed, the dynamics do not act to restore this symmetry. In fact, for small perturbations the gait will be attracted to the corresponding non-symmetric gait with the same model parameters (Figure 2.6) over many steps. Thus the instability of the symmetric gait is not catastrophic for small perturbations, meaning the model does not fall down.

Both gaits have three eigenvalues with a magnitude of unity. These three neutrally stable modes of both the symmetric and non-symmetric gaits are very similar and are defined by the

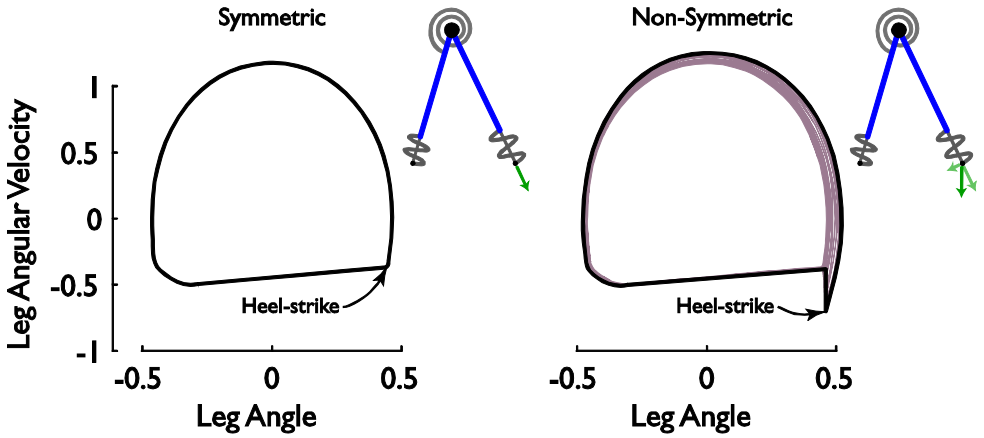

Figure 2.6. For a given set of parameters, two gaits exist that differ in the symmetry of the pendular leg motion. In the symmetric gait, the velocity of the foot at heel-strike (model on left) is parallel to the axis of the leg, resulting in a smooth contact transition. However, if this gait is perturbed, the dynamics do not restore symmetry, resulting in instability. In the non-symmetric gait, the velocity of the foot has both normal and tangential components (model on right) at heel-strike and the swing leg experiences an impulsive normal force to arrest the swing leg motion. This impulse scales to the normal velocity of the stance foot, stabilizing the leg motion over a stride. For small perturbations, the symmetric gait converges to the non-symmetric gait over many steps.

eigenvectors associated with each eigenvalue. One mode is associated with the speed of the walker and the other two associated with the vibration of leg spring compression. These neutrally stable modes suggest that the walking gait is stable but not speed stable; that is, the walker will not fall over in the presence of small perturbations and will respond by adjusting its speed and step length. The neutrally stable eigenvalues are most likely present because the walker conserves energy, that is, there is no way to dissipate energy added by a perturbation or disturbance. Energy dissipation, in the form of stance spring damping, would likely stabilize the neutrally stable eigenvalues, including the speed mode, and move them within the unit circle. Thus gaits with dissipation will have a unique steady state speed. Perturbing along neutrally stable eigenvectors should just change where energy is located and perhaps also change the step length and duty factor.

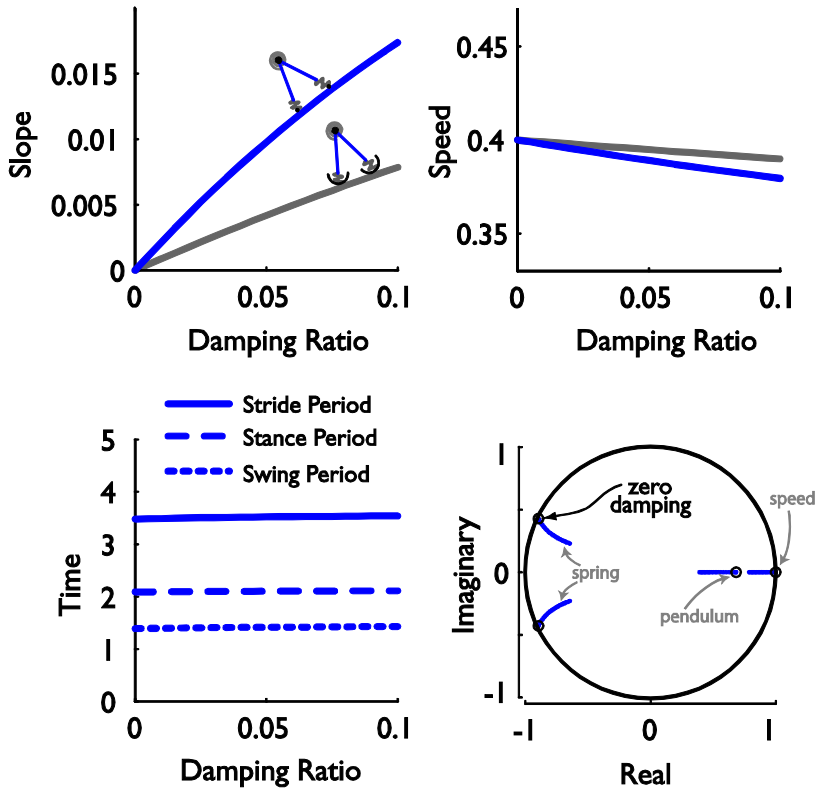

Figure 2.7. Gait properties of the compliant walker for increased damping of the leg spring. As the damping ratio increases, steeper slopes are needed to compensate for the energy lost in spring compression. Slope requirements are reduced when arcs are added to the feet. The stance, swing, and step period appear to be relatively insensitive to increased damping and slope, while the walking speed decreases slightly. Root locus analysis shows that increased damping and slope stabilizes the eigenvalues of the system relative to the undamped gait, denoted by the 'o' symbol. Eigenvalues within the unit circle are considered stable. Increased damping stabilizes the three neutrally stable eigenvalues and moves the stable eigenvalue closer to zero

Damping stabilizes gait at energetic cost

Model stability could certainly be gained by adding passive dissipation, which is an inevitable feature of any mechanical or biological system due to friction and viscosity. However, passive damping comes at the price of the metabolic cost associated with restoring energy back to the gait through active positive work. We will explore how damping in the leg springs affects stability and the energy expenditure. We searched for gaits over a range of damping ratios [0, 0.1]. For reference, a system with a damping ratio of 0.1 loses half of its amplitude over one cycle. Damped gaits were found by slowly increasing damping ratio from zero for the nominal walking gait while using the Newton search method to find subsequent fixed points. Since damping dissipates energy, either the slope or the stance thrust had to be increased for increasing damping ratio to maintain energy balance. The Newton search algorithm was modified to also vary a system parameter such that for a given damping ratio, it simultaneously found the initial conditions and energy input parameter (slope or stance thrust) that produced a repeatable walk gait. The other gait parameters, energy and the spring stiffness values, were held constant with values of: $K_{leg} = 22.0$ $K_p = 3.9598$ $E = 1.0499$.

Adding damping provided significant stabilization with little modification to the gait parameters (Figure 2.7). The slope parameter had to be increased with damping ratio to find repeatable walking gaits, compensating for increased energy lost due to dissipation. The cost of transport, which is equivalent to the slope, then appears to grow linearly with damping ratio. This cost can approximately be halved when an arc foot of radius 0.3 is added to the model, across the range of damping ratios. While walking speed decreases slightly with damping ratio, the other gait parameters such as stance, swing, and step period appear to be relatively insensitive to these changes. As the damping ratio is increased, the three neutrally stable eigenvalues decrease in magnitude and move within the unit circle. The model then becomes speed stable, such that only one gait speed exists for each slope-damping ratio combination. The other eigenvalue, which was stable for the non-symmetric nominal model, is further stabilized as well.

Adding leg mass alters energetics and stability of non-symmetric gait

While the assumption of negligible leg mass is not physically realizable, as with zero damping, we found that adding a modest amount of mass required relatively small additional energy expenditure and even stabilized the walking motion. We searched for gaits with leg mass over a range of (0, 0.2] with an approximate anthropomorphic positioning along the leg (c = 0.635). For reference, a leg mass of 0.16 represents an anthropomorphic scaling. Both symmetric and non-

symmetric walking gaits were found by slowly increasing leg mass from zero for the nominal walking gait while using the Newton search method to find subsequent fixed points. Since heel-strike collisions normal to the leg dissipate energy for significant leg mass, the non-symmetric walking gaits were found using the modified Newton search that simultaneously found the initial conditions and slope that produced a repeatable walk gait. Model parameters were then varied to find gaits with the gait parameters of the nominal walking gait. Here we only report gaits for these constant gait parameters.

As the leg mass increases for non-symmetric gaits, increasingly steeper slopes are needed to compensate for the energy lost in impulsive heel-strike impacts normal to the leg (Figure 2.8). Recall, that the non-symmetric walking gait gains some stability of the pendulum motion from an impulsive collision that resets the leg motion at heel-strike. These stabilizing collisions come at an energetic cost as leg mass becomes substantial. For an anthropomorphic leg mass (0.16), a slope of 0.017 is necessary to provide energy balance. However, slope requirements are once again greatly reduced when arcs are added to the feet, by an approximate factor of 14.

To maintain constant gait parameters of non-symmetric gait, the model parameters had to me modified linearly with leg mass (Figure 2.8). Had leg mass been varied while holding all other parameters constant, we would see a strong affect on the gait parameters, mostly due to a large change in the forward speed and frequency of leg swing. For fixed gait parameters, the total mechanical energy had to be reduced, simply reflecting that potential energy and the kinetic energy must fall as mass is redistributed towards the legs to maintain the same forward speed. With less mass at the hip to support, the leg stiffness decreases to maintain the same stance period. Hip stiffness, which we found to closely predict the period swing, increases linearly with leg mass. By fixing the gait parameters we have effectively simultaneously adjusted hip stiffness so that the ratio of hip stiffness to leg mass, and thus swing period remains constant. So the effect of leg mass itself is less important for maintaining the gait parameters than the natural frequency of the spring modes and the velocity at the hip. The symmetric gait required similar changes to model parameters but without a change in slope.

Adding leg mass affects the stability of the non-symmetric and symmetric gaits very differently (Figure 2.9). For the non-symmetric gait, leg mass stabilizes the eigenvalues of the system relative to the negligible mass gait, whereas the symmetric gait is further destabilized. Root locus analysis of the non-symmetric gait shows that increased leg mass not only modified the

eigenvalue associated with the pendulum mode but also the three neutrally stable eigenvalues. Adding leg mass stabilizes the two neutrally stable eigenvalues of the spring mode. The neutrally stable speed mode and stable pendulum mode merge within the unit circle at a mass of 0.08 and remain stable for increasing mass. For anthropomorphic leg inertia properties, the model is stabilized by an amount comparable to the model with significant damping (damping ratio of 0.1). For the symmetric gait, increased leg mass further de-stabilizes the pendulum mode, while adding some stability to the spring modes. The speed mode remains unchanged. Thus, increased leg mass does little to change the nature of the symmetric gait instability.

The symmetric gait has no energy loss even with significant leg mass because of the conservative elastic collision. However, this gait may not be physically relevant for walking robots or humans because any disturbance will cause the gait to move to a stable non-symmetric gait. The important point then is that stability of the pendulum mode can be gained for fairly small energy expenditure even with anthropomorphic leg mass. The cost of transport was only 0.0012 for a

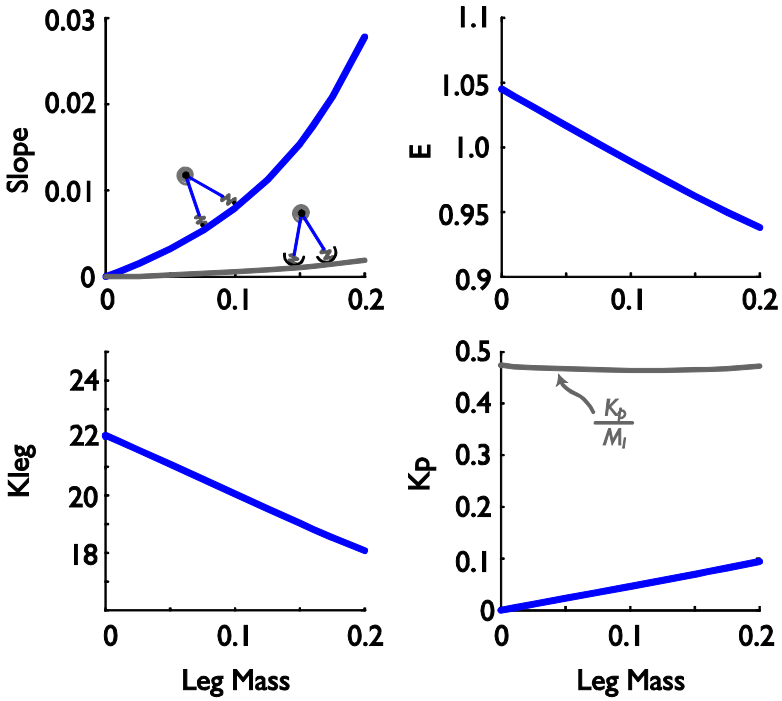

Figure 2.8. Model properties for increased leg mass and constant speed, step length, and duty factor. As the leg mass increases for non-symmetric gaits, steeper slopes are needed to compensate for the energy lost in impulsive heel-strike impacts normal to the leg. Slope requirements are greatly reduced when arcs are added to the feet. To maintain constant gait parameters for increasing leg mass, energy has to be reduced, simply reflecting that potential energy and the kinetic energy must fall as mass is redistributed towards the legs. Likewise, the leg stiffness decreases, as there is less mass at the hip to support, to maintain the same stance period. Hip stiffness increases, to maintain the ratio of stiffness to leg mass and swing period.

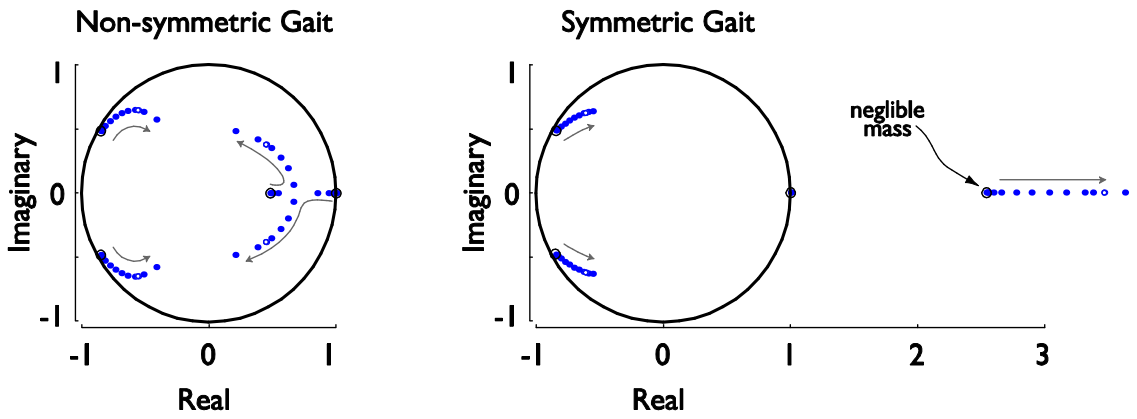

Figure 2.9. Leg mass affects the non-symmetric and symmetric gaits differently. Eigenvalues within the unit circle are considered stable. Root locus analysis shows that increased leg mass stabilizes the eigenvalues of the system relative to the negligible mass gait, denoted by the 'o' symbol. Increased leg mass stabilizes the three neutrally stable eigenvalues and maintains stability of the pendulum mode. For the symmetric gait, increased leg mass further de-stabilizes the pendulum mode, while adding some stability to the spring modes.

model with anthropomorphic leg mass and arc feet, which is approximately 2.5% the cost of transport in humans. From the dynamic walking perspective, we would then suggest designing a walking robot with relatively light legs that uses a simple energy input to maintain speed, as opposed to adding control to the swing leg to enforce a smooth conservative heel-strike collision. The energetic and computational cost for controlling symmetry would likely exceed the small amount of energy lost due from the non-symmetric stabilizing collisions.

Energetic Cost of Locomotion

The energy expenditure required to compensate for damping and leg mass cannot account for the cost of transport measured in humans. To stabilize the walking gait we added damping at the cost of energy expenditure. By adding leg mass we found a similar tradeoff. The cost of transport, equivalent to the slope down which the model walks, was at most 0.017 for a moderate damping ratio of 0.10. This cost of transport drops to 0.0078 when arc feet of radius 0.3 are added to the model for the same damping ratio. For anthropomorphic leg mass and similar arc feet, the heel-strike impacts that further stabilize the walking motion, only increase the cost of transport by approximately 0.0012. While we have confidence in our anthropomorphic leg mass estimation, we do not know what damping ratio is appropriate to represent passive dissipation performed by the body during walking. However, we find that the model cost of transport for moderate damping and leg mass is still well below the cost of transport value of 0.05 measured in human walking. Other factors such as damping at the hip, drag, and impacts of foot mass with the ground

could increase the requirements for adding energy back into the gait. However, analysis of these costs for a passive runner suggest that they are negligible for the speed range of walking (McGeer 1990a). Energetic analysis so far has left a gap between the cost of transport measured in the model and humans. But we have not accounted for worked performed by the leg springs to redirect the COM throughout gait. In fact, we have previously only discussed the leg springs in terms of its energy conservative behavior. However, the compliant legs are meant to globally represent the positive and negative work performed by muscle, tendon, and compliant structures in the leg. We could therefore prescribe some energetic cost to the work performed by the individual leg springs. We have already shown that the model can predict the individual limb mechanical work performed on the COM during human gait with reasonable accuracy. Therefore it makes sense that by accounting for this work we should be able to approximate the total mechanical work performed for a gait. However, without knowing the efficiency of the leg when producing this work we cannot prescribe a metabolic cost to the leg function. The efficiency of the leg would be approximately 25 % if muscle were performing all of the work (Margaria 1968) and move towards 100% if the work was performed entirely by elastic tendon. Assuming a constant fraction of work performed by muscle and tendon, we will simply use the mechanical work performed by the model as some indicator of metabolic work.

Energetic cost of speed and step length similar to collision models

While the compliant walking model is meant to improve upon existing rigid legged models, we also seek to verify that it retains their salient features. Specifically, this model must make new predictions while still verify the predictions made by the rigid models. The previous rigid legged models provided us with a framework to begin understanding the competing energetic costs of taking longer steps and forced leg swing. The sum of these two costs produces an energetic minimum at a certain step length, for a given speed, and closely matches the preferred speed-step length relationship in humans (Kuo 2001). We have already shown that, like the collision models, the hip spring stiffness, largely affects the step period, and energy which is somewhat analogous to push-off in the collision models, largely affects the step length. We will next show that the compliant model makes similar predictions about the energetic cost of taking longer steps, assuming that the spring work is treated as costly. We will not also verify the cost of leg swing since adding an axial leg stiffness does not affect the swing leg dynamics from previous cost models (Kuo 2001).

Work-energy principles predict that the work rate of push-off for the simplest walking model to be proportional to step length to the fourth power and step frequency to the third power (Equation 12) (Kuo et al. 2005). Though this relationship is derived under the assumption of impulsive push-off and heel-strike, the same relationship has been demonstrated in human walking (Donelan et al. 2002a). We seek to verify the same relationship for our compliant walking model.

$$E \propto \dot{M} L^4 f^3 \tag{12}$$

$$E = aL^4 + b \tag{13}$$

An array of gaits for both the simplest walker and springy walker were found over a range of step lengths with a constant step frequency of 0.69. Compliant walking gaits were found by varying K_{leg} , K_p and E, while duty factor was also held constant at 0.60. Two types of rigid gaits were found, the first being a gait that applies an impulsive push-off just before heel-strike, and second a gait that uses gravity to supply the energy lost at heel-strike. Rigid gaits were found by also varying K_p and the corresponding energy input parameter. Compliant walking gaits were found over a much smaller speed/step length range than for the simplest walker, owing to elastic rebound that results in skipping at higher speeds. The relationship between step length and push-off work rate is examined for both the simplest walker and the springy walker (Figure 2.10). As predicted previously (Kuo 2002a), the gait powered by gravity requires four times as much energy as the gait that uses an impulsive push-off. This result demonstrates that it is less efficient to do positive work on the COM over the entire step. When modeled as impulsive forces, it is then energetically advantageous to perform push-off immediately before heel-strike. Since the compliant walker produces a push-off over a finite time before heel-strike, we would expect that the work rate of push-off would lie between that of the two simplest models. Indeed this is the case, for most of the step length range. The above curves were fit to fourth order equations (Equation 13), to evaluate how well they fit the energetic equation above (Table 2.5) and to compare the relationship between step length and work rate among them.

The compliant model shows costs between the push-off and gravity powered models. For increasing step length, a larger amount of push-off work (36%) is required for the compliant walker than the impulsive push-off model, as evidenced by the larger *a* term. However, the gravity powered model is still the most costly. This result is not unexpected, since the simplest push-off walker theoretically uses the least amount of work to perform COM redirection during the step-to-step transition. It achieves this minimum by performing a short burst of push-off immediately before heel-strike. We can attribute then attribute extra push-off work in the compliant model to the fact that push-off occurs over a period of time and substantially overlaps the collision phase. Impulsive models of the step-to-step transition indicated that it is more costly to perform some amount of push-off after the start of heel-strike, even if push-off is performed in a short burst (Ruina et al. 2005). In fact, the cost of performing two impulsive collisions doubles when performing them simultaneously. By simply having some overlap between push-off and heel-strike, we would then expect the cost of push-off in the compliant model to increase over the simplest push-off model. Adding to the difference is the cost of performing push-off over significant period of time and displacement, even if performed before heel-strike. Greater COM displacement during the step-to-step transition means more work must be performed by each leg against gravity.

We also find a significant offset term, *b*, for the compliant model, which suggests that push-off work is required even at zero speed. Intuitively one would expect that the offset should equal to zero for both walkers. Why is it not zero for the springy walker? First, we note that the compliant gaits, which are not defined by speed and step length alone, were found by varying the parameters to maintain constant duty factor. It may be possible to lower the push-off work rate at the slower speeds by properly varying the duty factor, as shown in the next section. However, some push-off work even

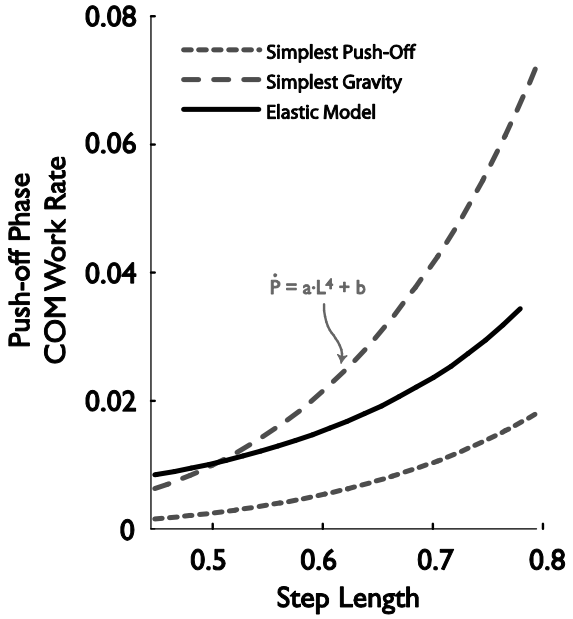

Figure 2.10. Fourth power relationship between step length and push-off work rate for the elastic walking model and simplest walking models powered by an impulsive push-off and gravity. Model gaits were found over a range of step lengths with a constant step frequency (0.69). For most of the step length range, the elastic walking had push-off costs between the two simplest walking models.

Table 2.5. Parameters of fourth order regressions of step length and push-off phase work rate for the simplest walking model powered by an impulsive push-off and gravity and an elastic walking model. All models were compared at the same speeds and step lengths and constant duty factor (0.6) for the elastic model.

$E = aL^4 + b$	R^2	a	b
Simplest Walker (Push-off)	0.994	0.0994	-0.0050
Simplest Walker (Gravity)	0.994	0.3975	-0.0201
Springy Walker	0.999	0.1349	0.0092

at very slow speeds appears to be a characteristic of the model dynamics. Since the legs are not rigid, the COM will always be moving back and forth along the stance leg to some degree, even at zero speed. Even if one were to start the COM at zero vertical velocity for zero speed (legs vertical), gravity would force the COM downwards, compressing the spring, and requiring positive work to raise the COM enough to allow the next foot contact. This work can be reduced for increasingly stiffer leg springs, though never eliminated. However, it is more likely that the leg stiffness of an compliant walking robot would be designed for faster speeds. Still, increasing the rigidity of the leg would be advantageous at very slow speeds and a method of locking out the leg spring could be used to reduce the energy requirements. In this case a small amount of hip torque could be used to replace the energy lost during the collision phase. Hip torque powered models have similar energetics as gravity powered walkers (Kuo 2002a), and would appear to be cheaper than an compliant model for very slow speeds.

Energetic costs depend on duty factor and are minimized for nominal value

The compliant model also makes predictions about energy use beyond those dependent on speed and step length. We note that speed and step length were sufficient gait parameters to uniquely define a rigid walking gait. However, the compliant walker is able to produce an array of gaits all with the same speed and step length, over a range of duty factors. We found that the duty factor significantly affects the amount of work performed by the legs during the step-to-step transition and over the entire stride. Undoubtedly, this new feature is a result of compression/extension capabilities of the springy walker, whereby the movement of the center of mass during double support is less restricted by the location of the feet, which roughly sets step length.

We found an array of gaits associated with the nominal speed of 0.4 and step length of 0.69, by varying the model parameters (Figure 2.11). To produce these gaits with constant speed and step

length, the overall system energy, E, and leg stiffness, K_{leg}, had to be increased while the hip spring, K_p, was decreased. These trends follow those found when the parameters were varied individually. Recall that, increasing K_{leg} and decreasing K_p both led to decreases in duty factor but had opposite effects on step period (frequency). We also find that the ground reaction forces increase monotonically for decreasing duty factor. Recall that, increasing the system energy and decreasing K_p increased the maximum vertical ground reaction forces. In rigid legged models, the magnitude of the impulsive force applied at push-off is proportional to the amount of work performed by that force. If this were true, we would expect that push-off work performed by the leg would also monotonically increase with decreasing duty factor. However, both the push-off work and total positive work calculated using the individual limbs method demonstrate a minimum in the middle of these gaits. The total positive work changes by up to 20% while the push-off work changes by up to 17%. Since the push-off work calculated using the individual limbs method was shown to be well correlated with the same measures in humans, we suggest that duty factor affects the energetic and metabolic cost of human gait. Duty factor may then be optimized to reduce metabolic expenditure at a given speed and step length.

Optimizing the amount of push-off work is equivalent to a minimum amount of energy stored in the stance leg spring just before the step-to-step transition, which is a function of leg stiffness and leg compression (Equation 14). This quantity is the same as the amount of energy stored in the leading leg spring at the end of the collision phase. Leg spring stiffness dominates the energy equation at low duty factors and leg spring compression dominates at high values, resulting in a bowl shaped minimum in the energy stored in the spring.

$$E_{st} = \frac{1}{2} \cdot K_{leg} \cdot \delta_{st}^2 \tag{14}$$

As duty factor increases above the optimal value, less positive work from push-off is performed on the COM before heel-strike begins and the angle between the leading leg and velocity of the COM decreases. The decreasing angle results in greater leading leg spring compressions and more negative work performed by the leading leg during the collision phase. Push-off work then also increases to balance the negative collision phase work and maintain steady walking speed. In summary, we find that as duty factor increases and thus the simultaneous positive and negative work performed during the step-to-step transition, so does the amount of spring compression.

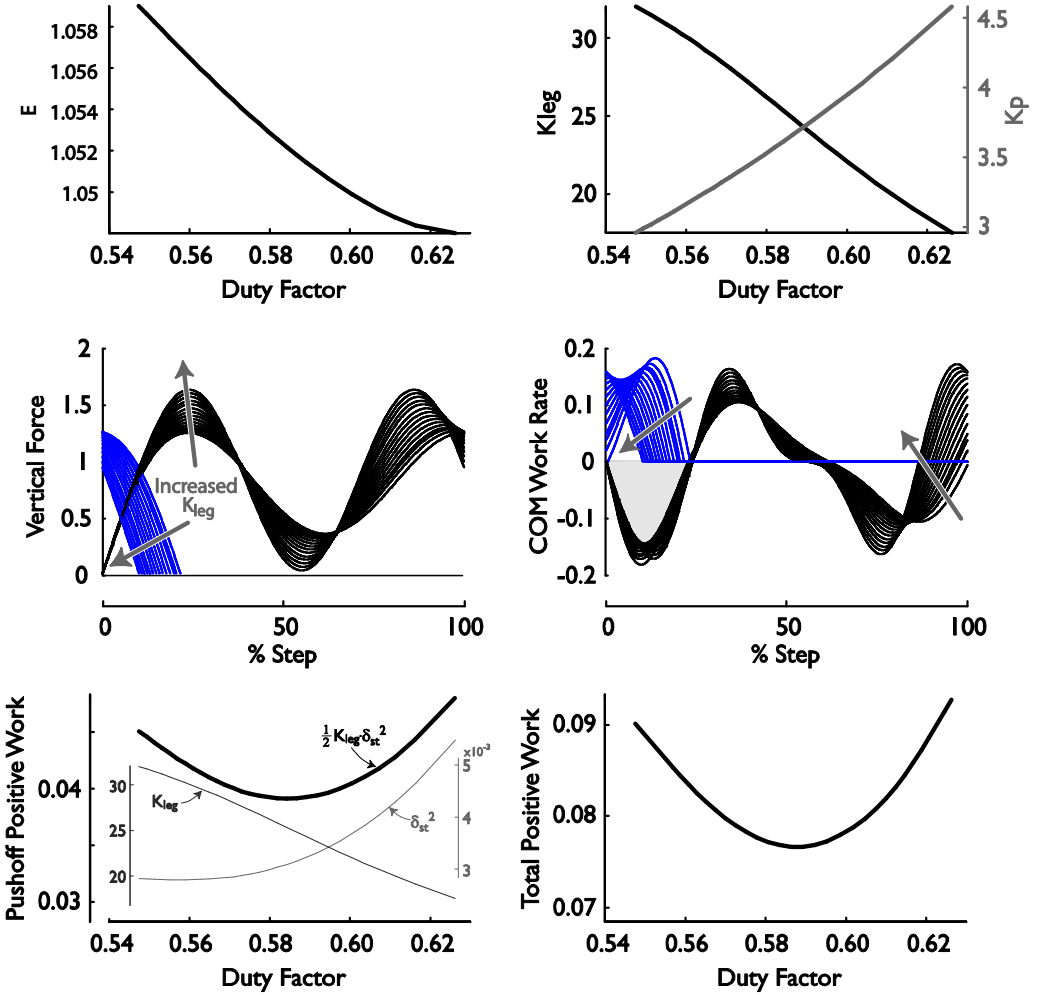

Figure 2.11. Duty factor can be independently controlled by choice of model parameters but with energetic consequences. The array of gaits shown has fixed speed of 0.4 and step length of 0.69. For increasing duty factor, energy, *E*, and leg stiffness, K_{leg}, must be decreased and hip stiffness, K_p, increased to maintain constant speed and step length (top). As duty factor decreases, the overlap between push-off and collision phases decreases and the peak ground reaction forces also monotonically increases (middle). Both the push-off work and total positive work are minimized for some intermediate value of duty factor (bottom). These bowl-shaped cost functions can be explained in terms of increased leg stiffness at low duty factors and increased spring compression at high duty factors, both of which determine the amount of energy stored in the leg springs.

To decrease the duty factor and keep the step period constant, it is necessary to decrease the period of spring bounce, and thus increase the stiffness of the axial leg spring. The energy of the system must also be increased to move the stiffer mass-spring system through the compression/extension cycle at a higher frequency. Although the maximum spring compression during the collision decreases as the duty factor decreases, the increasing spring constant more than compensates below a duty factor of 0.58 and the overall energy stored in the springs increases. This result also explains why the peaks of the vertical ground reaction forces also increase for decreasing duty factor. Overall, we find that larger push-off forces and work is required to move the COM through the faster compression/extension cycle needed to decrease duty factor.

Active Energy Supply

A compliant walking robot must surely also walk on level ground despite energy lost to dissipation (we cannot always count on a downward slope). We explored an approach that pumps energy into the leg spring during the second half of stance contact (McGeer 1990a), to compensate for damping in the leg springs. Stance thrust amounted to changing the set point of the stance spring in proportion to stance leg angle after the angle passed through zero (mid-support). We searched again for gaits over a range of damping ratios from 0 to 0.1. As previously, damped gaits were found by slowly increasing damping ratio from zero for the nominal walking gait. We used a modified Newton search algorithm to find the initial conditions and stance thrust parameter that produced a repeatable walk gait. We then used similar root finding methods to adjust the model parameters to find damped gaits with the same speed, step length, and duty factor parameters as the nominal undamped gait. Here we only report those gaits with constant gait parameters. We also repeated our search for gaits that used slope to compensate for damping for the same gait parameters. We then compare the consequences of using a slope or stance thrust for increased damping and constant gait parameters.

Using stance thrust to compensate for damping produces similar results for gravity powered gaits. The ratio of thrust had to be increased rather linearly as the damping ratio was increased to provide an energy balance against losses and produce repeated gaits (Figure 2.11). We also found increased damping and thrusting stabilizes the system similarly to the model with damping and slope. As the damping ratio is increased, the three neutrally stable eigenvalues again decrease in magnitude and move within the unit circle. A simple strategy of thrusting the leg spring is useful for replacing energy lost to dissipation. However, we also see that the method for adding back in energy lost to dissipation (gravity, thrusting) is less important than the damping itself for gaining stability. These two strategies do have different energetic consequences, though.

We calculated a cost of transport associated with the energy input parameters used to compensate for damping (Figure 2.12). For the sloped walkers, the COT was equal to the slope and for the stance thrust walkers; the COT was calculated by computing the work performed by changing the set point of the spring. Stance thrust work was calculated by integrating the stance spring force-set point work loop. We found that using stance thrusting to compensate for a range of damping ratios required approximately half the cost of transport as the slope powered model. We attribute this energy savings to the benefit of adding positive work to the gait just before heel-strike as was already shown from the energetics of the impulsive push-off and gravity powered rigid walking

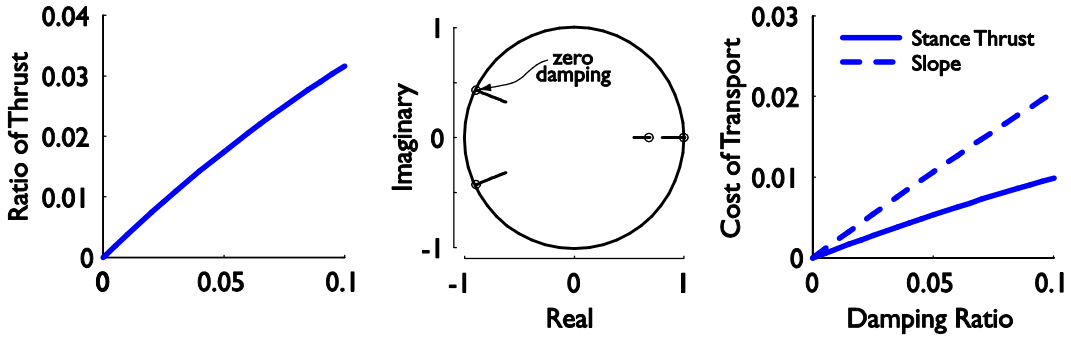

Figure 2.12. Model properties for increased damping ratio and thrust coefficient for fixed speed, step length, and duty factor. As the damping ratio increases, larger thrust coefficients are needed to compensate for the energy lost in spring compression (left). Root locus analysis shows that increased damping and thrusting stabilizes the system relative to the undamped gait, denoted by the 'o' symbol (middle). Similarly to the model with damping and slope, adding damping and compensating with stance thrust stabilizes the three neutrally stable eigenvalues. When comparing the cost of transport for damped gaits with constant gait parameters, thrusting the stance spring appears to be a cheaper method for damping compensation than gravity power.

models. Since gravity powered models have similar energetics to those powered by active torque about the hips, we suggest that stance thrust is a relatively economical means to compensate for dissipation while walking on level ground.

The use of leg springs and set point adjustment introduces a mechanism to perform some level of active control in addition to simply replacing energy lost to dissipation. Such control, whether by feedback, feed-forward, or a combination of the two, could greatly increase the stability margins over that which could be attained through passive dissipation alone, and would allow the model to maintain a steady walk pattern and speed in the face of much larger disturbances. By controlling the set point of the foot springs, energy can be added to or removed from the system, thereby compensating for energy fluctuations due to these external disturbances. An added controller would track the current system state and its corresponding energy, then choose a set point for the leg springs accordingly to achieve desired system energy and a corresponding gait. A discrete controller could easily be implemented by adjusting the ratio of thrust from step to step. Finally, adjustment of set point provides the model with a means to solve the foot clearance dilemma. A compliant walking machine that uses set point control to add energy and stability to the gait could also use this functionality to retract the foot during swing to achieve foot clearance around mid-stance. If this retraction is spread out over the first half of swing, the foot could clear the ground with relatively small modification to the swing leg dynamics. Nevertheless, adjustments to hip stiffness could easily be used to maintain swing period.

Other Behaviors

While this paper focuses on the typical walking gaits produced by humans and other bipeds, it is worth noting that a variety of other walking-like gaits exist. Many of these gaits border the typical walking gaits in parameter space and are easily found by extending the range of parameter searches. We have already shown that skipping naturally results by searching for gaits with increasing energy. However, a skipping gait can also be produced simply by allowing the nominal gait to build up speed on a shallow slope over many steps. Thus we consider skipping to be a walking-like gait because of its smooth connection with typical walking gaits and because the COM velocity is similarly redirected during double support. As speed slows for decreased energy, the M-shape feature of the ground reaction forces eventually flattens out to a single force peak. This paper restricted analysis to the speed range between the single peaked gait and skipping gaits. For even slower speeds, the force profile adopts a three-peak shape and can theoretically produce an infinite number of peaks as walking speed converges to zero or as leg

stiffness grows large (Geyer et al. 2006). Other gaits may produce an asymmetric force profile, where the first force peak can be three times larger than the second. Of these additional gaits, only skipping is ever seen in people, perhaps suggesting that the model is not adequate for these parameter extremes or that these gaits are extremely uneconomical. For example, producing a multiple-peaked force profile for slow walking would require very significant limb work to cycle the COM quickly along the length of the leg. Simply locking out the knee during single support and mimicking an inverted pendulum would certainly be more economical.

Discussion

The compliant passive dynamic model better approximates the measurable conditions of human walking, including ground reaction forces and work performed on the COM. The walking motion can be largely explained by the interaction of compliance and passive dynamic pendulum behavior. With an emphasis on simplicity, only three parameters were minimally required to characterize these motions. Injecting energy into the gait was found to be the easiest solution for increasing speed and without restrictions on how it must be accomplished. The stiffness parameters can then be used to tune the other gait parameters at a given speed. The periods of stance and swing are largely explained in terms of the natural frequency of the spring-mass and pendulum modes, respectively. The swing leg timing in particular is almost entirely determined as one half-period at the swing leg natural frequency. Overall, passive swing leg motion was found to have an important effect on energetics with changes in gait parameters. Swing dynamics also establish the behavior of the leading leg at heel-strike which in turn influences gait stability.

When applied to passive dynamic walking machines, leg compliance appears to be a necessary feature to achieve a cost of transport (COT) lower than is measured in humans. The lowest mechanical COT that has been achieved by a dynamic walking robot was found to match human values of 0.05 (Collins et al. 2005). Arc feet are also fundamental to achieving human-like kinetics at normal walking speeds and reducing the consequences of dissipation. Leg mass and damping are not necessarily bad features because they stabilize the walking motion for a small energetic penalty (COT < 0.01) when anthropomorphic feet (r=0.3) are used. Finally, we propose that modification of the leg spring set position serves as a convenient method to supply energy to the gait, achieve foot clearance, and further stabilize the gait through active control.

When studying human energetics, the model springs may approximate work performed by muscle. However, this need not be the case for compliant prosthetics, which could tune passive compliance to provide appropriately timed actuation for relatively insignificant cost. This result

sets an upper bound on the potential for elastic prosthetics to help amputees walk with improved energy economy. Current compliant prosthetic feet (Dynamic Elastic Response feet) require users to walk with relatively high energy expenditure compared to able bodied counterparts. This work suggests that this compliance may not be optimally tuned for walking economy.

Of note is the fact that the compliant model looks remarkably similar to carbon fiber running prosthesis. These designs are highly tuned for running economy but suffer from instability at slow speeds (it is impossible to stand still in them). In contrast, walking prosthetics are generally designed for the multi-functional demands of daily life, including standing still. It is worth asking whether walking prosthetics would look more like their running counterparts if they were first optimized for walking economy. Our findings suggest that amputees would be benefited when walking by having a more spring-like prosthetic leg with compliance tuned to body mass and leg length and an anthropomorphic roll-over shape. If so, it is possible that these legs could be made reconfigurable to accommodate other needs such as standing.

This model demonstrates how axial compliance produces many of measurable behaviors seen in normal human walking. However, the model does not explain what individual components of the leg are responsible for this elasticity. Different components of the leg likely contribute to its elasticity at different phases of a step. During heel-strike, the leg spring mostly approximates the behavior of the knee and pad of the heel. As the foot rolls over the ground, the ankle joint becomes more important so that by the end of the step at push-off, the leg spring approximates the combined behavior of the knee and ankle. Furthermore, the model provides no insight into the relative contribution of muscle and tendon to producing the global stiffness of the leg, nor how the work is distributed among joints. Finally, it is important to recognize that changes in the model leg stiffness do not necessarily predict changes in muscle activation or force since leg stiffness can be modified through a change in joint configuration. For example, a bent knee will act more compliant for the same muscle activation given a larger moment arm about the knee.

Though performed by a conservative spring, the compliance models work performed by muscle and should be considered when calculating COT or some other metabolic function. Recall that significant damping and leg mass could not alone account for the measured COT in humans. Given the reasonable accuracy with which the compliant model can reproduce the timing and amount of individual limbs push-off work, the model could serve as a useful tool to predict the energetic consequences of model and gait parameters. Our unpublished findings predict that

humans should reduce duty factor for increased walking speed to minimize the positive work performed on the COM. Leg stiffness would then be expected to increase with walking speed.

The relative timing of the push-off and heel-strike, characterized by the duty factor, appears to have significant energetic consequences. Our model produces an array of gaits with the same speed and step length but with varying double support periods. At normal walking speed, the push-off work varies by 18% suggesting that duty factor and step length must be optimized at a given speed. This model could serve a very important tool for investigate how push-off timing affects the energetic behavior of prosthetic feet. Anecdotal evidence from work in our lab indicates that these prosthetic feet may suffer from delayed push-off.

Energy saving mechanisms are thought to explain why we walk instead of run at low speeds. These arguments have traditionally focused on the use measures like percent recovery to judge energy economy. Percent recovery is a measure of how efficiently pendular motion exchanges between potential and kinetic energy during gait. Therefore, work performed along the leg during single support will decrease the measured percent recovery, even if that work is performed elastically. Above preferred walking speeds, percent recovery is known to decrease with increased speed. Eventually the recovery becomes so poor that people are thought to adopt a run to save energy in elastic structures.

More recently, dynamic walking approaches have suggested that the cost of redirecting the COM velocity at the step-to-step transition and the cost of leg swing dominant the energetics of walking. Percent recovery and COM redirection may appear to be at odds except when examined in terms of the compliant walking model. In the compliant model, the details of the COM motion during single support are entirely a function of the conditions at the double support period. For example, the amount of rebound at the middle of single support is dependent on the compression of the spring at the end of the collision phase. At this time point the energy in the leading leg spring is also equal to the amount of work perform in push-off and heel-strike. Thus there is a direct equivalence between the cost of performing the COM redirection and the amount of non-pendular energy exchange experienced during a step. It may be possible then that the percent recovery measure simply tracks the cost of the step-to-step transition at higher speeds.

Appendix 2.1 Effect of model parameters on initial conditions and ground reaction force profiles

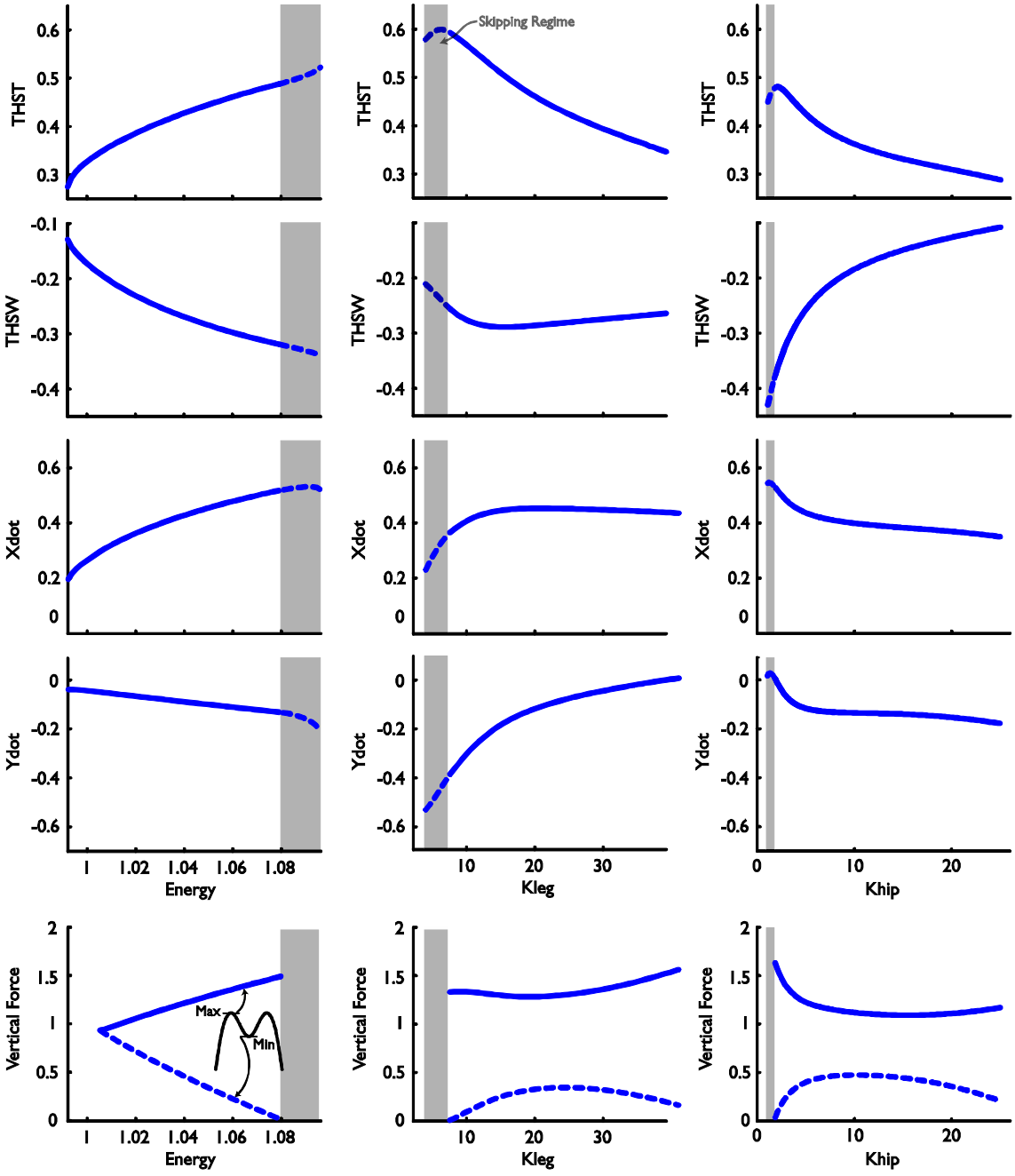

Chapter 3. The Role of Compliance in Walking and Running Gaits

Abstract

Bipeds tune the mechanical compliance of the legs for different locomotion gaits, controlling them to act like pendulums for walking, and more like axially-compliant springs for running. Mechanical properties such as leg compliance do not, however, always distinguish or determine different gaits. For example, a rugby ball rolling end over end can switch to a roll with a hop if simply given more speed (rather than needing a change in its mechanical properties). Spring-like and pendulum-like behaviors also poorly distinguish bipedal skipping, which seems to share elements of both. Perhaps gaits are determined by features other than the mechanical properties of the legs. Here we show that the amount and proportion of energy in the legs distinguishes between gaits much more so than leg compliance or other mechanical properties. A simple mathematical model demonstrates walking, running, skipping, and other bipedal gaits, all arising naturally from the passive dynamics of legs with fixed mechanical properties. The model has pendulum-like but axially-compliant legs, and smoothly changes from walking to skipping if simply given more energy, not unlike the rugby ball. Running requires a redistribution of energy into the axial compliance but not a change in compliance or other properties. Still other gaits arise naturally if the compliance is changed, such as a run without an aerial phase similar that observed in some birds. All gaits may be determined from the various ways that three separate motions may be coupled: the bouncing of a mass on a spring, the swinging of a simple pendulum, and the swinging of an inverted pendulum. Bipeds may tune leg compliance not to select gaits but to take best advantage of the ones that arise from passive dynamics.

Introduction

Human gaits such as walking and running have traditionally been treated as distinct paradigms with different dynamics. In walking, the legs are thought to act as coupled pendulums, whereas in running they compress and extend like springs (Figure 3.1a,b). The passive dynamics of these two modes may generate much of the leg motion and are likely critical to saving energy in both gaits. Such ideas have led to the spring-mass models for running and the inverted pendulum models and passive walkers for walking. A discussion of these locomotion models and their usefulness for describing the energetics and mechanics of walking and running has already been thoroughly treated (Alexander 1995; Farley and Ferris 1998; Kuo et al. 2005). However, inverted pendulum models cannot produce the ground reaction forces or COM trajectories seen in normal walking, suggesting that they do not completely account for the timing and amount of work performed on the COM during a step. Also, these models neglect a double support period, a gait parameter which may be tuned in normal walking to minimize metabolic cost (Alexander 1992). Also, traditional spring-mass running models (except McGeer 1990) neglect swing leg dynamics during single support and leg dynamics entirely during flight phase. McGeer's analysis suggests that the motion of the legs and their resulting configuration at heel-strike is a critical aspect of running stability and energetics. Humans can also walk and run with a single mechanical system, and neither robots nor human studies have yielded a single model that passively generates multiple gaits. Here we show that walking, running, and even skipping can be produced entirely by the dynamic modes of a remarkably simple model which combines pendulum and spring-like behavior.

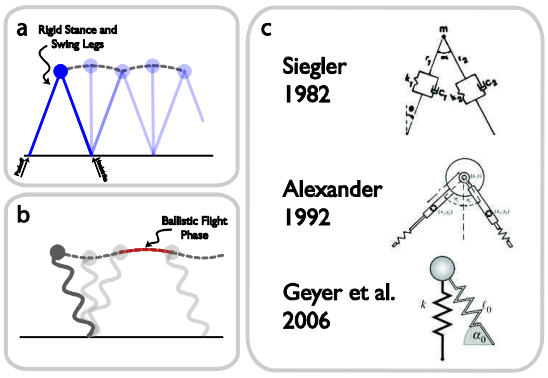

Figure 3.1. Models of legged locomotion. **a.** Inverted pendulum models approximate walking with rigid legs that perform no COM work during single support. **b.** Spring-mass models approximate running with a compliant stance phase and ballistic aerial phase. **c.** Several models have used axial leg compliance to produce more human-like walking features (Siegler et at. 1982) and both walking and running gaits (Alexander 1992; Geyer et al. 2006). However, each of these gaits either prescribes the ground reaction forces under the feet or the swing leg motion.

Several models have been developed that use leg compliance to produce more human-like walking features (Figure 3.1c), however, these models all prescribe aspects of the walking motion in some way (Alexander 1992; Geyer et al. 2006; Pandy and Berme 1988; Siegler et al. 1982). For example, Alexander's model of compliant walking prescribes the force profile under feet. The axial legs in this model then only acted to filter the interaction of the force profile and center of mass. The model of Geyer et al., produces a robust space of walking and running gaits by modifying only three parameters. However, this model does not incorporate swing leg dynamics and sets the angle of attack of the leading leg at heel-strike. Incorporating this type of control in a locomoting robot would require high-gain feedback to accurately target the angle of attack at each heel-strike. Humans do not appear to use end point control to fix the angle of attack, as will be later shown in Chapter 5. We believe that incorporating swing leg dynamics are beneficial for exploring what minimal level of control is necessary to achieve a walking gait. Actuation can be simply added to the hip in the form of a passive torsional spring which speeds up the natural motion of the legs (Kuo 2002a). By modeling the motion of the swing leg and treating the torsional stiffness as a model parameter we can examine how speeding up the oscillation of the swing leg affects gait parameters.

Methods

The simple compliant locomotion model is comprised of a single point mass at the pelvis, two axially-compliant legs with very light point mass feet, and a torsion spring acting between the legs (Figure 3.2a). The model is a simplification of a passive bipedal running model (McGeer 1990a) with the added capability of double support. We developed locomotion simulations that integrated the equations of motion for the model over the course of a step while handling discrete events (transitions) such as heel-strike and toe-off. A step was defined as the period between successive heel-strikes of the opposite foot. We then searched for symmetric, periodic gaits by varying the model parameters and initial conditions in a Newton method search. For definitions of symmetry and periodicity please see Chapter 2.

Since the model is passive, the details of the movement during a step are entirely a function of the initial conditions and model parameters. After non-dimensionalizing the governing variables, the model has only two physical parameters: the torsional hip stiffness, Kp, and axial leg stiffness, Kleg. Gait parameters, such as duty factor and step frequency, are set by tuning the two stiffness parameters and by selecting appropriate initial conditions for the simulation. The speed and type of gait depend on physical parameters as well as the total mechanical energy of the body center of

mass and axial springs, *E*, which is set by the initial conditions of the model states. The model has 3 degrees of freedom during single support, and thus the model energy and movement can be conceptually divided up into three modes: inverted pendulum, pendulum, and spring-mass, which

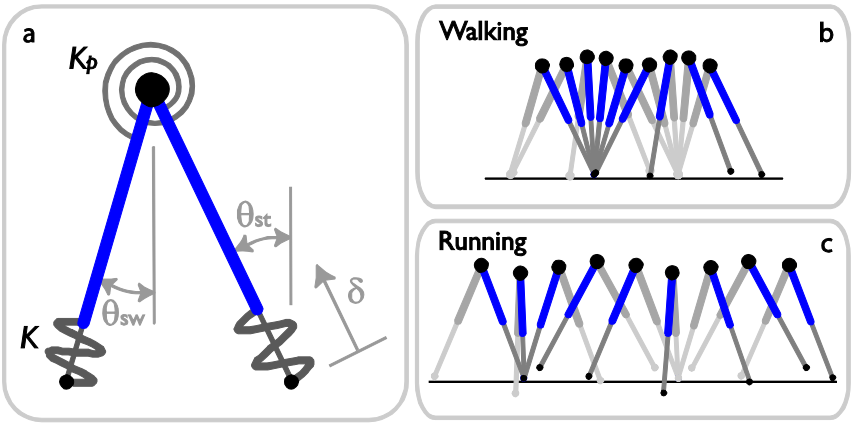

Figure 3.2. The simple compliant locomotion model. **a.** The model has three degrees of freedom during single support: the angle of the stance and swing legs, θ_{st} and θ_{sw}, and the displacement of the stance leg spring, δ. Only two degrees of freedom, the stance and swing leg angles are necessary to represent the model during double support. The model only has two non-dimensional physical parameters: axial leg stiffness, K_{leg}, and torsional hip stiffness, K_p. A third parameter, E, the total mechanical energy of the system, is also added to set bounds on gait speed and constrain the initial conditions. **b.** The COM motion smoothly oscillates up and down as the limbs continuously swing back and forth, switching between inverted pendulum and pendulum behavior in the stance and swing phases, respectively. **c.** The model also produces a running gait with similar motions. While running, the model COM oscillates up and down while the stance and swing legs oscillate back and forth.

correspond to three states: stance angle, θ_{st}, swing angle, θ_{sw}, and stance leg compression, δ.

Results

After adding compliant legs to our simple model, we found that the motion of both legs for an entire walking and running step can be generated completely passively (Figure 3.2 b-c). A variety of human-like gaits may be produced with one simple model, without enforcing ground reaction force patterns or prescribing motions (Figure 3.3). Vertical ground reaction force produced under one leg by these gaits over a stride match well when directly compared with corresponding sample human data. The model gaits were found simply by searching for repeated gaits (limit cycles) that matched the speed, step length and duty factors of the sample human data and was accomplished by tuning the stiffness parameters and initial conditions. To properly match the human model gaits, arcs of non-dimensional radius 0.3 were added to the model feet. This modification was necessary to match anthropomorphic features of the human foot-ankle-complex during walking (Hansen et al. 2004) and reduce collisions at a given step length. Since

no active control is used to generate these gaits and their associated force profiles, we see that the motions for these gaits are produced simply be the interaction of leg stiffness, inertia, and gravity.

The compliant model can reproduce gaits seen over a range of speeds

When walking, the model's compliant legs produce ground reaction forces and perform work on the body similar to humans. For very slow walking (not shown), the force measured under a single leg rises, remains relatively constant, and then falls. As walking speed is increased, the force profile adopts a characteristic double-peaked shape with the beginning of the first peak corresponding to leg loading during heel-strike and ending of the second peak to leg unloading during push-off. As the model walks faster and takes longer steps, more energy is stored in the stance spring (as evidenced by the larger peak ground reaction forces) and the vertical motion of the center of mass is increasingly affected by spring-mass mechanics. With increasing speed, the stance leg spring eventually stores enough energy such that the leg rebounds at mid-step and leaves the ground, producing a skipping gait. Thus skipping appears to be a natural extension of walking and the ultimate product of the increasing leg rebound at mid-step for increasing walking speeds. Unsurprisingly, the model also faithfully reproduces the ground forces seen in running gaits, which are characterized by a single peak of the vertical ground reaction force. Since the simple locomotion model accurately reproduces both walking and running gaits, we will use it to better understand the differences between these gaits.

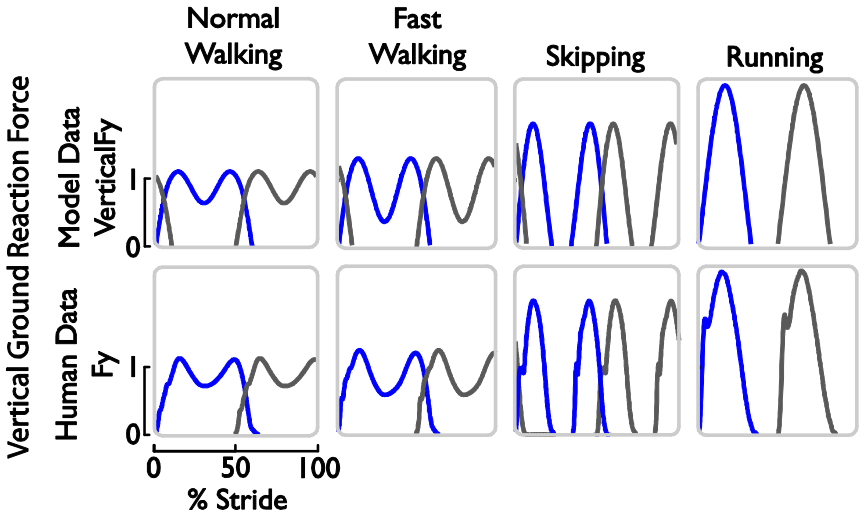

Figure 3.3. Comparison of ground reaction forces among model and example human gaits. Model gaits were found by matching human gait parameters and adding an arc of radius 0.3 to the foot. At a normal walking speed, the force profile adopts a characteristic double-peaked shape with the beginning of the first peak corresponding to leg loading during heel-strike and ending of the second peak to leg unloading during push-off. At faster walking speeds, the model produces larger peak ground reaction forces and a more noticeable dip in force at mid-support. With increasing speed, the stance leg spring eventually rebounds at mid-step, leaving the ground and producing a skipping gait. Human-like running gaits can also be produced and match results found from other spring-mass running models.

Several ideas distinguish walking and running gaits

Several definitions have been proposed to generally distinguish walking and running gaits. Alexander suggested that the varying shape of the ground reaction forces for walking and running could be characterized by a shape factor which scales the relative affect of two cosine terms in a force function (Alexander 1992). While it is clear that the force traces in these two gaits are very different, more observable differences are often used to distinguish them. The presence of an aerial phase has also been used to characterize running, relegating grounded gaits to walking. However, this definition breaks down for some running-like gaits (termed grounded or groucho running) seen in some birds (Rubenson et al. 2004) which may lack an aerial phase altogether and poorly distinguishes skipping gaits, which also have an aerial phase. Perhaps the most comprehensive distinction between walking and running was proposed by McMahon who described these gaits in terms of COM motion (McMahon et al. 1987). He proposed that in running gaits, the COM is lowest during the middle of single support, whereas in walking gaits, the COM is highest during the middle of single support. This definition is based on both empirical evidence and the theoretical models used to describe walking and running (Figure 3.1).

When comparing single support phases of walking and running, the COM motion and energy exchanges appear to very different (Figure 3.4). The distinguishing features are useful for understanding possible energy saving mechanisms used in these gaits (Farley and Ferris 1998). During the support phase of running, kinetic and potential energy vary together and can exchange with spring energy, which in humans could be partially stored by passive elastic structures. During the single support phase of walking, gravitational potential energy and kinetic energy vary opposite to each other since energy is exchanged from one form to the other. These energy saving mechanisms are thought to explain why we walk instead of run at low speeds and why we walk at a preferred speed (Farley and Ferris 1998). Measures like percent recovery, which attempt to quantify the amount of conservative pendulum energy exchange during walking have suggested that pendular energy exchange is less efficient at higher speeds above normal walking and that storing energy elastically in tendon may be more economical (Cavagna et al. 1976). However, we note that running also has a period where kinetic energy can be efficiently stored in a gravitational potential field, the flight phase. From now on, we will refer to these periods of efficient exchange as the gravity exchange phase. Though comparison of single support phases is useful for discussing energy saving mechanisms in walking and running, McMahon's definition may have lead to the false conclusion that the COM motion is overall very different during walking and running.

Walking and running appear to obey similar principles when viewed over an entire stride

When the COM motion of actual human data or that produced by the simplest locomotion model is viewed over a complete stride, we see a different story (Figure 3.4). Here we use data produced from the compliant model based on nominal walking and running gaits (Table 3.1). In both gaits the legs swing back and forth once per stride. The vertical COM motion appears oscillatory in both gaits and it no longer seems to make sense to ascribe walking to purely compass-like motion and running to bouncing. In fact, both gaits look like a bounce, albeit walking as a sudden bounce during double support. In both cases, there is also a large total force peak which coincides with a redirection of the COM and a period of low force at the middle of the gravity exchange phase. Perhaps a better way to distinguish walking and running is to compare them separately during the redirection phase (shaded gray) and the gravity exchange phase (shaded white).

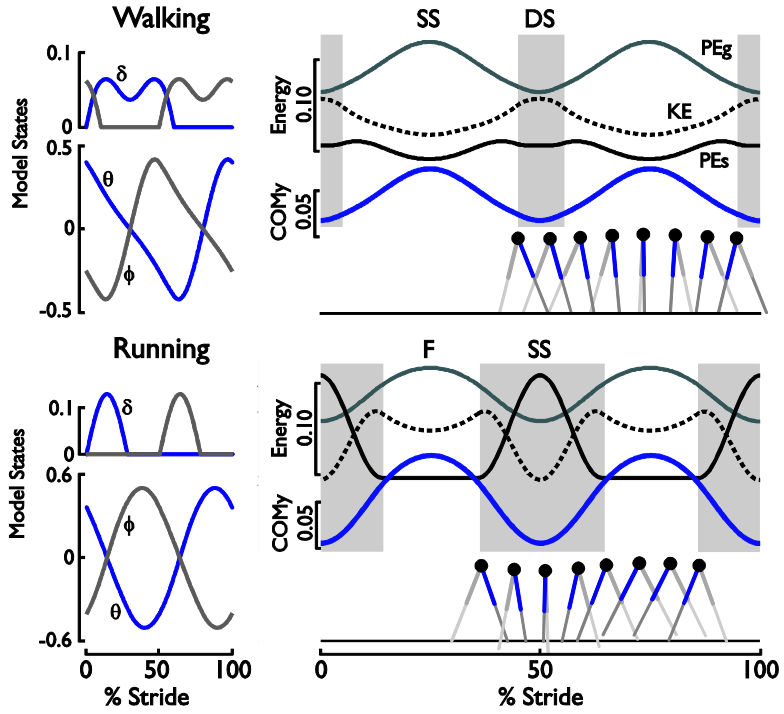

Figure 3.4. The COM motion of walking and running gaits appear similar when redirection phases are aligned and motion is viewed over a stride. Walking and running have been traditionally compared during the single support phase (SS) of each gait. However, when the gaits are aligned as shown, two new comparisons may be made. During the double support phase of walking (DS) and SS phase of running the COM is redirected upwards (shaded gray). In walking the redirection is accomplished through sequenced collisions and running by a single collision. During the SS phase of walking and flight phase of running (F), both models exchange potential and kinetic energy (shaded white). In running the exchange is perfectly conservative and in walking the exchange is at best 70% efficient. Both gaits also demonstrate rhythmic leg swing where the legs complete one back and forth cycle every stride.

Table 3.1. Model parameters and gait parameters for nominal walking and running gaits

	E	K_{leg}	K_p	Speed	Stride Length	Duty Factor
Walking	1.05	20.0	4.00	0.40	1.42	0.61
Running	1.43	15.5	4.10	0.95	2.24	0.35

Walking redirects COM motion with sequenced collisions whereas running uses a single collision

Walking makes use of sequenced force profiles to redirect the COM upwards. This sequencing of push-off and heel-strike can be used to minimize the energetic cost of redirecting the COM (Kuo 2002a; Ruina et al. 2005; Srinivasan and Ruina 2006). The double support period, where both legs push upwards, functionally results in a large vertical stiffness that is more than twice that of running at the same speed (Rebula 2008). This acts to quickly redirect the COM motion such the COM is moving upwards at the start of single support. Running uses a single elastic-like collision to redirect the COM, generally with shallow landing and takeoff angles. Running produces a comparatively lower vertical stiffness than walking and the COM is not redirected until the middle of single support. The theoretical cost of this redirection is less for walking at slow speeds and less for running at fast speeds (Ruina et al. 2005). The exchange of energy during the redirection phase does appear to be significantly different. In running, significant elastic energy is stored at mid-redirection and both kinetic and potential energy reach a minimum. In walking, elastic energy storage changes little as load is transferred from the trailing to leading leg, and kinetic energy reaches a maximum at mid-redirection due to pre-emptive push-off.

Walking and running similarly exchange potential and kinetic energy

Running conservatively exchanges kinetic energy with potential energy during flight as the COM moves in a parabolic arc. Walking can theoretically exchange kinetic energy with potential without loss, but estimates from human experiments show that at best this exchange is 70% efficient (Cavagna et al. 1976). Therefore running is always cheaper in this phase. The COM motion in this phase is closer to a circular, pendular arc.

At steady speed, the most basic task of walking or running gaits is to redirect the motion of the COM upwards after a period where gravity acted to bring it downwards (Ruina et al. 2005). Walking and running then appear to obey similar principles regarding the need to periodically redirect COM motion upwards after interaction with gravity. The only difference then is the details of how the redirection and gravity exchange are accomplished. We ask how these behaviors are differentially produced in the simplest locomotion model. We have already shown

that it is possible to create human-like gaits simply by tuning the spring stiffness parameters and the initial conditions. With inverted pendulum and spring-mass models in mind, we might expect to arrive at the sequenced redirections and pendular support that distinguish walking by using a stiff leg spring. Running gaits may then be found for relatively low leg stiffness values**.**

Walking and running gaits exist over a broad range of parameters

To understand how the model parameters and initial conditions affect gait parameters (speed, stride length) as well as the type of gait (walking, running) we swept the parameter space and total energy (bound on initial conditions) and searched for the existence of limit cycles (Figure 3.5). Three system parameters, K_p, K_{leg}, and E were varied individually about those of the nominal walking gait (Figure 3.4), while the other parameters were held constant. For each new parameter combination, we searched for fixed points and identified the resultant gaits. Walking gaits were found for a small range of energy values E = [0.99, 1.10] and a large range for the spring constants K_p = [1.1, 25.0], and K_{leg} = [2.2, 49.3]. Running gaits were found over a larger range of energy values E = [1.00, 1.10+], a smaller range of hip stiffness K_p = [2.3, 6.5], and for K_{leg} = [13.5, 62.5].

We found that changes in model parameters (Appendix 3.1, Figure 3.5) had similar effects on the stride parameters of walking and running gaits. Leg stiffness was found to positively correlate with stride frequency and negatively correlate with duty factor. Hip stiffness was found to be positively correlated with both stride frequency and duty factor. These trends follow from modification of the spring-mass and pendulum mode natural frequencies, as explained earlier (Chapter 2). The total mechanical energy was also positively correlated with speed and step length.

Surprisingly, we also found that walking and running gaits could exist for the same total mechanical energy and stiffness parameters. These findings are in contrast with the model of Geyer et al. which found an energy gap that divided walking and running gaits. Hence, walking gaits were only found at slow speeds and running gaits at faster speeds. To explore whether gaits co-exist over a larger region of parameter space, we performed a two-dimensional parameter sweep. Leg stiffness and hip stiffness were varied by a 4:1 ratio to maintain relatively constant duty factor and were swept simultaneously with the total energy. The sweep amounts to exploring an angled slice of the three-dimensional parameter volume.

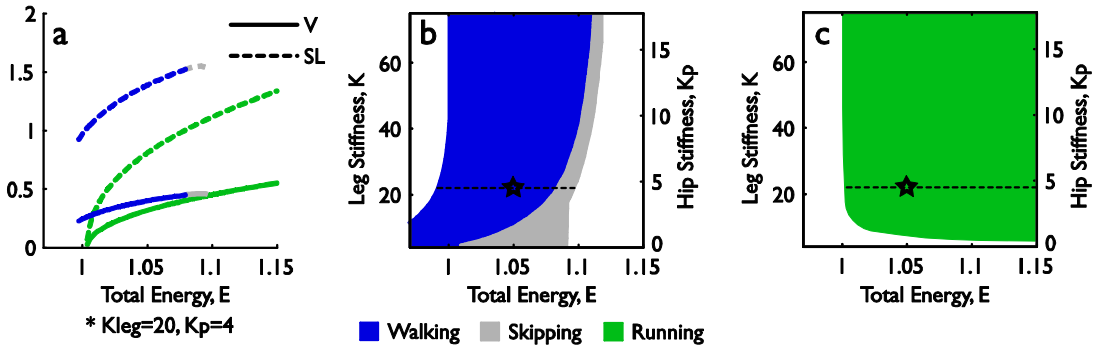

Figure 3.5. Stride parameters and gait regions as a function of stiffness and total energy. **a.** Total energy for fixed stiffness parameters positively correlates with speed and stride length for both walking and running. Skipping gaits naturally appear as walking gaits end for large energy values. Walking gaits are faster than the running gaits for energy values where both gaits exist. **b.** Walking gaits exist over a large range of parameter values. Skipping gaits border the running gaits at higher energy values. **c.** Running gaits exist for most of the parameter space and co-exist with a majority of the walking and skipping gaits. Parameters of the nominal walking gait are denoted by a star symbol.

We found that walking and running gaits co-exist over a large region of parameter space. In fact, running gaits overlapped with 85% of the walking-like gaits. For almost this entire region, walking is faster than running since the running gaits amount to hopping up and down with small forward speed in the chosen energy range. The ground reaction forces are also much higher in running in the overlap region and can be significantly reduced by walking (data not shown). We also found that the region of walking gaits are connected to an area of skipping gaits, meaning that the model smoothly transitions from walking to running as energy is increased.

If humans truly walk with stiff legs and run with compliant legs we would have expected to find walking and running in separate regions of stiffness values. If the existence of model gaits reflects the fact that humans prefer to walk at slow speeds and run at fast speeds, we might have expected to find a region of energy separating the two gaits. However, we have found that walking and running gaits can exist for the same total energy and stiffness over a broad parameter space. Walking gaits then don't necessarily emulate a stiff leg compared to running.

Initial conditions best distinguish between walking and running gaits

For fixed model parameters, only the initial conditions are left to distinguish the two gaits. These define the model states at the start of a step and ultimately determine how much energy is stored in the spring as the center of mass is being redirected upwards. Perhaps the gaits are best distinguished not by the total energy in the system or stiffness but by how the energy is distributed among the pendular and spring-mass modes.

To quantify the amount of energy stored in the different modes of the system, we define a metric called the spring fraction, which is the amount of energy stored in the springs at the middle of the redirection phase divided by the total system energy. This metric provides a basic quantification of the amount of spring-mass behavior in a gait. Since we have previously found that total energy is most closely correlated with speed, we used walking and running gaits over the previous range of total energies with fixed stiffness parameters and calculated their spring fraction.

The spring ratio categorization seems to separate the gaits in to two regimes: a walking-like regime and a running-like regime (Figure 3.6). For a large range of energies, there exists both a walking gait and a running gait. At slow speeds (energy), the walking-like regime is comprised of unique looking gaits that transition from a three-peaked ground reaction force profile to the more commonly recognized two-peak profile. At high speeds (energy) the walking-like regime transitions from normal looking walking to a skipping gait, demonstrating again that skipping naturally extends from walking as speed is increased. For a different set of stiffness parameters, we found that the model produces a grounded running gait seen in some bird species (Figure 3.7). With the new stiffness parameters fixed, the model smoothly transitions from a grounded running gait to a running gait with an aerial phase. This finding is supported by metabolic studies in the ostrich which shows that the gait parameters and metabolic cost of grounded running smoothly connects with aerial phase running (Rubenson et al. 2004).

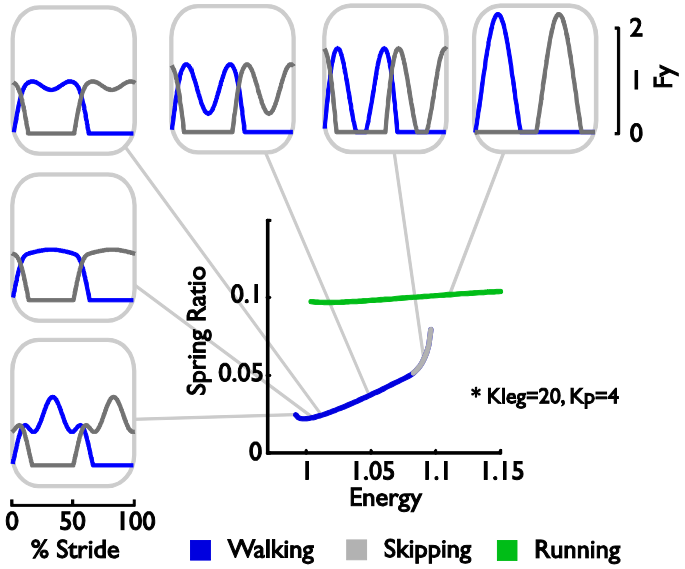

Figure 3.6. Spring ratio distinguishes walking and running gaits by characterizing the amount of spring-mass behavior in a gait. Walking and running gaits exist for the same model parameters but have distinct spring ratio measurements. When energy is varied for fixed stiffness parameters, walking gaits smoothly transition from a three-peaked force profile to a common two-peak profile and then to a skipping regime. Over this range, running gaits exhibit more spring-mass behavior than the walking-like gaits.

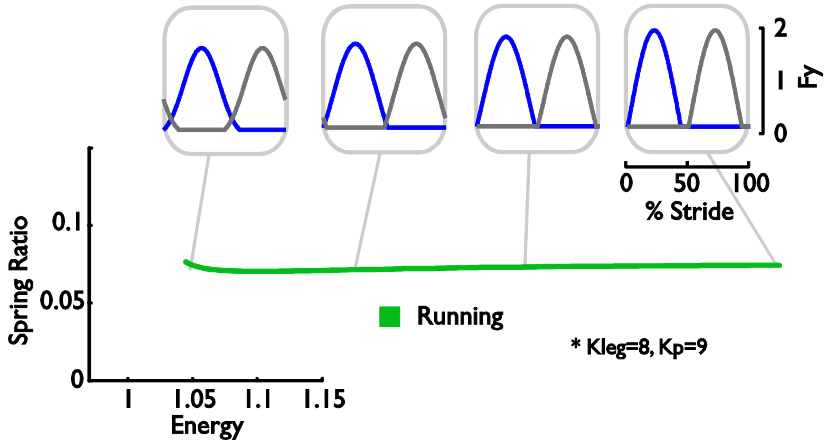

Figure 3.7. Model smoothly transitions between grounded and aerial running gaits. For a modified set of stiffness parameters, the model may exhibit force profiles characteristic of grounded running gaits. As energy is increased the model smoothly transition to the more common aerial running gaits and with similar spring ratio.

In contrast to the smooth transitions between walking and skipping or grounded running and aerial running, a transition between running and walking involves a distinct change in the initial conditions. This result follows from human experiments, which show that both kinematic and kinetic patterns abruptly change in the transition from walking to running (Hreljac 1995). McMahon and Cheng used a spring-mass model for running to predict that humans maintain constant leg stiffness independent of the speed of running. Here we show that leg stiffness need not be changed to transition from walking to running or speed up or slow down within these regimes.

Tuning the stiffness parameters can still be used to advantageously adjust gait parameters, and is likely to minimize the energetic cost of locomotion at a given speed. However, the most significant difference between walking and running gaits lies in the initial conditions, which determine how the energy of the system is distributed between pendular and spring-like modes. While compliant legs are needed to reproduce human-like walking motions, walking and running engage this elasticity differently, leading to a more inverted pendulum like behavior in walking and more spring-mass behavior in running. Walking uses the sequenced collisions to store less energy in the spring-mass motion and retain the majority of the energy in inverted pendulum behavior. Running uses a single collision to store a large amount of energy elastically.

Appendix 3.1 Affect of stiffness parameters on stride features

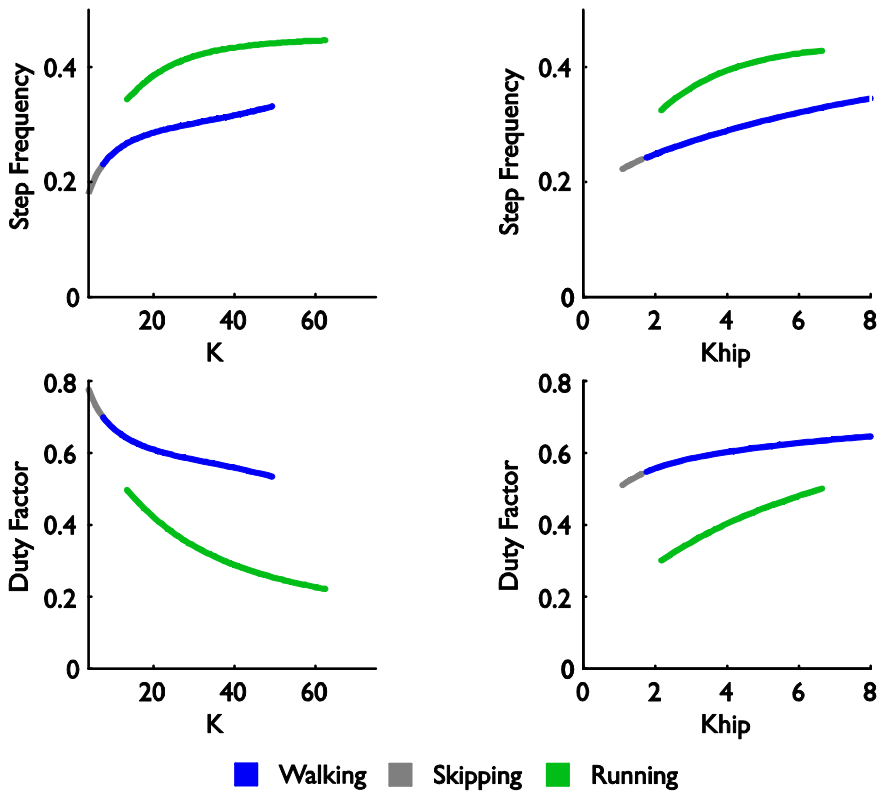

Chapter 4. Role of State Estimation in the Generation of Rhythmic Limb Behavior

Abstract

We use a simple walking model to study how the feedforward and feedback nature of central pattern generators (CPGs) can be optimally combined to produce steady walking motions. We interpret combined feedforward and feedback behavior in terms of a state estimation control scheme, whereby the neural oscillator acts as an internal model of limb dynamics that is updated by sensory information. The theory of state estimation suggests there is an optimal balance of feedforward and feedback control for improved performance given unexpected disturbances and imperfect sensing. To demonstrate this interpretation, we applied a controller with state estimation to a simple walking model under the presence of noise. The control system used an internal model of the limb dynamics to produce an estimate of the system state used to drive hip torque. The error signal, from model stretch sensors, was used to refine the state estimate via an estimator feedback gain, *L*, which scaled the relative influences of feedforward and feedback on the controller (i.e. small *L* produces pure feedforward and large *L* produces pure feedback control). Step-to-step variability was calculated from the standard deviation of leg angles and velocities at the beginning of each double support period. We show that a purely feedforward CPG is highly sensitive to unexpected disturbances and can take few steps before falling over. Pure feedback control analogous to reflex pathways can compensate for disturbances but is sensitive to sensory error. The model simulations demonstrate that step-to-step variability induced by the presence of noise is minimized when the relative roles of feedforward and feedback are appropriately balanced. In the presence of noise, there is an optimal combination that produces better performance over either feedforward or feedback alone. Errors increased as the L scaled either toward pure FF or pure FB, reaching a maximum of about 3.5 times the minimum position error and 4.2 times the minimum velocity error. Given these findings we suggest that CPG behavior is best understood when considering disturbances and imperfect sensing and that they serve a primary role to filter sensory information rather than to simply generate motor commands.

Introduction

Rhythmic pattern generating circuits located in the spinal cord have been well established in vertebrates over the past century. These circuits are thought to contribute to the basic walking motion, as evidenced by the fact that spinalized cats can produce stepping patterns that resemble normal walking (Grillner and Wallen 1985). Charles Sherrington was one of the first to demonstrate that decerebrate cats could produce basic stepping motions and largely attributed these motions to reflexes (Sherrington 1911). Sherrington proposed that simple reflexes are the fundamental units of movement and that complex tasks are produced by combining these simple reflexes. Around the same time, Thomas Graham Brown also isolated the spinal contributions of the stepping pattern (Brown 1914). However, he found that spinalized cats could produce stepping motions even when the afferents fibers were cut, suggesting that sensory feedback was not necessary to produce rhythmic motor behavior. These two competing ideas, central versus peripheral generation of rhythmic behavior, co-existed through much of the 20th century.

By the mid-1980's, the concept of motor programs renewed interest in central sources of motor commands and studies of de-afferentation emerged that again demonstrated that sensory feedback is not necessary to produce stereotyped rhythmic motor patterns (Knapp et al. 1963; Marsden et al. 1984; Rothwell et al. 1982). Today, the presence of spinal neural networks that produce rhythmic motor commands even when isolated from afferent feedback is well established for a large number of vertebrates (MacKay-Lyons 2002) and motor programs are thought shape the motor output in walking (Ivanenko et al. 2006). For example, isolated spinal cords from neonate rats are still able to produce fictive locomotor signals even when afferent fibers are dissected (Grillner and Wallen 1985). These neural networks are generally referred to as "central pattern generators" though this naming is largely the product of studies in invertebrates where the specific pattern generating neurons can be isolated. In humans, the existence of central pattern generators is still under speculation and most of our understanding of how they apply to humans is drawn as extensions from other vertebrate models.

With the discovery of central pattern generators, emphasis shifted toward feedforward motor pattern generation and away from patterns created solely through reflexive sensory feedback pathways. However, sensory feedback is known to play an important role in normal behavior (Cohen 1992), and feedforward control alone is known to perform poorly in the presence of disturbances. Furthermore, when limb dynamics and the metabolic cost of a motion is significant, movements are also likely to be more efficient when driven by sensory feedback.

Despite our evolving comprehension of the neural components of movement, we still lack a framework to understand how sensory feedback should be processed and combined with more feedforward components to produce efficient and accurate movements. We are left with two ideas about CPGs that are seemingly at odds: 1) CPGs can produce rhythmic bursting activity even when sensory feedback is removed (feedforward). 2) CPG oscillation can be entrained or modified with sensory feedback and this feedback is important for normal movement. We then ask, what benefit would be gained by combining both FF and FB?

Control theory may offer insight into how to address these issues, especially given knowledge of the uncertain conditions under which locomotion is achieved. For example, direct feedback is known to perform best when controlling a system that is faced with unexpected disturbances. Such a control strategy would make direct use of sensory information to generate motor commands but would be highly sensitive to imperfect sensory information. In contrast, a feedforward control strategy is robust to sensor error since motor commands are generated based on an intrinsic pattern. Biology must contend with similar imperfect conditions. Sensor error may take the form of noisy or inaccurate afferent signals from muscle spindles that are also limited by sensory precision. Disturbances may come from noisy or inaccurate force generation within the muscles or from outside disturbances such as from uneven terrain. Both types of uncertainty are significant even for healthy persons and often magnified due to locomotor impairments or aging (Horak et al. 1989; van Beers et al. 2002). Control systems have long used an approach called state estimation to process sensory information when faced with potentially noisy and inaccurate sensors. The scheme essentially generates a prediction of the system states by filtering sensory information through an internal representation of the system dynamics. The predicted states can then be used to generate motor commands through based on a feedback control strategy. We explore how state estimation theory can explain the combination of feedforward and feedback behavior and make predictions about how to best combine sensory feedback with intrinsic CPG patterning through adjustment of sensory feedback weightings.

We interpret the combined feedforward and feedback nature of CPGs in terms of an internal model that is updated by sensory information, or in other words, state estimation. Kuo (2002b) has previously proposed that neural oscillators can be interpreted as an internal model of limb dynamics. We are proposing that CPGs can be thought of as state estimators during rhythmic tasks such as walking. Under the state estimation interpretation, the internal model produces

feedforward commands even when the feedback is removed, resembling fictive locomotion in biology. The theory of state estimation suggests there is an optimal balance of feedforward and feedback control for improved performance in the presence of noise. In this sense, CPGs are not seen to simply produce motor commands for muscle activation but also to process sensory information through an internal representation of the limb dynamics.

We will test whether a state estimation controller applied to a compliant walking model can mimic observed behavior of CPGs, including their roles as sensory filters. We first show that either feedforward or feedback control can be used to produce identical limit cycles of leg motion under ideal conditions. However the pure feedforward controller is found to be extremely sensitive to unexpected disturbances, and demonstrates significant divergence from the nominal limit cycle. We then show that the pure feedback system also suffers from poor performance when sensory information is imperfect. We will demonstrate how an optimal combination of sensory feedback minimizes step-to-step variability in the presence of noise and that the overall behavior of the model mimics that of a CPG.

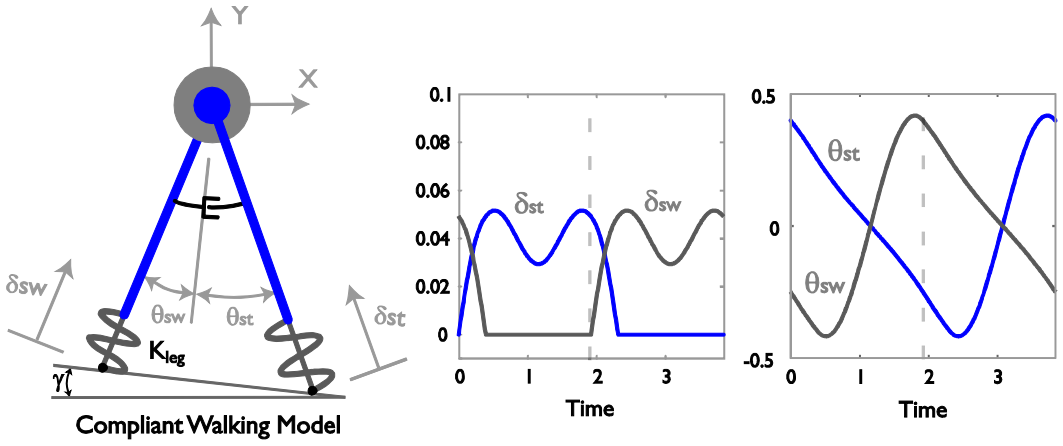

Figure 4.1. The compliant passive walking model has six degrees of freedom (left): the angle of the stance and swing legs, θ_{st} and θ_{sw}, the displacement of the axial leg springs, δ_{st} and δ_{sw}, and the horizontal and vertical location of the pelvis, x and y. The model also has three physical parameters: axial leg stiffness, K_{leg}, damping ratio of the leg stiffness, ζ, and slope, γ. At a nominal walking gait of 1.25 m/s, the model exhibits a characteristic shape of spring-mass behavior along the direction of the leg (middle) as the limbs continuously swing back and forth (right). The legs switch between inverted pendulum and pendulum behavior in the stance and swing phases, respectively.

Compliant Walking Model

As a simple model of limbs undergoing a rhythmic walking motion, we employed a compliant passive dynamic model of two-dimensional, biped walking. The model is comprised of a point mass at the pelvis and two damped axially-compliant legs with very light mass and point feet (Figure 1). We have previously shown that the model's compliant legs produce ground reaction forces and perform work on the body in a manner that resembles human walking (Chapter 1).

The model is further under the influence of active torques applied to the legs and may be generated from an intrinsic pattern (feedforward) or based on the states of limbs (feedback). These torques are meant to generally resemble the action of a torsional spring of stiffness, K_p, placed at the hip (see Chapter 1 and Equation 1). Spring-like torques are a convenient way to approximate the muscular effort necessary to force the legs to swing back and forth faster than the natural frequency of pendulum-like leg motion (Kuo 2002a). While forced leg swing requires metabolic expenditure, this action can be overall advantageous by limiting the need to take very long steps at faster walking speeds.

$$u = K_p \cdot f(\theta, \phi, t) \tag{1}$$

The model's dynamics contribute substantially to its gait. The model produces a double support phase of finite duration, a double-peaked vertical ground reaction forces as observed empirically, and smooth COM trajectories. If the initial conditions are chosen properly, this model can maintain a steady, rhythmic limit cycle in the absence of perturbations. We have also shown that this limit cycle can be stabilized against small disturbances by adding damping to the leg springs. The model must then walk down a shallow slope to recover energy lost in dissipation, and this choice of slope is unique for given damping and walking speed.

Walking simulations were developed to integrate the equations of motion, handle discrete events such as heel-strike and toe-off, and apply a smooth or impulsive transition to the next continuous state. For example, when the force produced by the trailing leg falls to zero during double-support, the model recognizes a toe-off event and smoothly transitions to single support, applying a ground contact constraint for the stance leg and locking the swing leg spring in place. The generic model has 6 degrees of freedom, where θ_{st} is the angle of the stance leg as measured from the counterclockwise vertical, θ_{sw} is the angle of the swing leg as measured from the counterclockwise vertical, δ_{st} is the instantaneous compression of the stance leg, δ_{sw} is the instantaneous compression of the swing leg, x is the horizontal location of the center of mass, and

y is the vertical location of the center of mass. Ground contact constraints further reduce the independent degrees of freedom during single and double support. Reduced equations of motion were then developed to simulate the single support period (Equations 2-4) and double support (Appendix 4.1),

$$\ddot{x} - (K_{leg}\delta_{st} + D\dot{\delta}_{st})\sin\theta_{st} + \sin\gamma = 0 \quad (2)$$

$$\ddot{y} + (K_{leg}\delta_{st} + D\dot{\delta}_{st})\cos\theta_{st} - \cos\gamma = 0 \quad (3)$$

$$\ddot{\theta}_{sw} + \sin(\theta_{sw} - \gamma) + \ddot{x}\cos\theta_{sw} + \ddot{y}\sin\theta_{sw} = u \quad (4)$$

$$D = \zeta \cdot \sqrt{4\,K_{leg}} \quad (5)$$

where K_{leg} is the stiffness of the axially compliant legs, D is the damping coefficient, γ is the slope, and u is the externally applied torque. Since the mass of the legs is assumed to be very small, the hip torque required to force leg swing is also small and has a neglible effect on the stance leg dynamics (u is absent from Equation 1 and 2). The damping coefficient, D, is determined based on the damping ratio, ζ, of the of the axial leg motion and stiffness, K_{leg} (Equation 5). All parameters and states are non-dimensionalized by total mass, uncompressed leg length, L_o, and the gravitational constant, g. Time is thus in units of $\sqrt{L_o/g}$. When inspecting the equations for single support we see that the dynamics resemble the actions of a system of coupled pendulums bouncing on a spring. Simulations of the model were implemented in Matlab and the limit cycle behavior was computed using numerical integration with the ode45 function. The relative integration error tolerance was 1e-8, and the absolute tolerance was 1e-9.

If the model is to undergo steady a state-state rhythmic walking motion, the initial conditions must be properly matched to the model parameters. Given ground contact constraints, the initial conditions of a step, which occurs at the beginning of double-support, are fully described by the four states: $[\theta_{st}\ \theta_{sw}\ \dot{x}\ \dot{y}]$. Limit cycles for each set of model parameters were found using a first-order Newton shooting method, which simultaneously found the initial conditions and slope that produced a steady walking gait. By modifying the model parameters we can control the features of the walking gait, such as speed and step length. We previously found that the overall speed of the gait is simply determined by the mechanical energy in the system set by the initial conditions (Chapter 2). The time of ground contact and step frequency, can be largely adjusted at a given speed by tuning the the leg stiffness, K_{leg}, and the spring-like active torques, u, applied to the legs. The leg stiffness largely adjusts the frequency of the spring-mass mode along the length of the leg and thus period of stance duration. The actuator adjusts the frequency of the inverted pendulum

mode or swing period. The damping ratio ζ determines how much speed is lost during one step cycle, roughly modeling the energy loss due to dissipatory effects, which can occur both continuously, as with friction, and over short intervals, as during foot contact at heel-strike.

To restrict the number of free parameters, the model conditions will be restricted to those corresponding to a moderate walking speed v = 0.4 (1.25 m/s). This constraint makes γ, D, and the initial conditions functions of three free parameters K_p, K_{leg}, and ζ. The following free parameter values are chosen for the nominal limit cycle (Figure 2c): K_p = 4.75, K_{leg} = 22, ζ = 0.1. At a speed of v = 0.4, this results in a slope of γ = 2.05e^{-2} , damping coefficient D = 0.94, and initial conditions $[\theta_{st}\ \theta_{sw}\ \dot{x}\ \dot{y}]$ = [0.434 -0.294 0.467 -0.114]. The parameter set is chosen to roughly correspond to a normal walking gait with step length s = 0.696 (0.696 m) and duty factor d = 60%.

Feedforward and Feedback Systems

In the ideal case in which unexpected disturbances are absent, identical limit cycles may be produced using any combination of feedforward and feedback control to pattern the active hip torque. A pure feedback control applies the active torque as a function of state only (i.e., the models's position and velocity) and not explicitly of time (see Figure 2b). In order for the model to exhibit periodic behavior, it is necessary that the torque actuator perform no net work over a stride. One simple feedback law is

$$\textbf{FB}: u(\theta_{st}, \theta_{sw}) = K_p \cdot (\theta_{st} - \theta_{sw}) \tag{6}$$

where K_p is a control feedback gain that could be set by a higher-level (descending) command. Essentially this control mimics the actions of a linear torsional spring, with stiffness K_p, and acts on both legs with a torque that is proportional to the angle between them. This direct feedback strategy is analogous to reflex pathways activated by muscle stretch sensation through Ia afferents. It may be verified that the FB control law provides neutral stability through application of Poincare maps (Chapter 1). When applied to a model with damping in the compliant leg springs, the model gains local asymptotic stability.

A pure feedforward control, however, applies the hip torque as a function of time only, regardless of the pendulum's state (see Figure 2a). The timing and amplitude of hip torque is prescribed to be that which would result from a passive torsional spring acting on two legs moving through the nominal trajectory. In absence of an analytical definition, the control law is simply

$$\textbf{FF}: u(t) = K_p \cdot (\theta^*_{st}(t) - \theta^*_{sw}(t)) \tag{7}$$

where $\theta^*_{st}(t)$ and $\theta^*_{sw}(t)$ are the time histories of the leg angles following the nominal trajectory. This feedforward strategy is analogous to the motor behavior recorded from spinal neurons in fictive locomotion preparations, where motor commands are generated by an intrinsically generated rhythm in the absence of sensory feedback. Unlike the control of a pendulum model of leg swing (Kuo 2002b), we will show that this feedforward implementation is generally unstable when applied to a passive walking model.

The pure feedforward and feedback control laws differ in behavior only when unexpected disturbances act on the system. We will consider two types of disturbances: process and sensor noise. Individual sensors provide incomplete information about the motion of local body segments and are subject to sensor noise, which adds unexpected errors, v, to the measurements of state. Error of this type is present due to limits on sensory precision and loss of accuracy by transmission of sensory information through multiple synapses and along axons (Kuo 2005). Physical disturbances are random external perturbations that cannot be predicted or corrected for ahead of time such as experience when walking over uneven terrain. Motor output variability also contributes to uncertainty and represents random fluctuations in muscle force in response to a motor command. We collectively refer to random physical disturbances and motor output

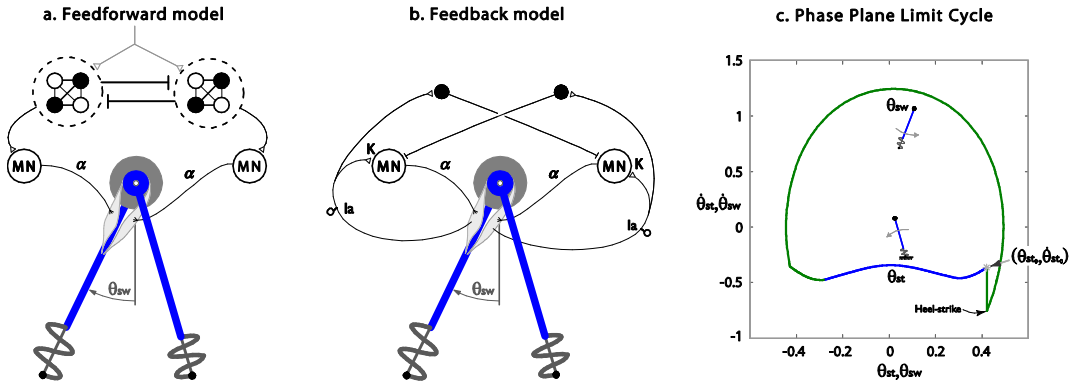

Figure 4.2. Model of pure feedforward and feedback circuits that produce rhythmic hip torque. **a.** The feedforward system is driven by two organizations of neuronal half-centers (enclosed by dashed circles) which are coupled through reciprocal inhibition and produce alternating bursts of activity driving motor neurons (MN). Muscles, activated by α motor signals, produce motion of the swing leg. **b.** The feedback system also produces rhythmic leg behavior, but only through activation of muscle stretch receptors (Ia afferents), which then generate reflexive motor commands and contralateral inhibition. If gain K_p is properly tuned, system will exhibit limit cycle behavior. **c.** Pure feedforward or feedback control can generate identical limit cycles, shown here in a phase plane plot of leg behavior over a stride. Limit cycle shown is for parameters K_p = 4.75, K_{leg} = 22, ζ = 0.1.

variability as process noise, w, which apply unexpected forces and torques to the model.

Equations (2-4) are therefore replaced by

$$\ddot{x} - (K_{leg}\delta_{st} + D\dot{\delta}_{st})\sin\theta_{st} + \sin\gamma = w_4 \tag{8}$$

$$\ddot{y} + (K_{leg}\delta_{st} + D\dot{\delta}_{st})\cos\theta_{st} - \cos\gamma = w_5 \tag{9}$$

$$\ddot{\theta}_{sw} + \sin(\theta_{sw} - \gamma) + \ddot{x}\cos\theta_{sw} + \ddot{y}\sin\theta_{sw} = u + w_6 \tag{10}$$

and the feedback law FB (Equation 6) is made a function of measured states corrupted by noise

$$x_m = x + v_1,\ y_m = y + v_2,\ \theta_m = \theta_{sw} + v_3 \tag{11}$$

$$\dot{x}_m = \dot{x} + v_4,\ \dot{y}_m = \dot{y} + v_5,\ \dot{\theta}_m = \dot{\theta}_{sw} + v_6 \tag{12}$$

rather than the actual states. Note that the measured swing leg angle will now simply be referred by θ_m. To characterize average behavior, these disturbances may be modeled as band limited white noise, as described below.

Sensitivity to Disturbances and Measurement Noise

We will use the compliant walking model under rhythmic hip torque activation to demonstrate two key principles related to motor control: pure feedforward systems are highly sensitive to process noise and pure feedback systems are sensitive to sensor noise. We first apply a 1% perturbation to the initial stance angle, which results in oscillatory behavior of the pendulum under FF control, as shown in Figure 3. To describe this behavior, we compute errors in the model position and velocity states from the nominal values directly at the beginning of each step. After completing 10 steps, the FF system diverges away from the nominal limit cycle and produces an error of 4.2% in θ_{st} and 9.0% in θ_{sw}. The errors continued to grow and the model falls by failing to achieve foot clearance before heel-strike after 17 steps. On the previous step, the model error had grown to 19.8% in θ_{st} and 48.3% in θ_{sw}. To demonstrate the sensitivity on parameter values, the maximum θ_{st} errors after 10 steps were computed for a range of values for K_p and ζ (see Figure 3b). The parameter domain was for feedback gains between 2 and 12, and ζ between 0 and 1.5. The maximum position error on θ_{st} is most influenced by the level of damping; however, the model was found to be relatively less sensitive to the perturbations for low feedback gains. Large errors, 10% and above, were found for values of ζ less than approximately 0.75, and errors above 5% were generally found for values of K_p above 3. The FF system is extremely unstable for low damping values and only consistently took 10 steps above $\zeta = 0.4$.

This high sensitivity at low damping levels is expected given the limited passive stability of similar walking models (Chapter 1), which suggests that the passive dynamics of the limbs have little tolerance for poorly timed hip torque. These results are in contrast to those found for the FF control of a simple pendulum model, which is globally stable and therefore more robust to command errors. Sensitivity can be reduced for low levels of K_p since the active control has a less significant effect on the motion of the swing leg as compared to the passive dynamics. However, for all parameter values the model eventually falls and higher values of damping only slow the divergence away from the limit cycle. Overall, we find that a walking model controlled with feedforward hip actuation to be highly sensitive to even small disturbances (~1%).

The performance of the FB system is far superior under the same conditions. Assuming accurate measurements of the state (i.e., $v_{1\text{-}6} = 0$) and using $K_p = 4.78$, the control law supplies a corrective hip torque based on the actual perturbed angle between the legs, so that the maximum error is 0.45% in θ_{st} and 0.60% in θ_{sw}. For an initial perturbation of 10% to the initial stance angle, the maximum error is 5.2% in θ_{st} and 7.4% in θ_{sw}. Settling time, defined as the number of steps required for error to go below 2%, is 5 steps for θ_{st} and 7 steps for θ_{sw}. Similar results are found over a range of feedback gains (2 to 12). However, this behavior is not invariant to the choice of the damping ratio. For a model with $\zeta = 0$, the perturbation causes the model to converge to a new limit cycle at a faster speed for a positive perturbation. Models with intermediate damping

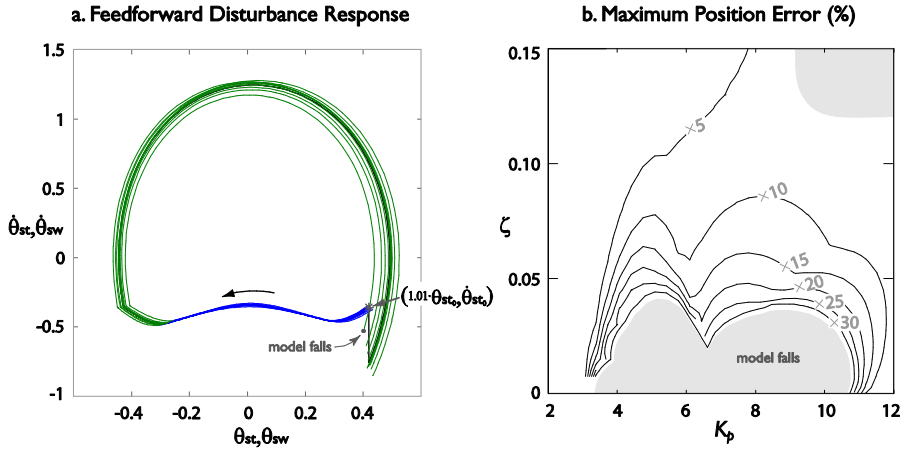

Figure 4.3. Feedforward systems are sensitive to physical disturbances. **a.** When the feedforward system of Fig. 2a is started with an initial stance angle with 1% error, model can exhibit unstable behavior and fast divergence away from limit cycle. Applied to a passive walking model, this control is highly sensitive to the presence of disturbances and the model falls over after 16 steps. **b.** Maximum stance angle position error after 10 steps due to 1% initial stance angle perturbation, as a function of parameters K_p (feedback gain) and ζ (damping ratio). Domain is restricted to parameter values that yield limit cycle behavior and for which the model takes at least 10 steps. Note that all parameter values result in greater than 1% position error, demonstrating high sensitivity to perturbations.

values do converge to their original limit cycle but with increasing settling time for decreasing damping ratio. Still, the pure FB system robustly prevents perturbations from growing indefinitly over many steps and averts model failure from a fall.

However, the FB system does not perform as well when measurements are imperfect and subject to noise. To assess sensitivity to measurement noise, we evaluated steady-state behavior, defined as root-mean-square (rms) errors of the model states. Variability is used as a performance metric because it generally reflects the ability of the controller to filter sensor noise and reject process disturbances, both of which tend to increase the overall variability of the legs states and adversely affect stability. Performance was measured over 200 steps, with simulated white noise, using noise parameters determined as follows. First, nominal disturbance noise w_{4-6} with zero mean and arbitrarily chosen covariance (Equation 13-15), and no measurement noise, was applied to the FB system,

$$w_4 = \left(c \cdot K_{leg}\delta_{sw_0} \sin\theta_{sw_0}\right)^2 \tag{13}$$

$$w_5 = \left(c \cdot K_{leg}\delta_{sw_0} cos\,\theta_{sw_0}\right)^2 \tag{14}$$

$$w_6 = \left(c \cdot K_p \cdot \left(\theta_{st_0} - \theta_{sw_0}\right)\right)^2 \tag{15}$$

where c is a weighting factor that scales noise values. The covariance values were calculated from the initial spring-like force at each of the degrees of freedom multiplied by the weighting factor (c = 1/500). These noise values produced steady-state root-mean-square errors on the measured states (Table 4.1). Root-mean-square error was computed at discrete instances, based on the deviations of the model states from the fixed point directly at the beginning of each step for 200 steps. These errors were used to determine nominal measurement noise characteristics: $v_{1\text{-}6}$ had zero mean and variances equal to 16 times the steady-state disturbance noise response. In other words, v_1 and v_2 had rms values of 2.41% and 0.48%, respectively. The factor of 16 was arbitrarily chosen so as to produce large steady state errors under pure FB control. For computations, band-limited white noise was simulated with normally distributed random numbers applied in discrete time with a zero-order hold and a step size 10 times smaller than the nominal step period.

Table 4.1. Root mean square error of model states for nominal disturbance noise applied to FB system.

State	x	y	θ_{sw}	$\dot{x}$	$\dot{y}$	$\dot{\theta}_{sw}$
RMS error	0.60 %	0.12 %	1.01 %	1.01 %	3.40 %	1.09 %

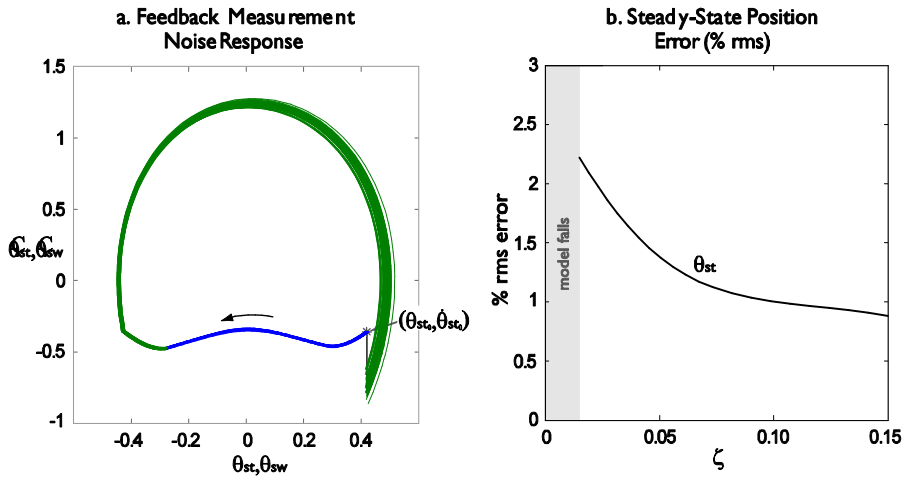

Figure 4.4. Feedback systems are sensitive to measurement errors. **a.** When the pure feedback system of Fig. 2b is subject to noise-like errors in state measurements, the error in state output persists while fluctuating about the nominal limit cycle. **b.** Steady-state stance angle position error, shown as percentage rms (root-mean-square), as a function of ζ (damping ratio). Steady state error is halved at higher damping ratios, while the model falls below a value of 0.015.

When the FB system operates with no disturbance noise but with nominal measurement noise as described above, the model states fluctuate about the fixed point (see Figure 4a). The steady-state rms errors are 1.13% in θ_{st} and 2.29% in θ_{sw}. Performing the same calculations for a range of parameter values for ζ (Figure 4b) but with identical noise attributes, we find that the FB system grows increasingly sensitive to measurement noise inversely proportional to damping ratio. The steady-state error can be reduced by more than a factor of 2 at high levels of damping but never eliminated. Below a value of $\zeta = 0.015$, the model fails to take the total 200 steps.

In contrast, the FF system is completely insensitive to measurement noise, because hip torque is applied according to an internally timed rhythm rather than noisy sensory measurements.

Hybrid Feedforward/Feedback Control

We have found that FF and FB are both sensitive and robust to different types of noise. FF control is extremely sensitive to unexpected disturbances and is even unstable when applied to the compliant walking model. Yet FF is entirely robust to sensor imperfections. A FB control scheme was able to stabilize the compliant model against disturbances but performed poorly when faced with sensor error. Given these opposite strengths and weaknesses of the two control schemes, we investigate whether combining them in some manner would be advantageous. To study the interaction of FF and FB, we require a system that will respond with pure FF and FB behavior at the extremes and with a relative mixture of the two based on some choice of parameters. Upon

developing the control scheme, we will simulate control of the compliant model with both types of noise and evaluate behavior for varying relative amounts of FF and FB.

The hybrid model adds sensory elements from the FB system to the intrinsic CPG behavior of the FF system. Fundamental to the hybrid model is the assumption that the neural oscillators model the dynamics of the compliant walking model, such that the bursting behaviors of the oscillators encode information about limb states. The predicted motion is then used to drive the FB system through control feedback gain, K_p. The oscillator output drives the hip torque that in the FB system would be driven directly from the sensed angle between the legs. We also assume the behavioral equivalent to α-γ co-activation such that muscle stretch receptors adjust sensitivity during movement, effectively signaling deviations from the expected movement. The sensors then signal unexpected disturbances and the resulting error signals, *e*, feed back to the oscillators through the CPG feedback gain or synaptic weighting, L, which updates the FF component based on the perceived movement. Essentially the CPG feedback gain scales the controller between FF and FB behavior. When *L* is 0, error information is ignored and the system generates autonomous rhythms. Hip torque is then applied based on the nominal leg angle trajectory, just as in the FF system. As *L* approaches infinity, the half-center oscillators are immediately entrained to the error signals, meaning the internal model will nearly exactly follow the sensed body state. This system

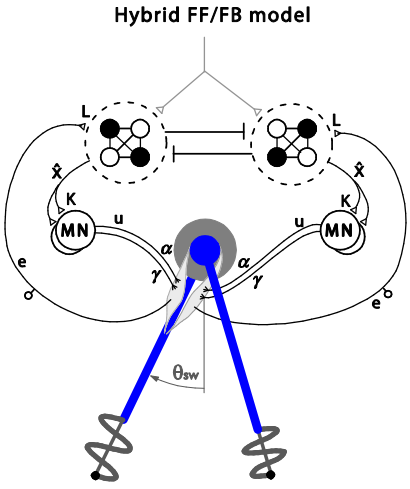

Figure 4.5. Hybrid system combines feedforward (FF) and feedback (FB) behavior. Half-centers (enclosed by dashed circles) produce bursts of α-γ co-activation with control gain $K_{p,}$ simultaneously activating motor neurons responsible for sending motor commands, u, to muscle groups that produce movement about the joint and to muscles connected to stretch receptors. Co-activation causes these stretch receptors to adjust sensitivity during movement so that afferents effectively provide error information, *e*, signaling unexpected disturbances. Sensory feedback, which then contains these error signals, entrains half-center oscillators with *CPG* feedback gain or synaptic weighting, *L*. When *L* is zero (afferents removed), error information is ignored and the system generates autonomous rhythms (feedforward). When *L* is very large, half-centers are immediately entrained to error signals and the system behaves essentially like a reflexive network (direct feedback). For any value of *L*, the hybrid system produces identical limit cycles, though with varying degrees of sensitivity to unexpected physical disturbances and measurement errors.

behaves essentially like the reflexive pathways of the pure FB control. Intermediate values of L, produce a controller between the two extremes, whereby sensory error information is filtered through the internal dynamics of the neural oscillators.

Mathematical implementation of the hybrid model will be expressed in state space notation. Defining the vectors and system matrices and adopting θ_{sw} as simply θ,

$$X \equiv \begin{bmatrix} x \\ y \\ \theta \\ \dot{x} \\ \dot{y} \\ \dot{\theta} \end{bmatrix}, \quad Y \equiv \begin{bmatrix} x_m \\ y_m \\ \theta_m \\ \dot{x}_m \\ \dot{y}_m \\ \dot{\theta}_m \end{bmatrix}, \quad W \equiv \begin{bmatrix} w_1 \\ w_2 \\ w_3 \\ w_4 \\ w_5 \\ w_6 \end{bmatrix}, \quad V \equiv \begin{bmatrix} v_1 \\ v_2 \\ v_3 \\ v_4 \\ v_5 \\ v_6 \end{bmatrix}, \quad A \equiv \begin{bmatrix} 0 & 0 & 0 & 1 & 0 & 0 \\ 0 & 0 & 0 & 0 & 1 & 0 \\ 0 & 0 & 0 & 0 & 0 & 1 \\ \frac{d\dot{x}}{dx} & \frac{d\dot{x}}{dy} & 0 & \frac{d\dot{x}}{d\dot{x}} & \frac{d\dot{x}}{d\dot{y}} & 0 \\ \frac{d\dot{y}}{dx} & \frac{d\dot{y}}{dy} & 0 & \frac{d\dot{y}}{d\dot{x}} & \frac{d\dot{y}}{d\dot{y}} & 0 \\ \frac{d\ddot{\theta}}{dx} & \frac{d\ddot{\theta}}{dy} & \frac{d\ddot{\theta}}{d\theta} & \frac{d\ddot{\theta}}{d\dot{x}} & \frac{d\ddot{\theta}}{d\dot{y}} & 0 \end{bmatrix}, \quad B \equiv \begin{bmatrix} 0 \\ 0 \\ 0 \\ 0 \\ 0 \\ 1 \end{bmatrix},$$

$\Gamma \equiv I_{6x6}$

the state-space equivalents to (8-12) are

$$\dot{X} = AX + Bu + \Gamma W \tag{16}$$

$$Y = X + V \tag{17}$$

There is one difference with the former system incorporating noise: the disturbance vector W has been expanded to include additional components $w_{1\text{-}3}$ that affect $\dot{x}$,$\dot{y}$, and $\dot{\theta}$ through Γ. The Jacobian matrix A was found by linearing the equation of motion (8-10) about a time point at the middle of single support. A separate matrix is calculated to estimate dynamics during double support and was found by linearizing the equations of motion for double support about the middle of that phase.

Since the CPG oscillators are assumed to model the behavior of the compliant walking model, the CPG's intrinsic state will be referred to as the state estimate, $\hat{X}$, with dynamics described by

$$\dot{\hat{X}} = A\hat{X} + Bu - Le \tag{18}$$

$$e = \hat{X} - Y \tag{19}$$

Reflected in the equations is the fact that the CPG has access to the motor command, u, and the sensory error, e, but not the values for the noise parameters. We also note that L is manifested as a 6x6 matrix of sensory weighting in this equation. Finally, a hybrid control $u = f(\hat{X})$ is constructed by applying the FB control law to the intrinsic state of the CPG, which now applies a torque in proportion to the estimate angle between the legs:

$$\textbf{HFB}: u(\hat{\theta}_{st}, \hat{\theta}_{sw}) = K_p \cdot (\hat{\theta}_{st} - \hat{\theta}_{sw}) \quad (20)$$

The estimator model described by (18) and (19) autonomously generates expected limb motion, and only requires feedback of sensory error, *e*, to correct that expectation. The hybrid model then demonstrates the ability to intrinsically generate motor activity even in the absence of sensory feedback. Sensory feedback can be eliminated either for L=0 or by removing *e*, equivalent to the fictive locomotion experiments where the afferents fibers are severed or blocked.

Optimal State Estimation Theory

We now discuss how the CPG feedback gain, *L*, will be chosen within the state estimation framework and implement a method for scaling this parameter between the FF and FB extremes. The main features of a state estimator are the same as our hybrid controller: an internal, forward model that uses a copy of the motor commands (efference copy) to estimate or predict system states and weighted sensory information which is used to correct the state estimate. The major task when developing a state estimation controller is determining *L*, which influences how strongly estimation errors update the internal model. There are many strategies for choosing L, but the optimal state estimation, or Kalman filter, approach is known to make optimal use of sensory information in the presence of both noise-like disturbances and measurement errors

Our hybrid system will use a single parameter, the CPG feedback index (CFI), to set the relative contributions of FF vs. FB (Kuo 2002b). The CFI is used in the design equations for the optimal state estimator as follows:

$$AP + PA^T - PV^{-1}P + 10^{CFI}\Gamma W \Gamma^T = 0 \quad (21)$$

$$L = PV^{-1} \quad (22)$$

where the vectors *W* and *V* are the covariance estimates for the process and sensor noise, respectively. The estimator gain *L* depends on the relative magnitudes of *W* and *V*, and the CFI inflates the influence of *W* over *V*. The estimator is theoretically optimal at CFI = 0, but simulations are needed to evaluate the overall performance because the walking model and control system are nonlinear. For increasing positive values of CFI, the entries of L grow large and the system approaches the pure FB extreme. For decreasing negative values of CFI, the entries of L approach 0 and the system behaves more like the pure FF system.

Performance of Hybrid Feedforward/Feedback System

We will consider performance as a function of the CPG feedback index (CFI) for nominal values of free parameters. Performance will be evaluated in terms of % rms error of the model states after each heelstrike. When designing the hybrid system model, we introduced noise-like disturbances $w_{1\text{-}3}$ acting on the velocity states. To ensure that $w_{4\text{-}6}$ remain the dominating influence as in the previous example, we set cov w_1 = 0.1cov v_1, cov w_2 = 0.1cov v_2, and cov w_3 = 0.1cov v_3.

Using the nominal parameter settings, we calculated CPG feedback gains for integer values of the CPG feedback index ranging from –5 to 5. Simulations were performed for 200 steps, and rms errors relative to the fixed point were calculated as described above. Simulations were also performed using pure FF and FB control under the same conditions to serve as limiting cases.

Results show that there is a hybrid combination of FF and FB that is least sensitive to the disturbance/measurement noise combination (see Figure 4.6). For the noise levels chosen, minimum steady-state errors were 1.87% rms in θ_{sw} and 3.24% rms in $\dot{y}$. This minimum was achieved with a CPG feedback index of 0, though the difference in error was negligibly small between feedback indices of -2 to 2. Errors increased as the CPG feedback index was increased in positive and negative directions, reaching a maximum of about 3.5 times the minimum θ_{sw} error and 4.2 times the minimum $\dot{y}$ error at a feedback index of -5. In the limiting case of pure FF control, the model was unable to take 15 steps at the nominal noise parameters before falling down. In contrast, the pure FB controller, though not ideal, was robust to falls for the noise parameters chosen.

Discussion

We found that for systems subject to both disturbances and imperfect sensing, there is an optimum balance of feedforward and feedback behavior that results in better performance than either FF or FB alone. Our results provide a context to understand two competing theories, which contend whether direct feedback, analogous to reflexes, or more hard-wired, motor programs are responsible for producing motor commands. These views differ on the role sensory feedback plays in generating motor commands: reflexive theory suggests that sensory information can be used directly to produce motor commands while motor program theory suggests that this sensory information can be largely ignored in lieu of internal representations of the body motions. Ignoring sensory information may be a useful strategy when sensory channels are noisy or inaccurate. However, sensory feedback is known to play an important role in normal behavior and

a feedforward control in the form of rhythmic motor programs was found to perform poorly in the presence of disturbances. State estimation theory explains that there is an advantage to combining a more hard-wired, top-down approach with a very dynamic feedback based approach even when sensory information is available and that this combination is best understood when considering disturbances and sensor noise. In this sense, CPGs are not seen to simply produce motor commands for muscle activation but also to process sensory information through an internal representation of the limb dynamics.

There were a few anomalies in which the results did not conform to expectations. Estimation theory predicts that errors should increase monotonically towards the feedforward and feedback extremes as the CPG feedback gains decrease or increase, respectively, from their optimal values. However, we found a relatively shallow change in percent root mean square error for CFI values between -2 and 2. This result may be partially explained by the presence of collisions which instantaneously change the angular velocity of the leading leg at heel-strike. These collisions effectively act as unexpected disturbances since the continuous time integration of sensory error within the internal model has no knowledge of them. Given these heel-strike disturbances, we

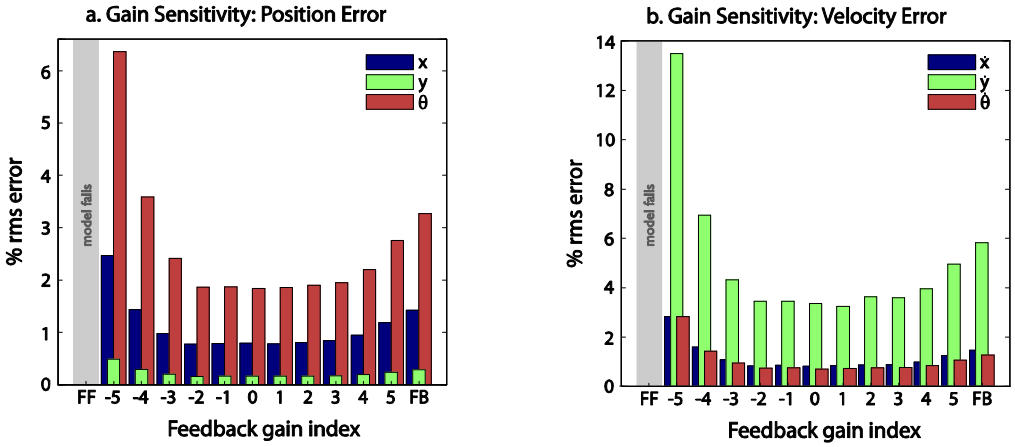

Figure 4.6. Steady-state position and velocity errors for hybrid system subject to noise-like perturbations and measurement errors, as function of *CPG feedback gain index* (CFI), which sets value of CPG feedback gain. Negative index values of increasing magnitude correspond to decreasing *L*, approaching pure FF system. Positive index values of increasing magnitude correspond to increasing *L*, approaching pure FB system. In the limiting case of pure FF control, the model was unable to take 15 steps at the nominal noise parameters before falling down. **a.** Position errors, in terms of % rms, are minimized for feedback gain index of 0 but are relatively insensitive between feedback indices of -2 to 2. Errors increase by a factor of 3.5 over minimal value for pure FF and FB systems. **b.** Velocity errors, in terms of % rms, are also minimized for index 0, with errors increasing by a factor of 4.2 over minimum.

found overall that pure FF was the least desirable method to control the passive walking model and was the only condition for the hybrid controller that could not take a significant number of steps before falling. However, these disturbances affect the model at all levels of feedback and may have washed out a distinctive optimum at a CFI of 0.

We were also generally limited by the amount of noise that could be applied to the passive walking model. Unlike, a swinging pendulum (Kuo 2002b) the passive model does not benefit from a global stability. With the pendulum, we can generally be confident that on average the pendulum will oscillate about an angle of zero. Though the passive model incorporates pendular motion, a limit cycle is attained by sequential step-to-step transitions that reset the pendular motion. The model falls down if the swing leg fails to clear the ground as it swings forward or if the hip on the stance leg fails to move over the support foot. Therefore there is a relatively narrow range of possible perturbations (compared to the simple swing pendulum) that can be applied while still achieving sequential steps. Furthermore, our calculation of L was based on a linearization of the equations of motion (matrix A, Equation 16) at points along the nominal limit cycle. For large levels of noise and significant departures from the limit cycle, the CPG feedback gain may have been improperly tuned for stabilizing the internal estimate of model states.

The model studied here was designed to mimic the basic features of normal walking kinematics. Though we modeled the propulsive properties of the legs with a passive spring, we expect that this actuation is also advantageously generated through feedback. Again, the advantage of feedback is that the timing is adjusted based on the actual state of the limb, and the disadvantage is sensitivity to sensory errors. Just as with the present model, a state estimator could optimally combine the advantages of feedback and a feedforward internal model to control the rhythmic compression and extension of the legs.

Applying the state estimation hypothesis to motor control (including posture and rhythmic movment) leads to interesting predictions. As suggested in Kuo 2002b, artificial corruption of a sensory channel should result in a decrease in its weight, assuming plastic adaptation of synaptic weighting is possible. In particular, an estimation scheme provides a convenient means to calculate and optimally respond to this sensory error. The magnitude of a feedback response to subsequent sensory perturbation would then be predicted to decrease with decreased weighting on that sensory channel. However, this result cannot be distinguished from a more hardwired reflexive strategy or other feasible motor control strategies with decreased feedback gains. A state

estimation filtering strategy can be distinguished from a more hardwired reflexive use of sensory information based on two criteria: 1) Temporal filtering of sensory information 2) Differential processing of sensory information during active (self induced) and passive (externally induced) movements.

For healthy persons with access to reliable sensory information, these two schemes are indistinguishable from one another and both predict a fast response to external perturbations. Under normal conditions (when all sensory information is providing similar and reliable information) the estimation tracking is expected to be fast, so that temporal response to a perturbation would likely be dominated by the feedback strategy. However, a neural realization of state estimation would show signs of temporal filtering of sensory signals (Kuo 2005). This temporal filtering can be witnessed when error is introduced on a single sensory channel such that the error updates the internal model states more slowly. The time scale of this sensory filtering will be dependent on the weighting of that sensory channel. When these sensory systems experience perturbations on all sensory channels, both strategies show fast responses of the body states that are limited by body dynamics and delays in generation of the motor commands. When these sensory systems experience perturbations on a single sensory channel, they show different rates of output response. The direct feedback strategy will still show a fast response because the sensory information is not processed before being used for feedback control. The state estimation strategy will show a slowed response as the perturbation introduced on a single sensory channel updates the internal model states more slowly. It should be noted that both of these control strategies predict that the magnitude of a feedback response to sensory perturbation increases with weighting on that sensory channel. However, a state estimation strategy can be differentiated from a direct feedback strategy based on the rate of the feedback response to sensory perturbations. State estimation predicts that the rate of the feedback response to sensory perturbation increases with weightings on that sensory channel whereas the rate of the feedback response is insensitive to this weighting when used in a direct feedback strategy.

By utilizing a forward model that makes use of efference copy, it is possible to cancel out the sensory effects of self motion, and thereby distinguish between intended motions (either produced by muscle work or expected interaction with the environment) and unintended motions. The state estimation hypothesis predicts that sensory information would be differentially processed for self or externally produced movements. Experimental evidence indicates that some sensory systems in insects and even primates use efference copies of motor commands to adjust their sensitivity

(Bellebaum et al. 2005; Poulet and Hedwig 2002; Roy and Cullen 2004; 2001). This sensory processing scheme therefore filters sensory information in a manner that emphasizes sensory signals generated by external unintended motions. For example, it has been shown that the vestibular nuclei in squirrel monkeys, which receives afferent signals from the vestibular semicircular canals, differentially processes self generated and externally produced head movements, suggesting the use of efference copy (Roy and Cullen 2001).

Internal models explain how sensory processing is accomplished but also give us insight into a possible method for motor learning, where errors in sensory prediction are used refine motor commands. For example, a forward model could provide the proper signals for motor learning by translating errors between the desired and actual sensory outcomes of a movement into the subsequent errors in the motor command. This learning is not possible under reflexive control because motor commands are generated by the movement itself and therefore there is not central motor command to correct.

Internal models have become an accepted paradigm for motor planning and learning for goal-directed, upper extremity movements (Hwang and Shadmehr 2005; Kawato 1999; Scott 2004; Wolpert et al. 1995). State estimation models of posture control have also successfully predicted the properties of human sway during sensory organization tests, where visual or proprioceptive information is rendered inaccurate by sway referencing (Kuo 2005). We suggest that the concept of internal models are not just relevant to upper extremity tasks, but that these principles are relevant at many levels of motor control, even for the most stereotyped of movements, such as walking. In humans, the existence of central pattern generators is still under speculation and most of our understanding of how they apply to humans is drawn as extensions from other vertebrate models. However, evidence for their existence in the humans is supported by several studies (Duysens and Van de Crommert 1998b; MacKay-Lyons 2002), including those that demonstrate phasic modulation of proprioceptive reflex gains during rhythmic tasks such as walking and arm cycling (Zehr 2005).

Finally, the hybrid model studied here was meant as a conceptual exercise rather than physiological model of human gait. It is our basic hypothesis that sensory processing is performed during locomotion in a manner akin to state estimation, where sensory information is filtered through an internal representation of the body dynamics. This hypothesis does then does not specify the details of feedback control strategies used or the details of how this is

accomplished in the nervous system (motor primitives, etc). The compliant walking model is complicated enough to produce specific features of the walking task but simple enough that feedback back rules can be generically represented. In the case of generating the rhythmic walking motion, a simple feedback rule whereby the legs extend and compress like linear springs reproduces the major features of sagittal plane COM motion in human walking.

Chapter 5. Direction dependent control of balance during walking and standing

Abstract

Human walking has previously been described as controlled "falling." Other evidence, however, suggests gait may also have self-stabilizing aspects requiring little control. Computational models suggest that the fore-aft component of walking may even be passively stable from step to step, whereas lateral motion remains unstable and requires control, as through active foot placement. Walking humans might then rely less on integrative sensory feedback, such as vision, for anterio-posterior (AP) balance than medio-lateral (ML). We tested whether healthy humans (N = 10) exhibit such direction-dependent control by applying low-frequency perturbations to the visual field (a projected virtual hallway) and measuring foot placement during treadmill walking. We found step variability to be nearly ten times more sensitive to ML perturbations than AP. Root-mean-square ML step variability increased approximately linearly with ML perturbation amplitude (R^2 = 0.81, P = 5.7e-4), with the slope defining the ML sensitivity, which was 9.4 times the AP sensitivity (P = 0.0005). For comparison, similar perturbations were applied during quiet standing, which was expected to be actively controlled in all directions, but less so in directions with large base of support (BOS). We measured variability of center of pressure as an indicator of active control, and found normal standing to have a reversed direction dependence compared to walking. The AP sensitivity was 2.3 times greater than ML (P = 0.039), suggesting that the low AP sensitivity of walking was not simply due to physiological limitations of visual processing. Tandem (heel-to-toe) standing yielded ML sensitivity 3.0 times greater than AP (P = 0.005), suggesting that the BOS indeed influences the degree of instability. The direction-dependent sensitivity of walking suggests that the central nervous system may gain stability in the AP direction through an uncontrolled series of falls.

Introduction

The central nervous system (CNS) uses sensory feedback for active control, particularly to compensate for instabilities. The upright human body, for example, is unstable and its balance is continuously stabilized through the integration of visual, vestibular, proprioceptive, and other sensory inputs. Other tasks may use sensory information in a discrete rather than continuous manner. In particular, walking has periodic dynamics, where the discrete step-by-step stability may be quite different from posture. This may therefore dictate differences in active control, as well as how sensory information is integrated and used for step-by-step stabilization. An implication of these differences is that clinical tests of standing balance may not capture some aspects of gait stability. Here we present an experimental study of the role of vision in the control of balance during walking, contrasted with its role in upright standing. We propose that the dynamics of walking may provide a degree of passive, step-by-step stability that is not present in standing.

The inverted pendulum dynamics of the upright body make posture unstable without control. The CNS actively balances the head, trunk, and legs on the ground with corrective torques based on sensory feedback (Horak and Macpherson 1996; Johansson and Magnusson 1991). Although local spinal reflexes certainly contribute to this control (Allum 1983; Carpenter et al. 1999), higher level integration of visual, vestibular, and other inputs is also important for stability (e.g., Nashner et al. 1982). Reduction of sensory information typically degrades posture control, and the combined loss of both visual and vestibular inputs makes posture considerably less stable despite the remaining presence of proprioceptive inputs (Black et al. 1983). Integrative feedback control is demonstrated even more directly by active body sway, which can be induced simply from experimental perturbations of the sensory inputs. For example, vision can be driven by an artificial visual field (e.g., Keshner and Kenyon 2000; Mahboobin et al. 2005; Peterka 2002b), and vestibular inputs can be manipulated by galvanic stimulation (e. g., Fitzpatrick et al. 1994; Inglis et al. 1995). The instability induced by multisensory loss demonstrates the necessity of integrative feedback, and the sensitivity of posture to driven inputs quantifies the contributions of sensory inputs to that integration.

Walking is potentially subject to similar instability as posture. This has led to the interpretation of walking as “controlled falling” (Perry 1992). Not only must walking be stabilized from step to step, but the head and trunk must also be continuously balanced as with posture (Keshner et al. 1988). The continuous balance component would then be expected to incorporate similar

integrative feedback, as evidenced by the sensitivity of postural sway to visual perturbations during gait (Keshner and Kenyon 2000; Warren et al. 1996). But unlike posture, it is also possible that walking exhibits some degree of step-to-step stability, as demonstrated by dynamic walking machines that can walk stably with no feedback control whatsoever (McGeer, 1990). The difference between continuous and step-to-step stability is demonstrated by a passive dynamic walking toy that is unable to stand up but can walk stably down a ramp (Coleman and Ruina 1998). Incorporating roughly human-like geometry and three-dimensional dynamics in a computational model of dynamic walking (Kuo, 1999), we found the fore-aft motion to exhibit passive dynamic stability, and the lateral motion a high degree of instability. The lateral instability is easily controlled through active adjustment of lateral foot placement with each step, driven by sensory feedback. But no feedback is necessary for the model's step-to-step stability in the fore-aft direction.

Applied to human walking, only the lateral component of active, step-to-step control would be expected to require higher level integrative feedback. This control would require sensation of body motion, similar to that used for continuous-time control of posture. But there would be little need for integrative feedback for the fore-aft motion, because lower level (e.g. spinal) feedback may be sufficient for the legs to support body weight and behave like pendulums. Indirect evidence for direction-dependent stability is given by previous observations that human subjects walking without vision have greater lateral step variability but no change in fore-aft step variability (Bauby and Kuo 2000b). The increase in lateral variability is analogous to the degradation of posture that results from removal of vision. If step-to-step stability is indeed different from postural stability, the difference might help explain why clinical tests of posture do not always predict gait ability (Shimada et al. 2003; Visser et al. 2008). The contribution of vision to step-by-step walking stability has yet to be quantified, but could be assessed by perturbing the visual field along multiple directions, as has been demonstrated in posture (Streepey et al. 2007b).

The purpose of the present study was to evaluate the sensitivity of step-to-step foot placement to perturbations of the visual field. We hypothesized that walking is passively unstable in the medio-lateral (ML) direction and therefore actively stabilized through integrative feedback control but passively stable (or rather, actively stabilized at lower levels of the CNS) in the anterior-posterior (AP) direction. We expected that ML foot placement would be highly sensitive to ML perturbations to the visual field, but that AP foot placement would be relatively insensitive to AP perturbations. To control for the possibility that observed sensitivities are simply due to direction-

dependencies in visual processing rather than the task dynamics, we also compared walking to an analogous set of continuous balance tasks. During standing, we expected the degree of instability, and hence sensitivity to visual perturbations, to depend on the base of support and therefore the type of stance. For both step-to-step balance during walking and continuous balance during standing, we hypothesized that the visual contribution to active control increases with the degree of passive instability.

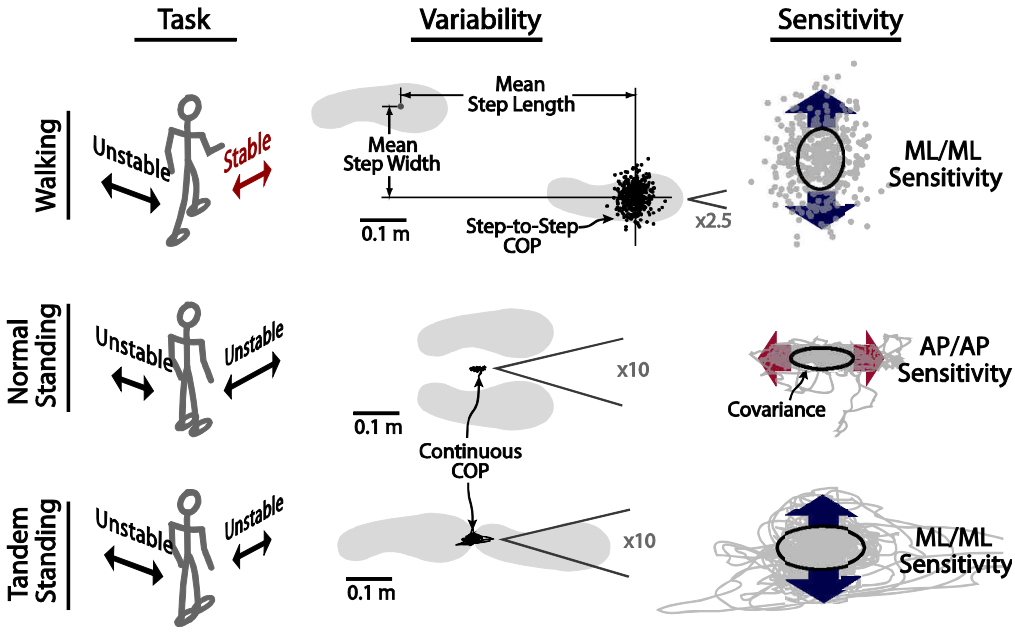

Figure 5.1. Predictions of sensitivity to visual perturbations, for walking, normal standing, and tandem standing. Previous computational models (Kuo 1999) predict that walking may have passive dynamic stability in the AP direction but instability in the medio-lateral (ML) direction, controlled with active foot placement. An indicator of active control is step variability, measured through the center of pressure (COP) under each foot. Models predict high sensitivity of ML (step width) variability to ML visual perturbations ("ML/ML sensitivity"). Ellipses denote covariance of step variability, computed from root-mean-square step deviations. The stability of standing is expected to depend on the base of support, with greater instability in the AP direction for normal standing, and the ML direction for tandem (heel-to-toe) standing. Variability of continuous COP, as opposed to step-to-step COP in walking, quantifies posture control. High AP/AP sensitivity to visual perturbations is expected during normal standing, and high ML/ML sensitivity during tandem standing.

Methods

We measured the effect of visual perturbations on COP variability, as an indicator of the degree of integrative control during both walking and standing (Figure 5.1). For walking, we used COP variability as a measure of discrete, step-to-step foot placement contributions to active control (Bauby and Kuo 2000b). For standing, we used COP variability as a measure of continuous application of torque against the ground. Given ideal sensors and no disturbances, both types of COP would be expected to exhibit no variability. But internal and external perturbations, along

with imperfect sensors, contribute to variability of discrete (foot placement) COP during walking, and continuous COP during standing. We induced visual sensory perturbations with a virtual reality environment, and quantified both types of variability with covariances, which describe the root-mean-square (RMS) variability in the ML and AP directions. During walking, these correspond to RMS variability in step width and step length, respectively. These variabilities were recorded as a function of visual field perturbations, yielding direction-dependent sensitivity measures. We applied oscillatory perturbations to the visual field during walking and two types of standing, with the feet placed side-by-side ("normal") or heel-to-toe ("tandem"). Sensitivities to perturbations were quantified as the change in RMS variability per unit change in perturbation amplitude, using step-to-step COP variability for walking, and continuous COP variability for standing.

From our computational models of walking, we expected greater instability in the lateral direction. This would be manifested as a high sensitivity of ML variability to ML perturbations, referred to as "ML/ML sensitivity," and a lower AP/AP sensitivity (Figure 5.1, right column). In contrast, we expected standing to be generally unstable, perhaps with the degree of instability depending on direction. Empirical observations suggest that normal stance is more unstable in the AP direction (Marigold and Eng 2006; Paulus et al. 1984), and tandem stance in the ML direction (Hong et al. 2007), perhaps due to differences in the base of support (Day et al. 1993; Henry et al. 2001; Horak et al. 2005). This leads to expectations of greater AP/AP sensitivity during normal stance, and greater ML/ML sensitivity during tandem stance.

Experiment

Volunteer human subjects performed walking or standing with visual field perturbations applied through a virtual reality display (see Figure 5.2). Ten subjects (6 male, 4 female, aged 24.3 ± 4.1 years; body mass 73.1 ± 15.4 kg;

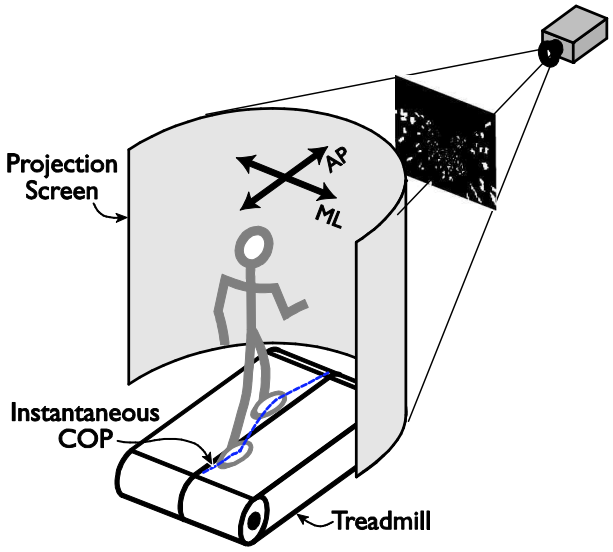

Figure 5.2. Experimental Setup: Virtual reality setup uses a single projector and curved rear projection screen to provide wide viewing angle and immersive feeling of moving within a tiled hallway. Force plates mounted underneath a split belt treadmill were used to record the center of pressure (dashed line).

leg length 0.92±0.08 m; mean ± s.d.) provided informed consent and participated in this study. All were healthy adults with no known visual conditions or impairments affecting daily walking function; including dizziness, vestibular conditions, somatosensory loss, or neurological disorders. Both walking and standing were performed on a split-belt instrumented treadmill used to record COP during each trial. The virtual reality display used a single video projector producing an image on a wide-view screen. The screen was 3 m high and 3 m wide, curved into a roughly semi-circular shape to provide about 180^{o} horizontal and 145^{o} vertical viewing angles, with subjects placed about 0.75 m away from the front of the screen. The image was rear-projected, with geometry distorted to compensate for screen curvature. We did not apply head tracking compensation, but to increase sense of immersion, subjects wore eyewear designed to block the field of view below the screen, including their feet and the stationary ground surrounding the treadmill. The visual field consisted of a virtual dark hallway tiled with randomly placed white rectangles (Warren et al. 1996).

Subjects were presented with oscillatory perturbations of the visual field in the form of translational sinusoids at 0.25 Hz in the horizontal plane. This low frequency was selected based on reports that perturbation frequencies between 0.20-0.25 Hz significantly affect balance while avoiding visual discomfort (Jeka et al. 2006; Sparto et al. 2006; Warren et al. 1996) and that vision is most sensitive below 1Hz (Yoneda and Tokumasu 1986). Lateral perturbations were applied as rotations about a vertical axis located at the vanishing point at the end of the virtual hallway. This was to ensure that the forward direction was always directed toward the center of the end of the hallway, so that any perceived self-motion induced only a balance correction but not a heading correction. Subjects were instructed to maintain a forward gaze by looking towards the end of the hallway and to use the visual information as naturally as possible as they walked down the hallway. Subjects were also informed that the visual stimuli might cause them to walk differently than usual and were instructed not to fight or consciously anticipate what they saw.

During the walking conditions, subjects walked at a constant speed of 1.25 m/s on the treadmill while viewing a virtual hallway, where the walls moved past them at the same speed as the treadmill belt. Prior to the study, subjects were given a 5 minute training trial to acclimate themselves to the virtual environment. They were then exposed to continuous perturbations of the visual flow in two sets of walking trials. The first set tested the effect of perturbation amplitude on step variability. Subjects were exposed to sinusoidal perturbations of the visual flow at amplitudes of 0, 0.05, 0.15, 0.25, and 0.35 m in both the M-L and A-P directions. The second set

tested the effect of perturbation direction, with translations in directions uniformly distributed at 0, 30, 60, 90, 120, and 150 degrees relative to M-L direction, all at the single amplitude of 0.25 m. Three additional trials were performed on five of the subjects to test the interaction of hallway speed and perturbation direction, in which the 0 m and 0.25 m perturbation amplitude conditions were repeated in both the ML and AP directions with the hallway nominally stationary and the walls not moving past the subjects (referred to as "No Flow" condition). This was similar to normal treadmill walking, where the visual field also does not translate relative to the body, except that perturbations were still superimposed on the otherwise stationary hallway. All walking trials were 5 minutes long and presented in random order, with a short break given after every third trial.

During the normal standing conditions, subjects stood on the treadmill with feet placed at shoulder width while viewing a stationary hallway. For the tandem standing conditions, subjects stood on the treadmill with one foot in front of the other in a heel to toe configuration. Subjects were allowed to choose which foot was placed forward and maintained the chosen configuration for all tandem trials. For all standing trials, subjects were additionally instructed to maintain an even weight distribution between the legs. All standing trials consisted only of two amplitudes and two directions. Sinusoidal perturbations in either the M-L or A-P direction were applied at amplitudes of 0 and 0.05 m in randomized trials that lasted 2 minutes.

We recorded instantaneous COP from continuous ground reaction force and moment signals for all trials. Ground reaction forces and moments were measured from force plates mounted underneath each treadmill belt. The forces and moments were sampled at 1200 Hz and low pass filtered with a 25 Hz cut-off frequency using a fourth order, zero-phase-shift Butterworth filter.

Analysis

Variability for walking and standing was quantified using COP as follows. In the walking trials, we measured RMS variability in step length and step width recorded from the instantaneous COP, which was estimated at mid-step over at least 350 steps. Mid-step was determined as the time point during a step when the vertical ground reaction force was at a minimum and below body weight. Step length was defined as the AP distance between the centers of pressure at mid-step of two consecutive steps plus the distance of treadmill travel during the step. The distance of travel was calculated as the product of treadmill belt speed and the time between consecutive mid-step events. Step width was defined as the lateral distance between the consecutive centers of pressure.

The step length and width measurements for left-right and right-left steps were then individually high-pass filtered at a cutoff of 15 steps before calculating RMS measures for all steps. The filter was used to remove low frequency components of step placement associated with slow changes in walking speed and heading. All length measurements were also normalized by the subject's leg length before computing statistics and group averages. Center of pressure estimates of foot placement during treadmill walking (Donelan et al. 2004) are less precise than kinematic measures (Bauby and Kuo 2000), especially for step length variability, because the foot remains relatively stationary with respect to the ground during the support phase while the COP progresses forward from the heel to the toe. Imprecision in mid-step event timing then adds to AP COP variability. We therefore concentrated not on absolute variability in step length and width, but in the changes in step variability across trials. Average step length and step width were also calculated to determine whether adding visual noise affects systematic control of foot placement. These checks ensure that the overall variability measured from foot placement is a result of the applied visual noise and not a change in control strategy. For the standing trials, the effect of the visual perturbations was assessed directly by measuring RMS COP displacement in both the M-L and A-P directions over a two minute interval. Before computing RMS measures, the COP data was first high-pass filtered at a cutoff frequency of 0.1 Hz to remove low frequency shifts in posture and weight bearing (Carpenter et al. 2001).

We defined the sensitivity metrics to quantify perturbation amplitude dependent changes in walking and standing variability. These were defined as the slope of the COP variability vs perturbation amplitude trends and labeled as follows: The ML/ML sensitivity for the walking trials corresponds to the slope of step width variability vs. ML perturbation amplitude. Similarly, AP/ML sensitivity for the standing trials corresponds to the slope of AP RMS COP displacement vs. ML perturbation amplitude.

We summarized changes in step width and step length variability with perturbation direction using subject-specific ellipses. Each ellipse was determined through a least squares circular regression of the RMS variability as a function of perturbation direction. Direction dependence was characterized by the elliptical eccentricity, defined as the ratio of the distance between the foci to the length of the major axis. (A circle has zero eccentricity, and a line segment has unit eccentricity).

We tested our hypotheses with the following statistical tests. To determine effects on average step length and width, we performed repeated measures analysis of variance (ANOVA) with perturbation amplitude and direction as factors. To determine effects on step variabilities, we performed repeated measures analysis of covariance (ANCOVA), with perturbation amplitude as one factor and direction as the other. This test yielded estimates of perturbation sensitivities, which were used to indicate whether visual information about side-to-side movement is more heavily weighted than that of fore-aft movement for controlling step-to-step balance during walking. For the standing conditions, we again used repeated measures ANCOVA to test whether AP/AP sensitivity was significantly greater than ML/ML sensitivity. Also calculated were ML/AP and AP/ML sensitivities for both walking and standing. Finally, we tested whether the directional eccentricity of the elliptical fits was significant for both step length and width variability, using a paired t-test. All statistical tests were performed with a maximum Type I error rate α of 0.05.

Results

Perturbations of the visual scene induced increases in variability during both walking and standing. The sensitivity to perturbation amplitude depended upon both the task (walking vs. standing) and the direction of perturbation (ML vs. AP). For all tasks, subjects showed greatest sensitivity in the direction of predicted instability: ML/ML sensitivity was greatest for walking and tandem standing and AP/AP sensitivity was greatest for normal standing. Details of these results and additional within-task comparisons are reported below, beginning with results for control conditions to facilitate comparisons.

During the walking control condition, subjects walked at 1.25 m/s with an average step length 0.683 m (± 0.033 SD, standard deviation) and step width of 0.159 m (± 0.041 SD). Step length (or AP) variability was 0.019 m (± 0.008 SD) and step width (or ML) variability was 0.025 m (± 0.007 SD), both expressed as root-mean-square (RMS) deviations of discrete, step-to-step COP. Step width variability was 31% greater than step length variability (P = 0.024, paired t-test). During the normal standing condition, AP variability was 0.0025 m (± 0.0009 SD) and ML variability was 0.0011 m (± 0.0004 SD), both expressed as RMS deviations of continuous COP. AP variability was 2.3 times greater than ML variability (P = 8.7e-5) in this case. During the tandem standing condition, subjects exhibited AP variability of 0.0050 m (± 0.0034 SD) and ML variability of 0.0043 m (± 0.0014 SD). Compared to normal standing, AP variability was 2.0

times greater (P = 0.060) and ML variability was 3.9 times greater (P = 6.6e-5) during tandem standing.

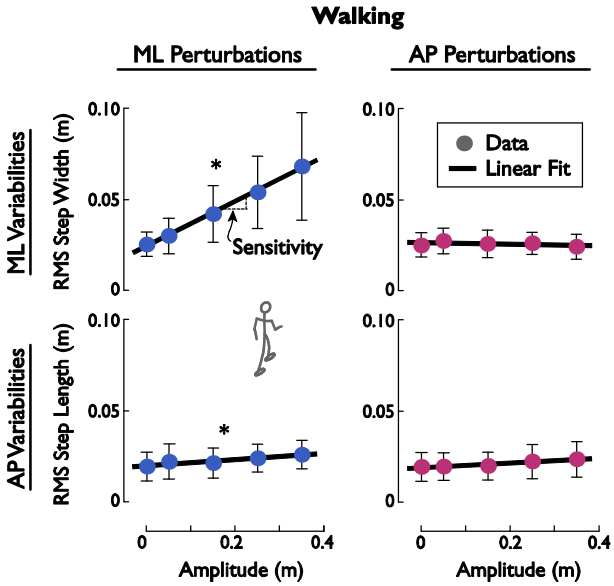

Figure 5.3. Variability of walking as a function of AP and ML visual perturbations. Step variability data (filled circles), defined as root-mean-square (RMS) deviations of step width and length, are plotted against perturbation amplitude. Linear regression fits (solid lines) to data yield slopes quantifying sensitivity to perturbations. Results show that step width generally exhibited greater variability than step length. Only ML perturbations produced significant changes in step variability; ML/ML sensitivity was 0.12 (P = 5.7e-4), and AP/ML sensitivity was 0.017 (P = 0.0047). Error bars denote standard deviation. Asterisks (*) denote significant sensitivity ($P < 0.05$).

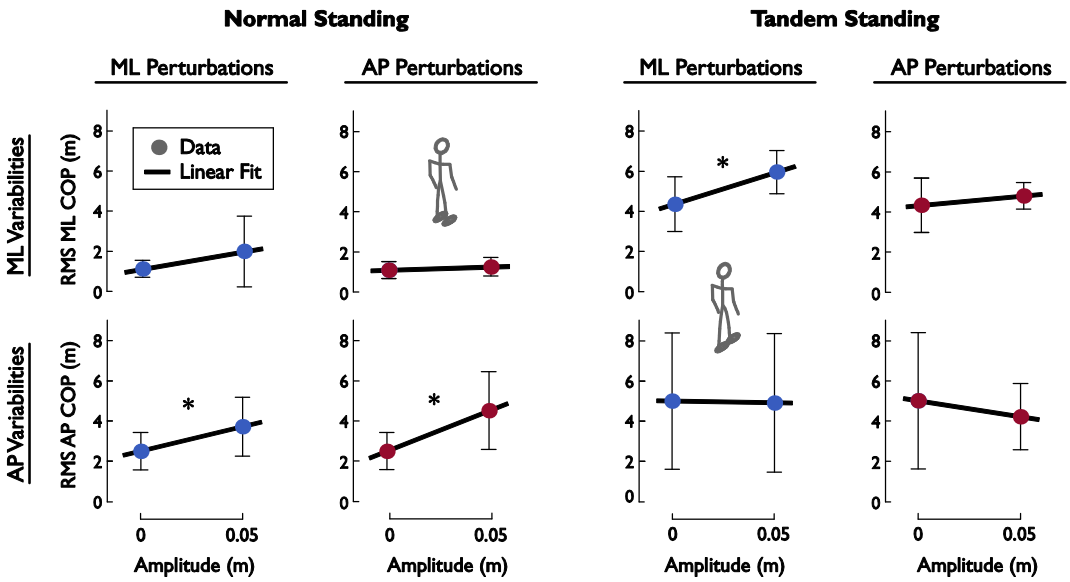

Figure 5.4. Variability of normal and tandem standing as a function of AP and ML visual perturbations. Center of pressure (COP) variability data (filled circles), defined as root-mean-square (RMS) deviations in the AP and ML directions, are plotted against perturbation amplitude. Linear regression fits (solid lines) to data yield slopes quantifying sensitivity to perturbations. During normal standing (left), AP variability was generally greater than ML variability, and more sensitive to visual perturbations in both directions; AP/AP sensitivity was 0.040 (P = 0.0044), and AP/ML sensitivity was 0.024 (P = 0.0005). During tandem standing, there was greater variability than normal standing. Only the ML/ML sensitivity was significant, with a value of 0.032 (P = 4.2e-5). Error bars denote standard deviation. Asterisks (*) denote significant sensitivity ($P < 0.05$).

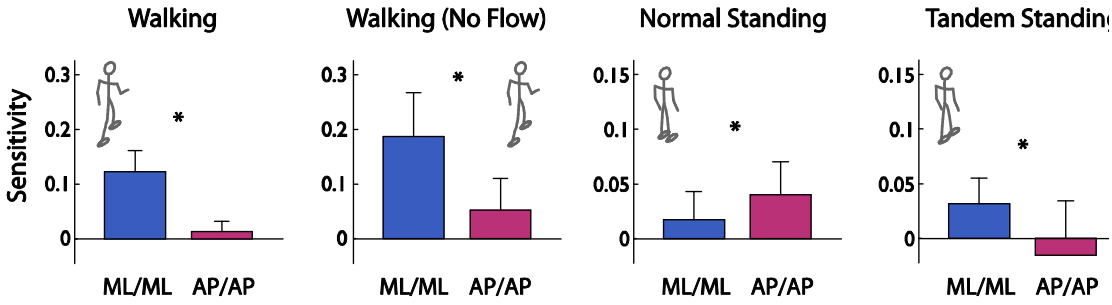

Figure 5.5. Summary of mean perturbation sensitivities for walking, normal standing, and tandem standing. Two sensitivities are compared: ML/ML (i.e., sensitivity of ML variability to ML perturbations) and AP/AP (see Figures 3 and 4). During walking and tandem standing, ML/ML sensitivity was significantly greater than AP/AP sensitivity (asterisks denote $P < 0.05$). The sensitivities were reversed for normal standing. The differential sensitivity remained in effect during walking with a nominally stationary visual field ("No Flow"), indicating that the contrast with normal standing is not due to differences in visual field motion. Walking sensitivities are consistent with model predictions of passive dynamic stability from step to step, and standing results are consistent with static stability expected from the base of support.

Visual perturbations had little effect on mean step parameters. Mean step length varied by at most 1.2% across perturbation directions ($P = 0.0014$, repeated measures ANOVA) and 2.6% across perturbation amplitudes ($P = 0.010$). Mean step width varied by insignificant amounts, 0.8% across direction ($P = 0.63$) and 7.4% across amplitude ($P = 0.51$). There was no evidence of significant amplitude-direction interaction ($P = 0.057$).

Visual perturbations had much greater effect on step variabilities, which varied approximately linearly with perturbation amplitude depending on perturbation direction (Figure 5.3). For example, the slope of ML variability due to ML perturbations (i.e., the ML/ML sensitivity) was 0.123 (± 0.075 SD), with a significant amplitude dependence ($P = 5.7e\text{-}4$), with $R^2 = 0.81$. Not only did ML perturbations affect step width variability, but they also caused an increase in step length variability, with AP/ML sensitivity of 0.017 (± 0.014 SD, $P = 0.0047$) with $R^2 = 0.82$. In contrast, AP perturbations had little effect at all; the sensitivities were much smaller—no greater than 0.013—and not significantly different from zero ($P = 0.34$ for ML/AP sensitivity, $P = 0.12$ for AP/AP sensitivity).

Variability during both types of standing also increased with perturbation amplitude (Figure 5.4), depending on the direction of perturbation. In normal standing, AP COP variability increased with both perturbation directions: AP/AP sensitivity was 0.040 (± 0.031 SD, $P = 0.0044$) with $R^2 = 0.83$, and the AP/ML sensitivity was a small but significant 0.024 (± 0.013 SD, $P = 0.0005$)

with R^2 = 0.94. In contrast, ML variability was relatively insensitive; the ML/ML sensitivity (P = 0.20) and ML/AP sensitivity (P = 0.30) were not significantly different from zero. During tandem standing, the ML/ML sensitivity was 0.032 (± 0.014 SD, P = 4.2e-5), with R^2 = 0.95. The other sensitivities were not significantly different from zero (AP/ML sensitivity, P = 0.87; AP/AP sensitivity P = 0.26; ML/AP, P = 0.20).

Perturbation sensitivities followed the trends predicted by task dynamics (Figure 5.5). During walking, the ML/ML sensitivity was about 9.4 times greater than the AP/AP sensitivity (P = 0.0005, repeated measures ANCOVA). But variabilities during normal standing exhibited an opposite trend, with an AP/AP sensitivity about 2.3 times greater than ML/ML sensitivity (P = 0.039, repeated measures ANCOVA). During tandem standing, the main sensitivity was ML/ML, which was 3.0 times greater than the AP/AP sensitivity (p = 0.0051). Even though variability was measured in different ways for walking and standing (continuous COP vs. discrete steps), the sensitivities to visual perturbations were of roughly the same order of magnitude. The most important comparison is therefore between sensitivities for each task, showing walking to be relatively far more sensitive in the ML direction than AP, and standing to have the converse effect, to a somewhat lesser degree.

Step variabilities also varied with perturbation direction intermediate to AP and ML (Figure 5.6). Perturbations in 30° increments resulted in variabilities that changed relatively smoothly between the two extremes. These increments also demonstrate how ML perturbations affected both step width and length variabilities, through the eccentricity of ellipses fit to polar plots of variability as a function of perturbation direction. Step width variability exhibited a significant eccentricity of 0.78 ± 0.08 CI (P = 9.5e-9), and step length variability an eccentricity of 0.60 ± 0.14 CI (P = 8.9e-6), both in the ML direction.

The effect of visual perturbations on walking was similar even with the nominally stationary visual field (see Figure 5.5, No Flow condition). In fact, the visual field condition had no significant effect on the primary sensitivities (normal flow vs. no flow: ML/ML P = 0.18; AP/AP P = 0.50). More importantly, ML/ML sensitivity was significantly greater than AP/AP sensitivity (by a factor of 3.58, P = 0.0079), even when the average speed of the visual field was zero relative to the subject.

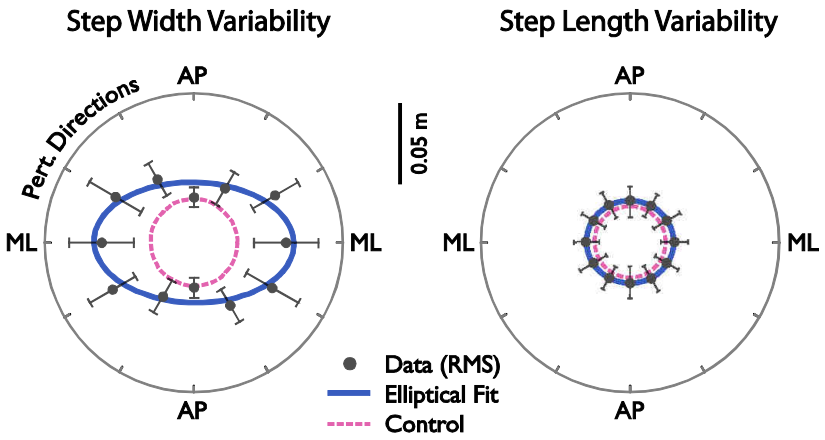

Figure 5.6. Step width and length variability as a function of visual perturbation direction. Data points show mean and standard deviation of RMS variability for perturbations with amplitude 0.25m, along with ellipses fit to these data (solid lines). Variabilities in the control conditions with no perturbations are shown for comparison (dashed circles). Both variabilities were greatest for perturbations in the ML direction, as demonstrated by significant eccentricity of subject-specific ellipses (P = 9.5e-9 for step width, P = 8.9e-6 for step length).

Discussion

This study was designed to determine whether human walking has passive stability in the AP direction, and instability in the ML direction. We perturbed the visual field in a variety of directions and amplitudes and measured the effect on foot placement variability. For comparison, we also tested the effect of visual perturbations on normal and tandem standing, hypothesizing that the base of support would determine directions of greatest instability. Our results revealed an amplitude and direction dependence of visual perturbations on step length and width variability during walking. During standing, COP variability was also sensitive to visual perturbations. The direction dependencies were consistent with our hypotheses: low sensitivity of step length to AP perturbations, high sensitivity of the AP component of normal standing, and high sensitivity in the ML direction during tandem standing. These findings have a number of implications for the control of walking and standing, and the role of integrative feedback in motor control in general.

Our results suggest that integrative visual feedback is used more for controlling lateral than fore-aft balance during walking. Direction-dependent sensitivity was predicted from the unstable lateral balance of dynamic walking models, which require active feedback only in the lateral direction (Kuo 1999). The observed high sensitivity of ML foot placement to ML visual perturbations suggests that vision is used to drive lateral foot placement. In contrast, there was no significant sensitivity of foot placement to AP perturbations, indicating little use of vision in that direction. In dynamic walking models and machines, passive stability is afforded by the pendulum-like motion of the legs and the step-to-step transition. These cause heelstrike collisions

to dissipate more or less energy when perturbations respectively add or subtract energy (Kuo 2002a; Wisse et al. 2005). This results in a motion that is stable over discrete steps (also referred to as "limit cycle" stability), despite having inverted pendulum instability in continuous time. Interestingly, we found ML perturbations to also affect step length variability, as indicated by significant AP/ML sensitivity. This may be due to dynamical coupling between step width and step length, as observed in our computational models (Bauby and Kuo 2000b). Passive dynamics may afford walking a degree of limit cycle stability in the AP direction without need for integrative control. But stability in the ML direction appears to depend on the integration of sensory feedback regarding ML motion of the body, for adjusting lateral foot placement.

We also observed direction dependence in the continuous-time control of standing. The higher sensitivity to AP than ML visual perturbations suggests that AP balance may be actively stabilized to a greater extent than ML balance. This direction dependence may be due to the configuration of the lower extremity, which in the sagittal plane resembles a multi-segment inverted pendulum. But in the frontal plane (ML direction) the two legs, pelvis, and ground form a four-bar linkage, which might be passively less unstable than an inverted pendulum. This may explain why subjects were quite insensitive to ML visual perturbations during normal standing. Others have also observed that increased stance width allows subjects to respond with smaller active postural responses, when perturbed either physically (Henry et al. 2001) or visually (Day et al. 1993; Hong et al. 2007) in the ML direction. The configuration is quite different in tandem standing, where the base of support is much reduced in the ML direction. Subjects weighted vision differently in that condition, consistent with how stability is expected to vary with configuration.

A potential concern regarding these results is that direction-dependent visual sensitivity might be an artifact of physiological limitations in visual processing. The low AP/AP sensitivity during walking might then be explained by poor ability to detect motion in that direction. This however appears unlikely, because subjects had high AP/AP sensitivity during standing. Another alternative explanation is that bulk flow of the visual field during walking somehow reduces visual sensitivity in the AP direction. But the AP/AP sensitivity was not significantly different even with a subjectively stationary hallway (see Figure 5.5, No Flow condition), and ML/ML sensitivity remained much greater, even though the nominal visual field was identical to that of standing. Other evidence suggests that the CNS can indeed sense perturbations to a moving visual field, because AP visual motion is still sensed and used for continuous-time stabilization of the

head and trunk during walking (Keshner and Kenyon 2000), and bulk flow has little effect on this control (Warren 1996). It therefore appears that the CNS does detect and respond to AP visual information during walking, but uses it selectively for continuous-time postural stabilization and very little for step-to-step, limit-cycle stabilization.

Our findings are subject to several limitations. The visual perturbations only produced an imperfect illusion of self-motion, due to the limited resolution and fidelity of the computer projected display, such as lack of stereoscopic head tracking in the virtual reality system. These limitations may have reduced the ability to detect significant sensitivities. Perturbations were also restricted to relatively low frequencies, where vestibular organs have low sensitivity, to avoid large conflicts between visual and vestibular input. Higher perturbation frequencies (and perhaps amplitudes) may induce greater conflict, which might produce different effects, as has been observed with sensory perturbations to posture (Peterka 2002b). Our estimates of COP during treadmill walking were also of limited precision in the AP direction, due to imperfect estimation of AP COP from a moving treadmill belt (Donelan et al. 2004a). This likely inflated estimates of AP step variability, but in a uniform manner having little effect on sensitivity measures. Finally, our measures of perturbation sensitivity were based on aggregate step variability rather than a correlation between individual perturbations and succeeding steps. We consider aggregate sensitivity to perturbations to provide better evidence of active control than previous studies using removal of vision (Bauby and Kuo 2000b). It would however be more direct to detect active foot placement control on a step-by-step basis.

A general theme of this study is that sensory feedback should be weighted based on stability requirements. Inherently unstable motor tasks require active feedback control for stability. Tasks or task directions with the greatest instability require more feedback, while others may require little feedback. Moreover, such feedback requirements should not be specific to vision. For example, proprioceptive perturbations have been applied using vibration of lower limb muscles, resulting in large effects on standing posture in the AP direction but small effects on walking (Courtine et al. 2007), consistent with the hypothesized direction of passive stability. Another example is aging, which has been associated with greater increases in ML than AP step variability (Dean et al. 2007a; Owings and Grabiner 2004a; b). This may be due to age-related deficits affecting not just vision but also a variety of other modalities. Another approach to the same theme is to perturb stability rather than sensory input. Accordingly, we have previously applied

external lateral stabilizers to artificially improve lateral stability of human subjects, with the result of reduced ML step variability (Donelan et al. 2004a).

Another theme is that discrete, step-to-step stability may be quite different from continuous-time stability. Our three-dimensional model of walking is unstable in the ML direction but stable in the AP direction (Kuo 1999). That same model, placed in the normal standing posture, is stable in the ML direction but unstable in the AP direction. It is, in fact, typical for dynamic walking robots to be designed solely for step-by-step, limit cycle stability, with little or no regard for standing stability (Coleman and Ruina 1998; Collins et al. 2005). Standing posture is characterized by continuous feedback control, much of it homonymous. For example, perturbations to the ankle trigger to feedback torques at the ankle (Park et al. 2004). There are also significant heteronymous contributions, but even these may be attributed directly to keeping the body upright. In contrast, step-by-step control of walking appears much more indirect and heteronymous. The hip torque that adjusts lateral foot placement is apparently triggered not by hip proprioceptors but by integrative information from the preceding step. The effect of that adjustment is to change body orientation, not directly but through the dynamics of the subsequent step-to-step transition.

Our findings may also have implications for the neural control of walking. Multiple levels of hierarchical feedback contribute to control, and are coupled through shared muscle groups, body dynamics, and interaction with environment. Neuronal circuits within the spinal cord produce a variety of short-latency reflexes and behaviors driven by proprioceptive and other local sensory feedback. These circuits are sufficient to produce walking in spinalized cats (Grillner and Wallen 1985), by supporting body weight and producing the basic stepping pattern. It is unclear whether humans have a similar degree of spinal control, but our results are consistent with other indirect observations that suggest this possibility (Duysens and Van de Crommert 1998a; MacKay-Lyons 2002). Dynamic walking models indicate that pendulum dynamics can account for much (if not all) of the stepping pattern, and interaction with step-to-step transitions can passively produce AP adjustment of foot placement with no need for active control. Humans may use spinal reflexes to produce low-level behaviors similar to the passive dynamics of models, making little use of integrative (e.g., visual and vestibular) feedback simply because it is not necessary. Higher level feedback may, however, be necessary for lateral stability. Even though spinalized cats can walk, they also tend to have poor lateral stability (e.g., Belanger et al. 1996; Brustein and Rossignol 1998), evidently lacking active, step-to-step foot placement control. These components rely more

heavily on visual, vestibular, and other feedback, integrated at the level of the brain stem and cerebellum. Hierarchical organization would allow spinal control to regulate most of the fore-aft walking motion, and higher levels of the CNS to integrate multisensory feedback for balance.

We have thus far assumed that vision is used integratively for walking balance, as it is for posture. An alternative possibility is that CNS performs directional weighting of vision separate from other inputs. Extrastriate areas, particularly the V5-MT region, are responsive to patterns of movement across many directions and are organized into columns that are sensitive to specific directions of motion. The anatomical arrangement of the MT and MST regions of the visual cortex, in direction-specific columns, provides a convenient means to weight particular directions of sensed motion. It is conceivable that task- and direction-dependent weighting is performed through selection and gating of these columns, perhaps contributing to cortical control of foot placement. Our preferred hypothesis, however, is that lateral foot placement control is a more automatic (and less cortical) response, sharing similar sensory integration circuitry to posture. Visual information might then contribute continuously to sensory integration in the brain stem and cerebellum (which also receive input from V5-MT). This could yield a single, model-based estimate of body state used to drive continuous-time posture control during standing and walking (e.g., Kuo 2005; Maurer et al. 2006), and also sampled step-to-step for driving discrete foot placement. This estimate might then be selectively weighted more for ML than AP control, without necessarily adjusting visual weighting at the cortical level. Although the present experiment uses vision for perturbations, a more general hypothesis is that multiple other sensors also contribute to state estimation and balance control, similarly weighted as a function of task dynamics. Just as we have assumed that the passive dynamics of our computational model can be realized by local reflexes in the human, these are mere working hypotheses that remain to be tested experimentally.

A potential application of this work is a new means to quantify balance during walking. Quantitative clinical assessments of posture such as computerized dynamic posturography (NeuroCom International, Clackamas, OR) typically apply sagittal plane perturbations, either by translating the body directly or by perturbing visual or somatosensory inputs during quiet standing. Although some tests appear related to fall risk, many do not assess non-sagittal motions, which are also considered clinically relevant to balance during walking (e.g., Marchetti and Whitney 2006; Schrager et al. 2008), and also predict fall risk well (Maki et al. 1994; Piirtola and Era 2006). Lateral COP variability during tandem stance and lateral step variability during

walking may be useful indicators of balance, and lateral perturbations to vision appear to reveal how visual information is integrated for this control. The influence of other inputs might be emphasized by artificially removing normal visual cues, akin to the "visual sway-referencing" used in dynamic posturography (Nashner et al. 1982). Virtual reality environments have previously proven useful for assessment of posture control (Keshner and Kenyon 2000; Streepey et al. 2007b). They could potentially also be used to selectively render ML or other visual cues inaccurate, and perhaps reveal poor integration of vestibular and other sensory information. Such perturbations or sway-referencing could then be applied to both walking and tandem stance, to provide data complementary to normal dynamic posturography.

Walking and tandem balance both appear to have inherent instabilities in the lateral direction. We have shown that visual perturbations induce substantial lateral variability in discrete foot placement during walking, and continuous COP variability during standing. These two measures serve as indicators of active balance control, and their sensitivity to perturbations quantifies the degree to which an input such as vision contributes to that control. In contrast to lateral balance, the fore-aft component of walking has little dependence on vision. The dynamics of the legs may afford passive, step-by-step stability to this component, so that the central nervous system has little need to control it with integrative feedback. The importance of dynamics is further highlighted by the visual dependence of standing, which can be reversed by changing the configuration of the legs and thereby the base of support. The CNS can selectively and flexibly weight sensory information for feedback control, both for continuous-time control of balance and step-by-step control of walking. It may also harness the self-stabilizing aspects of dynamic walking, where a series of uncontrolled falls can nonetheless be stable on a step-by-step basis.

Appendix 5.1 Supplementary Visual Perturbation Data

Summary statistics for control conditions and mean sensitivities for walking and standing conditions. Units are in meters.

	Walking	Walking (no flow)	Normal standing	Tandem standing
Step length (control)	0.683 ± 0.033	0.657 ± 0.025	--	--
Step width (control)	0.159 ± 0.041	0.152 ± 0.021	--	--
AP variability (control)	0.019 ± 0.008	0.015 ± 0.004	0.0025 ± 0.0009	0.0050 ± 0.0034
ML variability (control)	0.025 ± 0.007	0.016 ± 0.004	0.0011 ± 0.0004	0.0043 ± 0.0014
AP/AP sensitivity	0.013 ± 0.024	0.052 ± 0.052	0.040 ± 0.031 *	-0.011 ± 0.037
ML/ML sensitivity	0.123 ± 0.075 *	0.187 ± 0.090 *	0.017 ± 0.037	0.032 ± 0.013 *
AP/ML sensitivity	0.017 ± 0.014 *	0.026 ± 0.033	0.024 ± 0.013 *	-0.008 ± 0.032
ML/AP sensitivity	-0.004 ± 0.011	0.014 ± 0.011	0.003 ± 0.009	0.011 ± 0.014

Values are mean ± SD. Asterisks (*) denote statistically significance (ANCOVA, $P < 0.05$).

Chapter 6. Conclusion

We sought to address several individual motor control issues related to gait while building a hierarchical representation of how dynamics and control interact to pattern and stabilize the walking motion. We had proposed that adding compliance within the passive dynamics framework would provide a better representation of human-like walking features. To explore this hypothesis we developed simulations of a springy legged biped. Overall, we found that compliant and pendular dynamics explain much of the sagittal plane behavior of the limbs across a variety of gaits. While compliant legs produce more human-like walking motions, we found that they also retain significant pendular dynamics. We also proposed that spring-like limb behavior may be produced through muscle activation generated peripherally via reflex pathways (feedback) or centrally from neural oscillators (feedforward). We developed a model to demonstrate that these strategies may be optimally combined to produce steady-state motor behavior when faced with unexpected disturbances and imperfect sensing. The interaction of this musculoskeletal compliance, dissipation, and passive pendulum motion result in walking gaits that are stable in the sagittal plane. Aside from sagittal dynamics, we also valued the issue of whole body balance, since lateral dynamics remains unstable and require control to stay upright, as through active foot placement. We established that humans rely less on visual sensory feedback for anterio-posterior (AP) balance than medio-lateral (ML) given this directional instability in walking. The results of this thesis demonstrate how integrated models of control and dynamics may be useful for generating and testing a variety of hypotheses about human movement.

Compliant vs rigid legged dynamics

Human-like walking features include a smooth COM trajectory, a double-peaked vertical ground reaction force, and a significant duration of the step-to-step transition. Rigid legged models cannot reproduce these features at all, suggesting that they do not completely account for the work performed by the legs during gait. The compliant model excels compared to the rigid legged models in predicting the timing and actual quantity of work performed by the legs on the COM over a stride. The model is also ideal for exploring the costs of performing the step-to-step transition over significant time, and suggests that the relative timing of the push-off and collision phases, as determined by duty factor, have significant energetic consequences.

However, we do not mean to propose that compliant leg behavior replace pendulum behavior as the governing principle of walking dynamics, as has been previously suggested (Geyer et al. 2006). We cannot neglect the fact that rigid legged walking models have already served as powerful tools for predicting mechanical and metabolic costs of walking. Perhaps most remarkable is not how well the compliant model mimics actual walking but how successful predictions have been without compliance.

We also note that pendulum dynamics still significantly affect gait behaviors even with axial leg compliance. By parameterizing energy distribution with a spring ratio parameter, we found that all gaits incorporate some amount of pendular and spring-mass behavior, the relative amounts of which determine properties of the gait, such as type and speed. In this continuum of behaviors, walking acts more like an inverted pendulum relative to running and running acts more like a spring-mass system relative to walking. The model can then switch from a walk to a run by simply redistributing this energy from inverted pendulum dynamics to spring-mass for the same compliance. We also found that additional speed can be gained by simply injecting energy into the gait without having to modify properties of the compliance. However, these properties can be tuned to modify gait features, such as step length and duty factor, at a particular speed to improve energy economy. More work is needed to test whether humans actually adjust their leg stiffness to change these gait features.

This compliant behavior essentially models the work done by muscle and tendon to redirect the vertical motion of the body and speed up swing leg motion. Some control is needed to provide spring-like actuation from muscles though and could be potentially afforded by reflex loops and neural oscillators located in the spinal cord. Assigning a relative weighting of spring-like and pendular behaviors is really an evaluation of the relative impact of neuromuscular control and passive dynamics in generating gait. We find that compliant leg behavior (actuation) and passive dynamics are equally important in determining major features of walking and running behavior.

FF vs FB control

Contentious in the field of motor control has been the relative importance of central and peripheral generation of motor behavior for patterning rhythmic movements (Brown 1914; Grillner and Wallen 1985; Sherrington 1910). In contrast, upper body, volitional motor control theory has recognized the benefit of combining these two forms of control for producing robust

movements and learning from movement errors (Hwang and Shadmehr 2005; Kawato 1999; Wolpert et al. 1995). Perhaps the difference lies in the allowance of the motor cortex to flexibly make use of sensory information and the assumption that the spinal cord is relatively hard-wired and obeys fixed principles. We designed a walking model with hip actuation to demonstrate our interpretation of feedforward and feedback motor systems in terms of an internal model updated by sensory information for producing stereotyped, rhythmic movements. Applied to the neural oscillators presumed to locate in the spinal cord, the state estimation hypothesis suggests that CPGs serve a primary role to filter sensory information rather than to simply generate motor commands.

While this work was intended as a conceptual exercise to challenge the feedforward CPG interpretation, these ideas could be further tested through in vivo spinal preparations (Cazalets et al. 1992; Smith and Feldman 1987). If the motor and sensory pathways are left intact, electrical stimulation of the afferents could be used to artificially corrupt the feedback signal. The temporal filtering hypothesis discussed earlier could be assessed by corrupting the feedback pathway with varying levels of noise and the measuring the rate of the motor response to actual perturbations of limb position.

Active vs passive balance

We sought to distinguish walking balance and its subsequent utilization of sensory resources from standing balance, which is accepted to be unstable. Troublesome are comparisons of both walking and standing stability in the static sense and interpretations of walking as “controlled falling”. However, passive dynamics recognizes the self stabilizing properties of fore-aft balance and the need to actively balance against lateral instability. We used these concepts to show that humans rely less on integrative visual feedback for anterio-posterior (AP) balance than medio-lateral (ML). Standing balance was also found to have a reversed direction dependent sensitivity compared to walking.

Evidence that visual sensory information is processed differently for walking and standing balance may suggest that proper assessment of balance disorders or sensory impairments should involve several tasks, covering dynamic instabilities in all directions. Tasks that challenge only static balance in the AP direction may be best as predicting risk for standing falls and neglect potential loss of balance during walking or other movements. This idea is implicitly used in clinical practices, such as the Berg Balance Test, which use a variety of functional static and

dynamic tasks, including tandem stance, to assign a summary balance score. This score is significantly correlated with falls in the elderly (Bogle Thorbahn and Newton 1996). However, these functional assessment techniques do have limitations in their ability to specifically quantify and diagnose the cause of balance impairment. Dynamic posturography tests are able to distinguish sensory and motor impairments that affect static balance but do not have a dynamic walking balance equivalent (Allum and Shepard 1999; Nashner and Peters 1990; Peterka and Benolken 1995). Our results also question whether these tests conducted with a normal standing posture would diagnose lateral sensory deficits. Perhaps a dynamic posturography test for walking would be necessary to fully diagnose sensory impairments related to walking balance. Such a test could not only test lateral sensation but also stepping corrections related to walking balance. A simpler method might involve completing the dynamic posturography test with a tandem stance and measuring lateral motion, since we found this stance to have similar direction dependence as walking. This test would require that the visual surround be equipped to rotate laterally. The results of our study and others indicate that a virtual reality visual surround could instead be used to significantly perturb vision in all directions and significantly induce postural sway (Keshner et al. 2007).

Our findings demonstrate that a virtual reality environment is beneficial for studying how visual information is used to make foot placement decisions related to walking balance. Specifically, we have shown that visual errors in the form of oscillations can induce variability in foot placement and serve as a probe of the weighting or sensitivity to visual information. A similar paradigm may be useful for detecting or diagnosing gait balance impairment analogous to sensory organization tests that have been used for detecting standing postural imbalance. While the results directly indicate the influences of visual feedback on walking balance, these results should generalize to all sensory feedback channels and could possibly be validated through galvanic stimulation or tendon vibration experiments.

The applicability of our results to pathological gait should also be tested. Results were predicted based on a passive walking model and tested in healthy subjects. Predictions rely on the assumption that the sagittal plane motions of the walking subjects make use of passive principles. We have provided evidence for this in healthy subjects but the same may not be true for persons with sensory or motor pathologies. Therefore the clinical relevance of these findings for the diagnosis and treatment of such pathologies will need further validation in patient populations.

References

Adamczyk PG, Collins SH, and Kuo AD. The advantages of a rolling foot in human walking. *J Exp Biol* 209: 3953-3963, 2006.

Alexander RM. 3 Uses for Springs in Legged Locomotion. *Int J Robotics Res* 9: 53-61, 1990.

Alexander RM. A model of bipedal locomotion on compliant legs. *Philos Trans R Soc Lond B* 338: 189-198, 1992.

Alexander RM. Simple models of human movement. *Appl Mech Rev* 48: 461-470, 1995.

Allum JH. Organization of stabilizing reflex responses in tibialis anterior muscles following ankle flexion perturbations of standing man. *Brain Res* 264: 297-301, 1983.

Allum JH, and Shepard NT. An overview of the clinical use of dynamic posturography in the differential diagnosis of balance disorders. *J Vestib Res* 9: 223-252, 1999.

Anand V, Buckley JG, Scally A, and Elliott DB. Postural Stability in the Elderly during Sensory Perturbations and Dual Tasking: The Influence of Refractive Blur. *Invest Ophthalmol Vis Sci* 44: 2885-2891, 2003.

Bardy BG, Warren WH, Jr., and Kay BA. Motion parallax is used to control postural sway during walking. *Exp Brain Res* 111: 271-282, 1996.

Barth DG, Schumacher L, and Thomas SS. Gait Analysis and Energy Cost of Below- Knee Amputees Wearing Six Different Prosthetic Feet. *Journal of Prosthetics & Orthotics* 4: 63-75, 1992.

Bauby CE, and Kuo AD. Active control of lateral balance in human walking. *J Biomech* 33: 1433-1440., 2000a.

Bauby CE, and Kuo AD. Active control of lateral balance in human walking. *J Biomech* 33: 1433-1440, 2000b.

Belanger M, Drew T, Provencher J, and Rossignol S. A comparison of treadmill locomotion in adult cats before and after spinal transection. *J Neurophysiol* 76: 471-491, 1996.

Bellebaum C, Daum I, Koch B, Schwarz M, and Hoffmann KP. The role of the human thalamus in processing corollary discharge. *Brain* 128: 1139-1154, 2005.

Bent LR, Inglis JT, and McFadyen BJ. When is vestibular information important during walking? *J Neurophysiol* 92: 1269-1275, 2004.

Black FO, Wall C, 3rd, and Nashner LM. Effects of visual and support surface orientation references upon postural control in vestibular deficient subjects. *Acta Otolaryngol* 95: 199-201, 1983.

Blake AJ, Morgan K, Bendall MJ, Dallosso H, Ebrahim SB, Arie TH, Fentem PH, and Bassey EJ. Falls by elderly people at home: prevalence and associated factors. *Age Ageing* 17: 365-372, 1988.

Bogle Thorbahn LD, and Newton RA. Use of the Berg Balance Test to predict falls in elderly persons. *Phys Ther* 76: 576-583; discussion 584-575, 1996.

Brown TG. On the nature of the fundamental activity of the nervous centres; together with an analysis of the conditioning of rhythmic activity in progression, and a theory of the evolution of function in the nervous system. *J Physiol (Lond)* 48: 18-46, 1914.

Brustein E, and Rossignol S. Recovery of locomotion after ventral and ventrolateral spinal lesions in the cat. I. Deficits and adaptive mechanisms. *J Neurophysiol* 80: 1245-1267, 1998.

Carpenter MG, Allum JH, and Honegger F. Directional sensitivity of stretch reflexes and balance corrections for normal subjects in the roll and pitch planes. *Exp Brain Res* 129: 93-113, 1999.

Carpenter MG, Frank JS, Silcher CP, and Peysar GW. The influence of postural threat on the control of upright stance. *Exp Brain Res* 138: 210-218, 2001.

Cavagna GA, and Margaria R. Mechanics of walking. *J Appl Physiol* 21: 271-278, 1966.

Cavagna GA, Thys H, and Zamboni A. The sources of external work in level walking and running. *J Physiol* 262: 639-657, 1976.

Cazalets JR, Sqalli-Houssaini Y, and Clarac F. Activation of the central pattern generators for locomotion by serotonin and excitatory amino acids in neonatal rat. *J Physiol (Lond)* 455: 187-204, 1992.
Cohen AH. The Role of Heterarchical Control in the Evolution of Central Pattern Generators. *Brain Behavior and Evolution* 40: 112-124, 1992.
Coleman MJ, and Ruina A. An uncontrolled walking toy that cannot stand still. *Phys Rev Lett* 80: 3658 - 3661, 1998.
Collins S, Ruina A, Tedrake R, and Wisse M. Efficient bipedal robots based on passive-dynamic walkers. *Science* 307: 1082-1085, 2005.
Cordo PJ, and Nashner LM. Properties of postural adjustments associated with rapid arm movements. *J Neurophysiol* 47: 287-302, 1982.
Courtine G, De Nunzio AM, Schmid M, Beretta MV, and Schieppati M. Stance- and locomotion-dependent processing of vibration-induced proprioceptive inflow from multiple muscles in humans. *J Neurophysiol* 97: 772-779, 2007.
Day BL, Steiger MJ, Thompson PD, and Marsden CD. Effect of vision and stance width on human body motion when standing: implications for afferent control of lateral sway. *J Physiol* 469: 479-499, 1993.
Dean JC, Alexander NB, and Kuo AD. The effect of lateral stabilization on walking in young and old adults. *IEEE Trans Biomed Eng* 54: 1919 - 1926, 2007a.
Dean JC, Alexander NB, and Kuo AD. The effect of lateral stabilization on walking in young and old adults. *IEEE Trans Biomed Eng* 54: 1919-1926, 2007b.
Dillingham TR, Pezzin LE, and MacKenzie EJ. Limb amputation and limb deficiency: epidemiology and recent trends in the United States. *South Med J* 95: 875-883, 2002.
Doke J, Donelan JM, and Kuo AD. Mechanics and energetics of swinging the human leg. *J Exp Biol* 208: 439-445, 2005.
Donelan JM, Kram R, and Kuo AD. Mechanical and metabolic determinants of the preferred step width in human walking. *Proc R Soc Lond Ser B-Biol Sci* 268: 1985-1992., 2001.
Donelan JM, Kram R, and Kuo AD. Mechanical work for step-to-step transitions is a major determinant of the metabolic cost of human walking. *J Exp Biol* 205: 3717-3727, 2002a.
Donelan JM, Kram R, and Kuo AD. Simultaneous positive and negative external mechanical work in human walking. *J Biomech* 35: 117-124., 2002b.
Donelan JM, Shipman DW, Kram R, and Kuo AD. Mechanical and metabolic requirements for active lateral stabilization in human walking. *J Biomech* 37: 827-835, 2004a.
Donelan JM, Shipman DW, Kram R, and Kuo AD. Mechanical and metabolic requirements for active lateral stabilization in human walking. *J Biomech* 37: 827-835, 2004b.
Duysens J, and Van de Crommert HW. Neural control of locomotion; The central pattern generator from cats to humans. *Gait Posture* 7: 131-141, 1998a.
Duysens J, and Van de Crommert HW. Neural control of locomotion; The central pattern generator from cats to humans. *Gait Posture* 7: 131-141., 1998b.
Farley CT, and Ferris DP. Biomechanics of walking and running: from center of mass movement to muscle action. *Exerc Sport Sci Rev* 26: 253-285, 1998.
Farley CT, Glasheen J, and McMahon TA. Running springs: speed and animal size. *J Exp Biol* 185: 71-86, 1993.
Fitzpatrick R, Burke D, and Gandevia SC. Task-dependent reflex responses and movement illusions evoked by galvanic vestibular stimulation in standing humans. *J Physiol* 478 (Pt 2): 363-372, 1994.
Fukunaga T, Kubo K, Kawakami Y, Fukashiro S, Kanehisa H, and Maganaris CN. In vivo behaviour of human muscle tendon during walking. *Proc R Soc Lond B Biol Sci* 268: 229-233, 2001.
Gabell A, Simons MA, and Nayak US. Falls in the healthy elderly: predisposing causes. *Ergonom* 28: 965-975, 1985.

Gailey RS, Wenger MA, Raya M, Kirk N, Erbs K, Spyropoulos P, and Nash MS. Energy expenditure of trans-tibial amputees during ambulation at self-selected pace. *Prosthet Orthot Int* 18: 84-91, 1994.
Garcia M, Chatterjee A, Ruina A, and Coleman M. The simplest walking model: stability, complexity, and scaling. *J Biomech Eng* 120: 281-288, 1998.
Geyer H, Seyfarth A, and Blickhan R. Compliant leg behaviour explains basic dynamics of walking and running. *Proceedings of the Royal Society B-Biological Sciences* 273: 2861-2867, 2006.
Grillner S, and Wallen P. Central pattern generators for locomotion, with special reference to vertebrates. *Annu Rev Neurosci* 8: 233-261, 1985.
Hansen AH, Childress DS, and Knox EH. Roll-over shapes of human locomotor systems: effects of walking speed. *Clin Biomech (Bristol, Avon)* 19: 407-414, 2004.
Henry SM, Fung J, and Horak FB. Effect of Stance Width on Multidirectional Postural Responses. *J Neurophysiol* 85: 559-570, 2001.
Herbert LM, Engsberg JR, Tedford KG, and Grimston SK. A comparison of oxygen consumption during walking between children with and without below-knee amputations. *Phys Ther* 74: 943-950, 1994.
Hirai K, Hirose M, Haikawa Y, and Takenaka T. The development of Honda humanoid robot. In: *Robotics and Automation, 1998 Proceedings 1998 IEEE International Conference on*1998, p. 1321-1326 vol.1322.
Holt KG, Wagenaar RC, LaFiandra ME, Kubo M, and Obusek JP. Increased musculoskeletal stiffness during load carriage at increasing walking speeds maintains constant vertical excursion of the body center of mass. *J Biomech* 36: 465-471., 2003.
Hong SL, Manor B, and Li L. Stance and sensory feedback influence on postural dynamics. *Neurosci Lett* 423: 104-108, 2007.
Horak FB, Dimitrova D, and Nutt JG. Direction-specific postural instability in subjects with Parkinson's disease. *Exp Neurol* 193: 504-521, 2005.
Horak FB, and Macpherson JM. Postural orientation and equilibrium. In: *Handbook of Physiology, Section 12: Exercise: Regulation and Integration of Multiple Systems*, edited by Rowell LB, and Shepherd JT. New York: Oxford University Press, 1996, p. 255-292.
Horak FB, Shupert CL, and Mirka A. Components of postural dyscontrol in the elderly: a review. *Neurobiol Aging* 10: 727-738, 1989.
Hreljac A. Determinants of the gait transition speed during human locomotion: kinematic factors. *J Biomech* 28: 669-677, 1995.
Hwang EJ, and Shadmehr R. Internal models of limb dynamics and the encoding of limb state. *J Neural Eng* 2: S266-278, 2005.
Inglis JT, Shupert CL, Hlavacka F, and Horak FB. Effect of galvanic vestibular stimulation on human postural responses during support surface translations. *J Neurophysiol* 73: 896-901, 1995.
Ishikawa M, Komi PV, Grey MJ, Lepola V, and Bruggemann GP. Muscle-tendon interaction and elastic energy usage in human walking. *J Appl Physiol* 99: 603-608, 2005.
Ivanenko YP, Poppele RE, and Lacquaniti F. Motor control programs and walking. *Neuroscientist* 12: 339-348, 2006.
Jahn K, Strupp M, Schneider E, Dieterich M, and Brandt T. Differential effects of vestibular stimulation on walking and running. *Neuroreport* 11: 1745-1748, 2000.
Jahn K, Strupp M, Schneider E, Dieterich M, and Brandt T. Visually induced gait deviations during different locomotion speeds. *Exp Brain Res* 141: 370-374, 2001.
Jeka J, Allison L, Saffer M, Zhang Y, Carver S, and Kiemel T. Sensory reweighting with translational visual stimuli in young and elderly adults: the role of state-dependent noise. *Exp Brain Res* 174: 517-527, 2006.

Johansson R, and Magnusson M. Human postural dynamics. *Crit Rev Biomed Eng* 18: 413-437, 1991.
Kawato M. Internal models for motor control and trajectory planning. *Curr Opin Neurobiol* 9: 718-727, 1999.
Kay BA, and Warren WH, Jr. Coupling of posture and gait: mode locking and parametric excitation. *Biol Cyber* 85: 89-106, 2001.
Keshner EA, and Kenyon RV. The influence of an immersive virtual environment on the segmental organization of postural stabilizing responses. *J Vestib Res* 10: 207-219, 2000.
Keshner EA, Streepey J, Dhaher Y, and Hain T. Pairing virtual reality with dynamic posturography serves to differentiate between patients experiencing visual vertigo. *J Neuroeng Rehabil* 4: 24, 2007.
Keshner EA, Woollacott MH, and Debu B. Neck, trunk and limb muscle responses during postural perturbations in humans. *Exp Brain Res* 71: 455-466, 1988.
Knapp HD, Taub E, and Berman AJ. Movements in monkeys with deafferented forelimbs. *Exp Neurol* 7: 305-315, 1963.
Kram R, Domingo A, and Ferris DP. Effect of reduced gravity on the preferred walk-run transition speed. *J Exp Biol* 200: 821-826, 1997.
Kuo AD. Energetics of actively powered locomotion using the simplest walking model. *J Biomech Eng* 124: 113-120, 2002a.
Kuo AD. An optimal state estimation model of sensory integration in human postural balance. *J Neural Eng* 2: S235-249, 2005.
Kuo AD. The relative roles of feedforward and feedback in the control of rhythmic movements. *Motor Control* 6: 129-145, 2002b.
Kuo AD. A simple model of bipedal walking predicts the preferred speed-step length relationship. *J Biomech Eng* 123: 264-269., 2001.
Kuo AD. Stabilization of Lateral Motion in Passive Dynamic Walking. *Int J Robotics Res* 18: 917-930, 1999.
Kuo AD, Donelan JM, and Ruina A. Energetic consequences of walking like an inverted pendulum: step-to-step transitions. *Exerc Sport Sci Rev* 33: 88-97, 2005.
Lee CR, and Farley CT. Determinants of the center of mass trajectory in human walking and running. *J Exp Biol* 201: 2935-2944, 1998.
Lovely RG, Gregor RJ, Roy RR, and Edgerton VR. Effects of training on the recovery of full-weight-bearing stepping in the adult spinal cat. *Exp Neurol* 92: 421-435, 1986.
MacKay-Lyons M. Central pattern generation of locomotion: a review of the evidence. *Phys Ther* 82: 69-83, 2002.
Mahboobin A, Loughlin PJ, Redfern MS, and Sparto PJ. Sensory re-weighting in human postural control during moving-scene perturbations. *Exp Brain Res* 167: 260-267, 2005.
Maki BE, Holliday PJ, and Topper AK. A prospective study of postural balance and risk of falling in an ambulatory and independent elderly population. *J Gerontol* 49: M72-84, 1994.
Marchetti GF, and Whitney SL. Construction and validation of the 4-item dynamic gait index. *Phys Ther* 86: 1651-1660, 2006.
Margaria R. Positive and negative work performances and their efficiencies in human locomotion. *Int Z Angew Physiol* 25: 339-351, 1968.
Marigold DS, and Eng JJ. The relationship of asymmetric weight-bearing with postural sway and visual reliance in stroke. *Gait Posture* 23: 249-255, 2006.
Marsden CD, Rothwell JC, and Day BL. The use of peripheral feedback in the control of movement. *Trends Neurosci* 7: 253-257, 1984.
Maurer C, Mergner T, and Peterka RJ. Multisensory control of human upright stance. *Exp Brain Res* 171: 231-250, 2006.
McGeer T. Passive bipedal running. *Proceedings of the Royal Society of London: B Biological Sciences* B240: 107-134, 1990a.

McGeer T. Passive Dynamic Biped Catalogue. In: *The 2nd International Symposium on Experimental Robotics II* Springer-Verlag, 1991, p. 465-490.
McGeer T. Passive dynamic walking. *Int J Robotics Res* 9: 62-82, 1990b.
McGeer T. Passive walking with knees. *Robotics and Automation, 1990 Proceedings, 1990 IEEE International Conference on* 3: 1640-1645, 1990c.
McMahon TA, and Cheng GC. The mechanics of running: how does stiffness couple with speed? *J Biomech* 23 (suppl. 1): 65-78, 1990.
McMahon TA, Valiant G, and Frederick EC. Groucho running. *J Appl Physiol* 62: 2326-2337, 1987.
Morris R, Harwood RH, Baker R, Sahota O, Armstrong S, and Masud T. A comparison of different balance tests in the prediction of falls in older women with vertebral fractures: a cohort study. *Age Ageing* 36: 78-83, 2007.
Movshon JA, Adelson EH, Gizzi MS, and Newsome WH. The analysis of moving visual patterns. In: *Pattern Recognition Mechanisms*, edited by Chagas C, Gatass R, and Gross C. New York: Springer Verlag, 1985, p. 117-151.
Murray MP, Mollinger LA, Gardner GM, and Sepic SB. Kinematic and EMG patterns during slow, free, and fast walking. *J Orthop Res* 2: 272-280., 1984.
Nashner LM, Black FO, and Wall C, 3rd. Adaptation to altered support and visual conditions during stance: patients with vestibular deficits. *J Neurosci* 2: 536-544, 1982.
Nashner LM, and Peters JF. Dynamic posturography in the diagnosis and management of dizziness and balance disorders. *Neurol Clin* 8: 331-349, 1990.
Niino N, Tsuzuku S, Ando F, and Shimokata H. Frequencies and circumstances of falls in the National Institute for Longevity Sciences, Longitudinal Study of Aging (NILS-LSA). *J Epidemiol* 10: S90-94, 2000.
Oddsson LI, Wall C, McPartland MD, Krebs DE, and Tucker CA. Recovery from perturbations during paced walking. *Gait Posture* 19: 24-34, 2004.
Oie KS, Kiemel T, and Jeka JJ. Multisensory fusion: simultaneous re-weighting of vision and touch for the control of human posture. *Brain Res Cogn Brain Res* 14: 164-176, 2002.
Owings TM, and Grabiner MD. Step width variability, but not step length variability or step time variability, discriminates gait of healthy young and older adults during treadmill locomotion. *J Biomech* 37: 935-938, 2004a.
Owings TM, and Grabiner MD. Variability of step kinematics in young and older adults. *Gait Posture* 20: 26-29, 2004b.
Pandy MG, and Berme N. Synthesis of human walking: a planar model for single support. *J Biomech* 21: 1053-1060, 1988.
Park S, Horak FB, and Kuo AD. Postural feedback responses scale with biomechanical constraints in human standing. *Exp Brain Res* 154: 417-427, 2004.
Paulus WM, Straube A, and Brandt T. Visual stabilization of posture. Physiological stimulus characteristics and clinical aspects. *Brain* 107 (Pt 4): 1143-1163, 1984.
Perry J. *Gait Analysis: Normal and Pathological Function*. Thorofare, NJ: Slack, Inc., 1992.
Peterka RJ. Sensorimotor integration in human postural control. *J Neurophysiol* 88: 1097-1118, 2002a.
Peterka RJ. Sensorimotor integration in human postural control. *J Neurophysiol* 88: 1097-1118, 2002b.
Peterka RJ, and Benolken MS. Role of somatosensory and vestibular cues in attenuating visually induced human postural sway. *Exp Brain Res* 105: 101-110, 1995.
Peterka RJ, and Black FO. Age-related changes in human posture control: sensory organization tests. *J Vestib Res* 1: 73-85, 1990.
Peterka RJ, and Loughlin PJ. Dynamic regulation of sensorimotor integration in human postural control. *J Neurophysiol* 91: 410-423, 2004.

Piirtola M, and Era P. Force platform measurements as predictors of falls among older people - a review. *Gerontology* 52: 1-16, 2006.
Poulet JF, and Hedwig B. A corollary discharge maintains auditory sensitivity during sound production. *Nature* 418: 872-876, 2002.
Rothwell JC, Traub MM, Day BL, Obeso JA, Thomas PK, and Marsden CD. Manual motor performance in a deafferented man. *Brain* 105 (Pt 3): 515-542, 1982.
Roy JE, and Cullen KE. Dissociating self-generated from passively applied head motion: neural mechanisms in the vestibular nuclei. *J Neurosci* 24: 2102-2111, 2004.
Roy JE, and Cullen KE. Selective processing of vestibular reafference during self-generated head motion. *J Neurosci* 21: 2131-2142, 2001.
Rubenson J, Heliams DB, Lloyd DG, and Fournier PA. Gait selection in the ostrich: mechanical and metabolic characteristics of walking and running with and without an aerial phase. *Proc Biol Sci* 271: 1091-1099, 2004.
Ruina A, Bertram JE, and Srinivasan M. A collisional model of the energetic cost of support work qualitatively explains leg sequencing in walking and galloping, pseudo-elastic leg behavior in running and the walk-to-run transition. *J Theor Biol* 237: 170-192, 2005.
Schrager MA, Kelly VE, Price R, Ferrucci L, and Shumway-Cook A. The effects of age on medio-lateral stability during normal and narrow base walking. *Gait Posture* 28: 466-471, 2008.
Scott SH. Optimal feedback control and the neural basis of volitional motor control. *Nat Rev Neurosci* 5: 532-546, 2004.
Sherrington C. *The integrative action of the nervous system*. New Haven,: 1911.
Sherrington CS. Flexion reflex of the limb, crossed extension-reflex, and reflex stepping and standing. *J Physiol (Lond)* 40: 28-121, 1910.
Shimada H, Obuchi S, Kamide N, Shiba Y, Okamoto M, and Kakurai S. Relationship with dynamic balance function during standing and walking. *Am J Phys Med Rehabil* 82: 511-516, 2003.
Siegler S, Seliktar R, and Hyman W. Simulation of human gait with the aid of a simple mechanical model. *J Biomech* 15: 415-425, 1982.
Sienko KH, Balkwill MD, Oddsson LIE, and Wall C. Effects of multi-directional vibrotactile feedback on vestibular-deficient postural performance during continuous multi-directional support surface perturbations. *Journal of Vestibular Research* In Press: 2009.
Simon D. Kalman Filtering. *Embedded Systems Programming* 14: 72-79, 2001.
Smith JC, and Feldman JL. In vitro brainstem-spinal cord preparations for study of motor systems for mammalian respiration and locomotion. *J Neurosci Methods* 21: 321-333, 1987.
Sparto PJ, Redfern MS, Jasko JG, Casselbrant ML, Mandel EM, and Furman JM. The influence of dynamic visual cues for postural control in children aged 7-12 years. *Exp Brain Res* 168: 505-516, 2006.
Speers RA, Kuo AD, and Horak FB. Contributions of altered sensation and feedback responses to changes in coordination of postural control due to aging. *Gait Posture* 16: 20-30, 2002.
Srinivasan M, and Ruina A. Computer optimization of a minimal biped model discovers walking and running. *Nature* 439: 72-75, 2006.
Streepey JW, Kenyon RV, and Keshner EA. Field of view and base of support width influence postural responses to visual stimuli during quiet stance. *Gait Posture* 25: 49-55, 2007a.
Streepey JW, Kenyon RV, and Keshner EA. Visual motion combined with base of support width reveals variable field dependency in healthy young adults. *Exp Brain Res* 176: 182-187, 2007b.
van Beers RJ, Baraduc P, and Wolpert DM. Role of uncertainty in sensorimotor control. *Philos Trans R Soc Lond B Biol Sci* 357: 1137-1145, 2002.
Visser JE, Carpenter MG, van der Kooij H, and Bloem BR. The clinical utility of posturography. *Clin Neurophysiol* 119: 2424-2436, 2008.

Wall C, 3rd, Oddsson LI, Patronik N, Sienko K, and Kentala E. Recovery trajectories of vestibulopathic subjects after perturbations during locomotion. *J Vestib Res* 12: 239-253, 2002.
Warren WH, Kay BA, and Yilmaz EH. Visual control of posture during walking: functional specificity. *J Exp Psychol Hum Percept Perform* 22: 818-838, 1996.
Whitney SL, Marchetti GF, Schade A, and Wrisley DM. The sensitivity and specificity of the Timed "Up & Go" and the Dynamic Gait Index for self-reported falls in persons with vestibular disorders. *J Vestib Res* 14: 397-409, 2004.
Winter DA. Human balance and posture control during standing and walking. *Gait & Posture* 3: 193-214, 1995.
Wisse M, Schwab AL, van der Linde RQ, and van der Helm FCT. How to keep from falling forward; elementary swing leg action for passive dynamic walkers. *IEEE Trans on Robotics* 21: 393-401, 2005.
Wolpert DM, Ghahramani Z, and Jordan MI. An internal model for sensorimotor integration. *Science* 269: 1880-1882., 1995.
Yoneda S, and Tokumasu K. Frequency analysis of body sway in the upright posture. Statistical study in cases of peripheral vestibular disease. *Acta Otolaryngol* 102: 87-92, 1986.
Zehr EP. Neural control of rhythmic human movement: the common core hypothesis. *Exerc Sport Sci Rev* 33: 54-60, 2005.